5-2012

Increased geranylgeranylated K-Ras contributes to antineoplastic effects of farnesyltransferase inhibitors.

Mandy A. Hall

Increased geranylgeranylated K-Ras contributes to antineoplastic effects of farnesyltransferase inhibitors.

By

Mandy Ann Geryk Hall, B.S.

APPROVED:

_____

Dennis P.M. Hughes, PhD, MD, Supervisory Professor

_____

Eugenie S. Kleinerman, MD

_____

Gary Gallick, PhD

_____

Francois Claret, PhD

_____

Michael Blackburn, PhD

_____

APPROVED

_____

George M. Stancel, PhD, Dean, The University of Texas
Graduate School of Biomedical Sciences at Houston

Increased geranylgeranylated K-Ras contributes to antineoplastic effects of farnesyltransferase inhibitors.

A

DISSERTATION

Presented to the Faculty of
The University of Texas
Health Science Center at Houston
And
The University of Texas
M.D. Anderson Cancer Center
Graduate School of Biomedical Sciences

In Partial Fulfillment
of the Requirements
for the Degree of

DOCTOR of PHILOSOPHY

By

Mandy Ann Geryk Hall

Houston, TX
May 2012

DEDICATION

To my parents who have always pushed me to do better than I think I am able to do. You are both always there for me to support me in every way you can. You have always encouraged me to do whatever I want in life, thank you.

Sam and Page thank you for always helping us any way you can and for always being there for us.

Mackenzie Marie and Sara Hayden, my girls, thank you for loving me unconditionally and for teaching me to be a more patient person. I love seeing your faces light up, Mommy loves you.

To my husband, Bo, for being there for me all the times I have needed you. You are always there to bring my spirit up and to make me see everything is going to be fine. I could not imagine being where I am today without you, I love you.

ACKNOLEDGEMENTS

Thank you to my advisor, Dr. Dennis Hughes, for the opportunity to do research and my thesis in your laboratory. I admire your positive attitude and ability to remind me of my achievements and provided guidance on my research when my experiments give me trouble. Thank you for being very understanding in all aspects throughout my time in your laboratory.

I would like to thank all past and present members of the Hughes' lab. Especially Dr. Laura Nelson, whom corrected countless spelling mistakes, answered unlimited questions, and was always there to give me advice. Yanwen Yang, thank you for your expertise in molecular biology and trouble shooting for various experiments. Our laboratory is very lucky to have both of you. Limin Zhu, thank you for all of your hard work with parts of the senescence portion of this thesis.

Thank you to Dr. Patrick Zweidler-McKay for all of your advice and reagents when we were neighbors and when your laboratory was my second home. Thank you, Dr. Karen Clise-Dwyer, Karen Ramirez, and Kim Acklin in the South Campus Flow Cytometry Facility for all of your help, advice and training on the Influx Cell Sorter.

I would also like to thank everyone in the Pediatrics department for making the last six years truly enjoyable. I wish you all the best of luck and I am going to miss all of you.

I also thank all of my past and present committee members for all of your guidance and support. I aspire to reach the level of success each of you have achieved in your careers: Dr. Eugenie S. Kleinerman, Dr. Gary Gallick, Dr. Francois Claret, Dr. Michael Blackburn, Dr. Vidya Gopalakrishnan, and Dr. Timothy McDonnell. I especially would like to thank Dr. Kleinerman for encouraging me to finish my research project to the end.

Thank you to all of my friends and family for all of your encouragement and support throughout the years.

Increased geranylgeranylated K-Ras contributes to antineoplastic effects of farnesyltransferase inhibitors.

Publication No. _____

Mandy Ann Geryk Hall, B.S.

Supervisory Professor: Dennis P. M. Hughes

The Ras family of small GTPases (N-, H-, and K-Ras) is a group of important signaling mediators. Ras is frequently activated in some cancers, while others maintain low level activity to achieve optimal cell growth. In cells with endogenously low levels of active Ras, increasing Ras signaling through the ERK and p38 MAPK pathways can cause growth arrest or cell death. Ras requires prenylation – the addition of a 15-carbon (farnesyl) or 20-carbon (geranylgeranyl) group – to keep the protein anchored into membranes for effective signaling. N- and K-Ras can be alternatively geranylgeranylated (GG'd) if farnesylation is inhibited but are preferentially farnesylated.

Small molecule inhibitors of farnesyltransferase (FTIs) have been developed as a means to alter Ras signaling. Our initial studies with FTIs in malignant and non-malignant cells revealed FTI-induced cell cycle arrest, reduced proliferation, and increased Ras signaling. These findings led us to the hypothesis that FTI induced increased GG'd Ras. We further hypothesized that the specific effects of FTI on cell cycle and growth result from increased signal strength of GG'd Ras.

Our results did show that increase in GG'd K-Ras in particular results in reduced cell viability and cell cycle arrest. Genetically engineered constructs capable of only one type of prenylation confirmed that GG'd K-Ras recapitulated the effect of FTI in 293T cells. In tumor cell lines ERK and p38 MAPK pathways were both strongly activated in response to FTI, indicating the increased activity of GG'd K-Ras results in antiproliferative signals specifically through these pathways. These results collectively indicate FTI increases active GG'd K-Ras which activates ERK and p38 MAPKs to reduced cell viability and induce cell cycle arrest in malignant cells. This is the first report that identifies increased activity of GG'd K-Ras

contributes to antineoplastic effects from FTI by increasing the activity of downstream MAPKs.

Our observations suggest increased GG'd K-Ras activity, rather than inhibition of farnesylated Ras, is a major source of the cytostatic and cytotoxic effects of FTI. Our data may allow for determination of which patients would benefit from FTI by excluding tumors or diseases which have strong K-Ras signaling.

TABLE OF CONTENTS

LIST OF FIGURES

APPENDIX FIGURES

LIST OF TABLES

ABBREVIATIONS

Endoplasmic reticulum	ER
Extracellular-signal-related kinase	ERK
Farnesylated	F'd
Farnesyltransferase inhibitors / inhibition	FTI
GTPase activating protein	GAPs
Guanosine diphosphate	GDP
Guanine nucleotide exchange factors	GEFs
Galectin-3	Gel-3
Geranylgeranylated	GG'd
Geranylgeranylation	GG'n
Geranylgeranyl transferase inhibitors / inhibition	GGTI
Growth factor receptor-bound protein 2	Grb2
Guanosine triphosphate	GTP
Guanosine triphosphatase	GTPase
Hypervariable region	HVR
c-Jun N-terminal kinases	JNKs
Kilodaltons	kDa
Kinase suppressor of Ras 1	KSR1
Mitogen-activated protein kinase	MAPK
Mouse Embryonic Fibroblasts	MEFs
Neurofibromatosis type 1	NF1
Peripheral blood mononuclear cells	PBMCs
Platelet-derived growth factor	PDGF
Phosphatidyl inositol-dependent kinase 1	PDK-1
Phosphatidylinositol 3-kinases	PI3K
Protein kinase C	PKC
Plasma Membrane	PM
Ras-guanine-nucleotide-releasing factor	Ras-GRF
Ras-guanyl nucleotide-releasing protein	Ras-GRP
Receptor tyrosine kinases	RTK
SL3-3 enhancer factor 1	Sef-1
Son of sevenless	SOS
Tipifarnib	TF
T-lymphoma invasion and metastasis-inducing protein	TIAM

CHAPTER 1: Introduction

INTRODUCTION

Ras

In human cancer there is a 30% incidence of activating mutations in *Ras* genes, therefore Ras proteins are extensively studied. However, despite over thirty years of research, interacting proteins and regulators of Ras are still being discovered. Ras proteins are small guanosine triphosphatases (GTPase) that regulate cellular growth, differentiation, survival, and death (1-3). There are four Ras proteins created by 3 Ras genes; H-Ras, N-Ras, K-Ras A and K-Ras B. K-Ras A and B are splice variants. K-Ras A is expressed temporally and spatially and it is actively expressed in the adult kidney, intestine, stomach, liver, uterus, lung, pancreas, salivary glands, seminal vesicles, bone marrow, and cecum. H-Ras, N-Ras, and K-Ras B are expressed ubiquitously. Further review of these proteins excludes K-Ras A, as it is tissue specific and is not expressed in most cell lines used in this thesis.

The specificity for each Ras isoform is determined by differential patterns of expression, distinct intracellular processing and differential localization displayed by the fully processed protein products. The function of each individual species of Ras differs depending on the cell type and the availability of interacting modulator and effector proteins, which is what contributes to the complexity of Ras signaling (4). The biologic impact of Ras signaling is dependent on both the subcellular localization of Ras and the specific interacting partners present at these locations. These binding partners can determine the intensity and duration of Ras signaling, which in turn determines if the signal is proliferative, cytotoxic, or cytostatic.

Ras Structure

Ras proteins are comprised of 6 β-strands and 5 α-helices. Ras is a 21 kDa protein which contains a G domain (amino acids 1-166) and a C-terminal membrane targeting and effector domain known as the hypervariable region (HVR- amino acids 166-189) (Figure 1). The G domain contains 5 G motifs which allow Ras to bind GDP or GTP. G1 consists of the P-loop which binds the α and β phosphates of GDP or GTP (5). G2 contains threonine-35 and is known as the switch 1 domain. G3 is comprised of a DXXG motif and binds Mg^{2+} and the γ phosphate of GTP. G5 contains a SAK consensus sequence which supports the guanine base recognition site. The two regions in Ras important for activation by GEFs are switch I, which comprises amino acids 25-40, and switch II which comprises amino acids 57-75(6). The effector domain (amino acids 32-40) is the binding site for Ras effectors (described below) (7).

The HVR comprises two known important features: the linker domain with limited known functions and the targeting domain where posttranslational modifications such as prenylation and palmitoylation are esterified to Ras proteins (further discussed below). The prenylation (farnesyl or geranylgeranyl) group associated with Ras and the number or lack of palmitoylation groups determines what membrane and which proteins each Ras family member associates with (8-18). These post translational differences are what allow the highly homologous Ras proteins to interact with a wide array of intercellular membranes and downstream effectors.

Figure 1

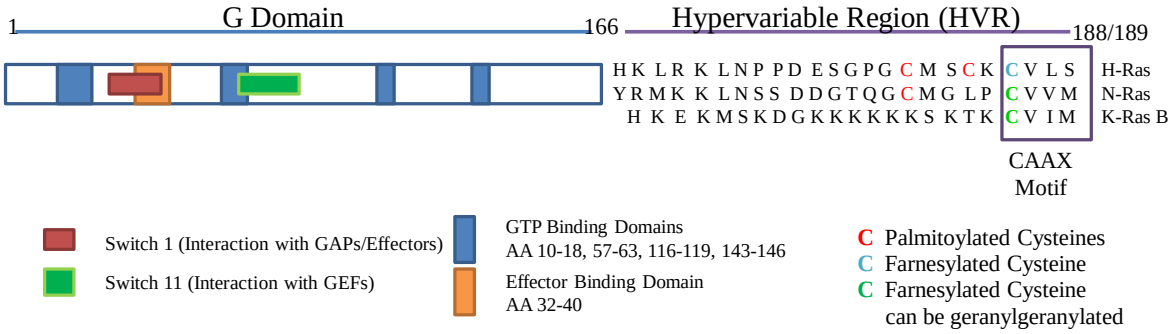

Figure 1. Structure of the three Ras proteins. All three Ras proteins have a highly homologous G domain which contains the GTP (orange) and effector (blue) binding domains. The G domain also contains switch 1 (red) and switch 11 (green) which undergo conformational changes upon Ras binding guanine nucleotides. The hypervariable region (HVR) is distinct among the Ras proteins. The HVR contains amino acid residues that are post-translationally modified and allow Ras to interact with membranes. Cysteines that can be plamitoylated are red, two available sites on H-Ras one on N-Ras. H-Ras can only be farnesylated while N- and K-Ras can be farnesylated or GG'd.

Ras post translational modifications and processing: Prenylation, palmitoylation, and ubiquitination.

Prenylation

For full activity, it is commonly thought that Ras must be membrane-bound. Ras is associated with the membrane mainly by the post translational process, prenylation. Prenylation is the irreversible addition of a lipid to the C-terminal cysteine of membrane-associated proteins (19-21). This lipid modification increases the hydrophobicity of the protein

and enhances the interaction with membrane lipids as well as with other proteins (20, 21). There are two forms of prenylation: farnesylation (15-carbon) and geranylgeranylation (GG'n) (20-carbon). There are pharmacological inhibitors which have been created to inhibit these processes (discussed below). Prenylated proteins contain a CAAX motif which consists of a required cysteine (C) followed by two aliphatic amino acids (A) (leucine, isoleucine, or valine) with a C-terminal serine, methionine, glutamine, or leucine (X) (22, 23). This CAAX motif, along with the linker region at the C-terminus of proteins, determines what prenyl group is added to the protein (24). Some proteins can only be farnesylated and others only GG'd, while some can have either modification added to their C-terminus. The amino acid in the X position determines which prenyl group associates with the protein. If the X is a serine or glutamine, a farnesyl group will be added to the C-terminal cysteine of that protein. If the X is a leucine, then a geranylgeranyl group will be added to the C-terminal cysteine of the protein. However, if the X is a methionine then the protein can be either farnesylated or GG'd. N-Ras and K-Ras B both have a methionine in the X position and are able to be GG'd if farnesylation is blocked (25). Farnesylation and GG'n of proteins occur in the cytosol (8).

Fully processed Ras is prenylated, protealyzed, and carboxymethylated. Once Ras is farnesylated, Rce1 proteolyzes the AAX and Icmt carboxymethylates the C-terminal cysteine. Knockout of the Rce1 gene in mice is lethal (26). Both Rce1 and Icmt are endoplasmic reticulum (ER) proteins which reside on the cytosolic surface of the ER (8). MEFs without *Rce1* and *Icmt* have mislocalized farnesylated wild type (WT) (N-,H-,K-) and oncogenic (H- and K-) Ras, but when WT K-Ras was mutated to be GG'd, the absence of these genes did not disrupt Ras localization (26). Absence of these genes did not disrupt GG'd protein localization, suggesting the longer alkyl chain has a greater affinity for the membrane and is less likely to have disrupted localization without fully processed protein. Farnesylation may be comparatively reversible while GG'n is a more permanent anchor for membrane association and signaling (26). *Icmt*-deficient Embryonic Stem cells (EM) have mislocalised K-Ras to the cytoplasm while some K-Ras was still able to localize to the plasma membrane (PM) (27). K-Ras which is still localized at the PM could be GG'd K-Ras. Additionally the difference between Rce1 and Icmt deficiencies could be due to differences in the cell types used. This difference in localization could be due to a more dramatic change from not having proteolytic cleavage and carboxymethylation, as these two steps could both affect the degree of mislocalized Ras.

Palmitoylation

Ras proteins have additional modifications that allow them to further interact with membranes. H-Ras and N-Ras are both palmitoylated. Palmitoylation (*S*-acylation) is the covalent and reversible attachment of 16-carbon fatty acid palmitate to cysteine residues of membrane-targeted proteins. Not only does palmitoylation allow Ras proteins to interact with membranes and other proteins but it also aids in determining the subcellular trafficking of proteins among subcellular membrane components. Palmitoylation is a reversible and dynamic process. H-Ras has two cysteine residues that can be palmitoylated with a half life of 60 minutes while N-Ras has only one with a half life of 20 minutes (8). The trafficking of these proteins is very different with these modifications. N- and H-Ras are both distributed through the secretory pathway. Activation of these two proteins stimulated de-palmitoylation and redistribution to the ER or Golgi, where they are re-palmitoylated. This cycle prevents nonspecific accumulation of H and N-Ras on membranes. Palmitoylation of H-Ras on Cys181 stabilizes H-Ras to the PM, while palmitoylation on Cys 184 facilitates redistribution between the PM and microdomains (28). Palmitoylation is necessary for PM localization as H-Ras targeting domain mutants where cysteine residues are mutated cannot be trafficked to the PM (15). Reversible palmitoylation and positioning of the palmitoyl group regulate Ras localization and signal output (8, 11, 12, 29).

K-Ras B does not have a palmitoylation site but does have a stretch of six lysine residues (polybasic region) that are positively charged to allow it to further interact with membranes, as membranes are negatively charged. Additionally a third motif distinct from the prenylation site, palmitoylation, or polybasic sites, has been identified. This motif contains acidic residues in the HVR that stabilize palmitoylation, and basic amino acids that may interact electrostatically with acidic phospholipids at the cell surface (11).

Ubiquitination

Ras can also be ubiquitinated. Mono- and di-ubiquitination have been found to restrict the activity of H- and N-Ras yet promote the activity of K-Ras (30). Ubiquitination increased K-Ras affinity for Raf, PI3K, and RalGDS in kinase assays (30). Ubiquitinated H-Ras and N-Ras alters their subcellular localization to endosomes, preventing activation of Raf, while ubiquitination of K-Ras does not alter its localization at the PM (31, 32). Ubiquitination of K-Ras enhances the strength of its signaling output, possibly by stabilizing K-Ras-GTP (30, 33). The deubiquitinating enzyme USP17 inhibited H-Ras and N-Ras localization to the PM but still

allows them to function at the ER and Golgi (32), demonstrating Ras can facilitate signal transduction at sites other than the PM.

Unprenylated WT Ras is still active in Normal non-transforming cells

It has been thought that Ras must be membrane bound in order to be active and increase signaling of downstream effectors. However, two independent groups have found normal non-oncogenic Ras is active when it is not prenylated in normal cells. One group found accumulation of unfarnesylated H-Ras in the cytosol by using $Ras^{G12V,C186S}$ and Ras^{C186S} in 293T cells. $Ras^{G12,C186S}$ inhibited activation and membrane translocation of Raf by forming a stable complex with Raf in the cytosol (34). In contrast WT, unprenylated Ras^{C186S} showed no inhibitory effect on either Raf activation or Raf translocation (34). These results demonstrate that unfarnesylated oncogenic Ras interacts with Raf in the cytosol to inhibit its membrane translocation, thereby not allowing for Raf activation, while unfarnesylated normal Ras does not. Unprenylated WT Ras in three normal renal cell types stimulated by platelet-derived growth factor (PDGF) can activate mitogen-activated protein kinase (MAPK) and phosphatidylinositol 3-kinases (PI3K) (1). In normal cells unprenylated Ras may still be active in the cytosol and able to activate downstream effectors even when it is not membrane-bound.

Ras localization

Ras proteins are distributed to specific regions of a cell based on which post-translational modifications have been added to individual Ras proteins. Specific effector pathways have been identified for Ras proteins in specific cellular localizations. Thus it is important to identify differences in localization of wild type (WT) and mutant Ras proteins. It is also important to identify differences in localization between N-Ras, K-Ras, and H-Ras proteins themselves.

Farnesylated and GG'd K-Ras associate with microtubules and can then associate with the PM, since in cells treated with paclitaxel, a microtubule inhibitor, K-Ras was found almost exclusively in intracellular locations (35). H-Ras and Rho A and B were not associated with microtubules and this observation suggests other portions such as the six lysine residues in the K-Ras HVR allows association with tubulin polymers (35). WT H-Ras is normally in equilibrium between lipid rafts and noncholesterol-dependent microdomains, while constitutively active H-Ras is in nonraft microdomains (Figure 2) (9). GTP bound H-Ras is localized in non-raft regions and GDP bound H-Ras is in lipid raft regions, conversely GTP bound N-Ras resides in lipid raft microdomains and GDP bound N-Ras resides in non-raft

regions (Figure 2) (9, 36). WT and constitutively active K-Ras both cluster in the disordered plasma membrane, however mutating K-Ras so that it can be only GG'd reduces clustering (Figure 2) (9). This result suggests K-Ras requires a farnesyl moiety for normal microlocalization. GG'd K-Ras is more tightly bound to the membrane, demonstrated by resistance to 1 M salt extraction (15). This finding suggests GG'n is a more permanent anchor and has the potential to produce a more sustained signal. H-Ras associates with distinct signaling domains when it is WT or oncogenic, while K-Ras localization changes depending on its prenylation status and does not change whether it is WT or oncogenic (9). These differences in spatial localization between Ras proteins contributes to differential signal outputs from these highly homologous proteins (9).

Figure 2

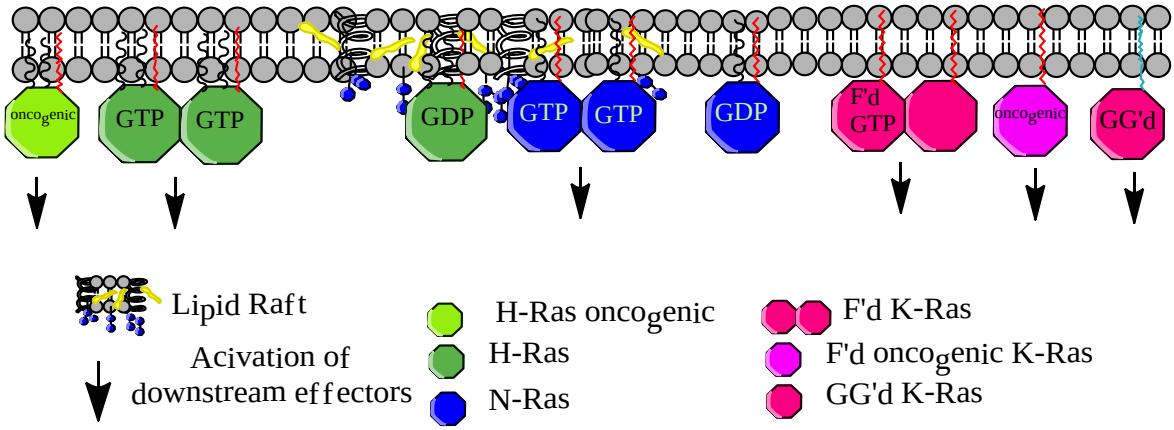

Figure 2. Spatial arrangement in the plasma membrane determines signaling specificity among the Ras proteins. Oncogenic H-Ras, GTP bound H-Ras, GDP bound N-Ras, and all K-Ras are localized in the disordered plasma membrane. GDP-bound H-Ras and GTP bound N-Ras associate with lipid rafts. Farnesylated K-Ras clusters in the plasma membrane while GG'd K-Ras reduces clustering in the plasma membrane. Arrows indicate Ras which is active and can activate downstream effectors.

To selectively localize Ras to specific compartments, mutant H-Ras constructs have been created. These experiments were designed to selectively determine which downstream effectors the Ras proteins interact with at specific subcellular compartments. For example, to selectively exclude H-RasV12 from the PM, cysteines 181 and 184 were mutated to serines (H-RasV12 SS), which does not allow association of palmitoylation groups (37). The remaining constructs were created with oncogenic H-Ras, which was not able to be prenylated since the N-terminus (amino acids 1-66) was fused to proteins that reside in specific subcellular

localizations (37, 38). As only the N-terminus was fused to other proteins, structural folding of Ras may be altered, allowing effector proteins which would not normally associate with oncogenic H-Ras to have access and bind to these mutant H-Ras proteins. Differences between the HVDs of the Ras proteins were not accounted for when producing these constructs. As each protein has different post translational processes associated with them these experiments likely have binding interactions which may have limited biological relevance.

GEFs and GAPs

Ras is the founding member of a family of small GTPases (39). It cycles through active and inactive states by binding to guanine nucleotide exchange factors (GEFs), which allow for the exchange of guanosine triphosphate (GTP) from guanosine diphosphate (GDP) and GTPase activating protein (GAPs) which exchange GTP to GDP. Ras bound to GTP is active and inactive when bound to GDP. There are three main classes of Ras GEFs: son of sevenless (SOS), Ras-guanine-nucleotide-releasing factor (Ras-GRF), and Ras-guanyl nucleotide-releasing protein (Ras-GRP). The interaction of SOS with Ras after receptor tyrosine kinases (RTK) activation has been thoroughly examined (Figure 2). After growth factors bind RTK, the receptors dimerize and autophosphorylate (40). Growth factor receptor-bound protein 2 (Grb2) adaptor protein associates with SOS in the cytoplasm and is recruited to the membrane after receptor phosphorylation (40). SOS is then able to activate plasma membrane (PM) bound Ras. During the interaction between Ras and SOS (a GEF), switch 1 leads to disruption of the nucleotide-binding site and GDP dissociation, and switch II mediates anchoring of Ras to Sos (6).

Figure 3

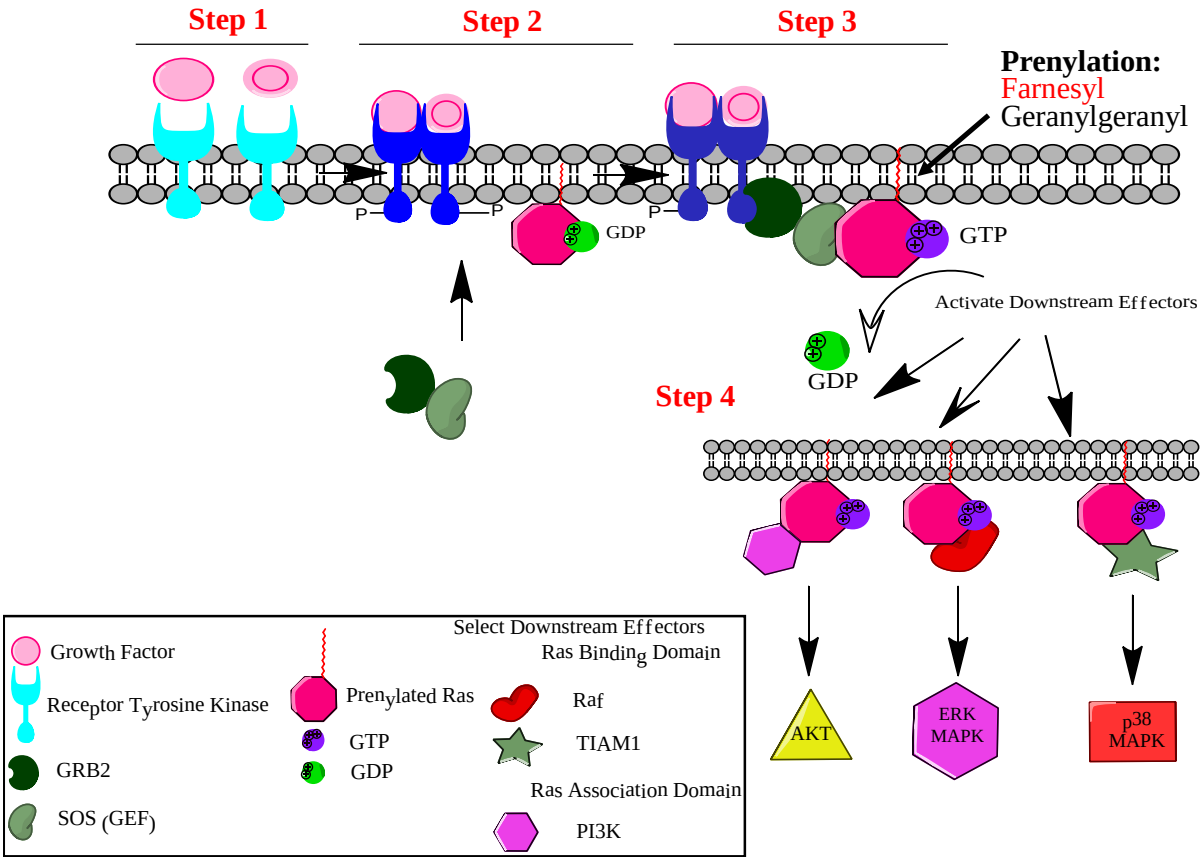

Figure 3. Activation of Ras and select downstream targets by activation of receptor tyrosine kinases (RTKs). Step 1: Extracellular growth factors bind to RTKs which are embedded into the plasma membrane. Step 2: The receptors dimarize and autophosphorylate. Adaptor molecules such as GRB2 interact with the GEF SOS in the cytoplasm, and are recruited to RTKs when they are phosphorylated at specific residues. Inactive GDP-Ras is localized in the PM by addition of a prenylation group. Step 3: Prenylated Ras is embedded into the membrane and is activated by SOS which allows for the exchange of GTP from GDP when GRB2 is phosphorylated by RTKs. Step 4: Ras can then activate specific downstream effectors depending on its localization within the plasma membrane. Three downstream effectors depicted are PI3K, Raf, and TIAM1, which activate AKT, ERK, and p38 MAPK respectively.

Ras-GRPs are GEFs that can associate with endomembranes to activate Ras. GRP2 and GRP3 localize to the Golgi where they can activate N-Ras and H-Ras (41). GRP2 activates K- and N-Ras and is stimulated by tetradecanoylphorbol acetate (TPA, a small molecule that stimulates protein kinase C (PKC)) and inhibited by increased cytosolic levels of calcium (42). Once stimulated by TPA, GRP2 can activate K- or N-Ras at the PM (42). GRP activation at specific localizations and interaction with select Ras species suggests spatial and temporal activation of Ras is dependent on various factors in a cell.

P120^{GAP} was the first identified GAP found to interact with the effector domain of Ras to turn off Ras signaling (43). Other GAPs such as Ca^{2+}-promoted Ras inactivator (CAPRI) and Ras GTPase-activating-like protein (RASAL) have been identified as Ca^{2+} dependent and regulate Ras activation based on Ca^{2+} concentrations within a cell (44, 45).

Neurofibromin is a Ras-GAP which acts as a tumor suppressor and its expression is lost in the disease neurofibromatosis type 1 (NF1) (46). In neurofibroma cells from NF1 patients, activated Ras is upregulated in Schwann cells and not fibroblasts (3). However, in *NF1*-deficient mice, embryonic fibroblasts exhibit enhanced Ras activation, and prolonged extracellular-signal-regulated kinase (ERK) activation (47). These findings demonstrate differences in Ras activation between patients and mice, however both demonstrate NF1 as an inhibitor of Ras activation.

Cell types in different species and different tumor types are likely to have differential activation of GAPs and GEFs to activate/deactivate Ras. If Ras is associated with a GEF and active, then the effector domain (amino acids 32-40) becomes an active binding site for Ras effectors (7).

Ras target proteins

In cells that have low levels of endogenous Ras protein, a modest increase in Ras signaling promotes proliferation; however high sustained levels induce growth arrest and senescence (4, 48). Some cells, however, escape growth arrest, probably by down-regulating tumor suppressor genes such as p53 (49). There are numerous Ras effectors that result in a wide variety of responses. Identified Ras effectors include: Raf, PI3K, RalGDF, Rin1, T-lymphoma invasion and metastasis-inducing protein (TIAM), Af6, Nore1, PLCε and PKCξ. Our work specifically focuses on Ras-Raf, Ras-TIAM, and Ras-PI3K signaling (Figure 3).

Raf was the first discovered Ras effector and is often associated with proliferative effects. However, research has also discovered if the Raf pathway is over-stimulated this can have anti-proliferative effects and result in cell death (50-52). Raf has three isoforms which preferentially associate with specific Ras isoforms (7, 53, 54). Activation and recruitment of Raf by Ras activates the ERK MAPK pathway. There are multiple MAPK pathways that regulate a wide variety of cellular activities. A well-studied group of this family includes the ERK 1/2, c-Jun N-terminal kinases (JNKs), and p38 MAPKs. There are three evolutionarily conserved sequential kinases: a MAPK, a MAPK kinase (MAPKK), and a MAPKK kinase (MAPKKK) (51, 55). The MAPKKKs are serine/threonine kinases that are often activated

through phosphorylation by a small GTP-binding protein such as Ras. MAPKKK activation leads to phosphorylation and activation of a MAPKK which then phosphorylates, thereby activating, a MAPK. Once activated, MAPKs phosphorylate their respective substrates. ERK 1/2 are most often activated as a result of mitogen or growth factor signals. JNK and p38 MAPKs are primarily activated by environmental stress and inflammatory cytokines. p38 can also be activated through Ras mediated activation of T-cell lymphoma invasion and metastasis-inducing protein 1 (TIAM1), which also contains a Ras-binding domain (56). TIAM1 is a GEF that activates Rac. Rac is an identified activator of Mirk, which in turn can activate MKK3/6 the upstream activator of p38 MAPK (57). There is overlap and crosstalk in these signaling cascades which regulate the balance of cell survival. NIH3T3 cells co-transfected with oncogenic H-Ras and p38 MAPK resulted in p38 MAPK activation (58). p38 MAPK activation provided a negative feedback mechanism for overcoming the proliferative ERK signals activated by oncogenic H-Ras (58). Over stimulation of MAPK family members has been shown to offset the balance of growth signals of a cell, driving it to cell death (50, 52, 59). ERK1/2 signaling is regulated by their subcellular localization which in turn regulates which substrates will be phosphorylated and activated (60). Scaffold proteins form integrated structures to determine the amplitude and duration of signals created from signaling cascades. Casar et al. found scaffolds serve to direct spatial control of ERK1/2 signals by regulating ERK activity in a subcellular specific nature (53). Cells were transduced with localization specific H-RasV12. In cells with RasV12 at lipid rafts, ERK1/2 localized with cPLA2, whereas cells expressing H-RasV12 at the disordered PM ERK1/2 colocalized with RSK1 (53).

PI3K directly and preferentially interacts with H-Ras or N-Ras as opposed to K-Ras (61). Ras binding and activation of PI3K allows lipid phophatidylinositol (3,4,5) triphosphate (PIP_3) to be produced which then recruits phosphatidylinositol-dependent kinase 1 (PDK1). PDK1 and AKT are then translocated to the PM where PDK1 phosphorylates AKT. AKT has 3 isoforms which modulate proliferation and cell death (61-64). N-Ras binds PI3K which produces 3,4,5-trisphosphate which binds AKT and allows for its activation through phosphorylation. Once activated, AKT can then phosphorylate Bad on serine 136 (62). Phosphorylation of Bad inhibits its binding to anti-apoptotic proteins Bcl-2 and Bcl-xL allowing AKT to promote cell survival (64).

In BHK (derived from hamster kidney tissue) and COS (derived from an African green monkey) cells, K-Ras is a potent effector of Raf-1, while H-Ras preferentially activates PI3K

(7, 8). Effector domain mutants have been made to determine which signaling pathways are necessary for specific Ras activity in H-Ras and K-Ras (65). In endometrial cells H-Ras preferentially activated PI3K to promote cell survival, while K-Ras activated Raf-1 and ERK signaling to promote apoptosis (65). K-Ras B can also be phosphorylated by PKC to promote translocation of K-Ras B to the mitochondria, causing cell death by interacting with Bcl-xL (64, 66).

Ras interacting proteins

Gelactins are β-galactoside binding proteins that contain a COOH-terminal carbohydrate domain, a NH_2-terminal proline, and glycine-rich domain (67). K-Ras-GTP directly interacts with Galectin-3 (Gal-3) when in nanoclusters at the PM which interact to magnify signaling of ERK through K-Ras (68, 69). Over-expression of Gal-3 in breast cancer cells increased WT K-Ras-GTP and decreased expression of WT N-Ras-GTP (69). Inhibitors of ERK inhibited oncogenic Gal-3 mediated apoptotic resistance and anchorage-independent growth (69). The Gal-3 and K-Ras interaction may induce a conformation change which makes K-Ras inaccessible to GAPs, and therefore increase K-Ras-ERK signaling specifically (68, 69).

Other scaffolding proteins have been identified and also contribute to the strength and intensity of Ras downstream signaling. Kinase suppressor of Ras 1 (KSR1) has been shown to interact with ERK at the PM, while SL3-3 enhancer factor 1 (Sef-1) regulates ERK at the ER and Golgi (53, 70).

Mutant verses Wild Type

Amino acid substitutions at critical positions in Ras allow the protein to become constitutively active and can result in malignant transformation of cells (39). Various substitutions have been identified the most common reported are Gly 12, Gly 13, and Gln 61, which bind to the β- and γ- phosphate of GDP and GTP (71). These mutants diminish GAP-mediated GTP hydrolysis, thereby increasing the activity of Ras and its downstream signaling. Mutations in Ras isoforms have different frequencies and prevelances in cancer (Table 1). K-Ras mutations are the most common reported. *Ras* mutations occur with some frequency in the following cancers with the listed frequencies (72):

K-Ras	
Pancreas	80-90%
Colon & Rectum	30-60%
Lung	27-60%
Liver	12-26%
Ovary	0-48%
Cervix	20%
Endometrium	10-40%
Breast	1-12%
Thyroid	0-60%
Testis	12-43%
Leukemia	6-40%
Head & Neck	0-30%

N-Ras	
Liver	20%
Skin	20%
Thyroid	0-60%
Testis	12-43%
Leukemia	6-40%
AML	22-40%

H-Ras	
Small intestine	31%
Prostate	4-10%
Stomach	0-41%
Bladder	7-66%
Thyroid	0-66%
Head and neck	0-30%

Table 1: Ras mutational frequency in cancer. Yellow indicates overlap between K-Ras and N-Ras, green indicates all three Ras proteins have reported mutations, and blue indicates overlap between K-Ras and N-Ras mutations.

Ras activation was analyzed in 191 AML patients. 22% of patient samples had Ras mutations, whereas 25 patient samples had strong Ras activity in the absence of *Ras* mutations. In younger patients, increased Ras activation/activity was predictive for overall survival rate in patients receiving high-dose-1-β-D-arabinofuranosylcytosine therapy (anti-viral agent) (73).

Given the differences between mutant and WT Ras, the cellular signals they create are very different. Signaling consequences of transfecting / transducing oncogenic H-, N-, or K-Ras are likely create a different biological outcome from transfecting / transducing WT Ras. As many cancers have a specific oncogenic Ras prevalence, research using oncogenic forms may have biological relevance in relation to the disease with that mutant Ras species. Creating oncogenic Ras has been shown to alter H-Ras and N-Ras signaling (9). A large percentage of research has been conducted with oncogenic H-Ras, which is likely to have relevance to diseases which harbor mutant H-Ras. However, these findings are not likely to correlate with diseases which have mutant N- or K-Ras or WT Ras. These proteins distribute to distinct subcellular locations in order to create signaling cascades with specific biological outcomes.

To understand the complicated network of Ras signaling, the transfected / transduced Ras needs to have biological relevance. A GG'd H-Ras would not endogenously occur in a cell and would behave differently than GG'd N-Ras since N-Ras has only one not two palmitoylation sites. The difference of K-Ras and its polybasic domain is necessary for its specific localization and interaction with effector proteins and microtubules. While creating mutant proteins allows for determination of specific signaling cascades and interactions, caution needs to be taken for interpretation of the results and the implications they may have.

Subcellular localization influences which signaling partners H-, N, or K-Ras interacts with (17, 29, 38, 54, 62, 74). The extent of activation generated by Ras is dependent on stability of the Ras-GTP effector complex and the rate at which Ras cycles through newly formed Ras-GTP effector complexes (62). Clustering, scaffolding proteins, and GEFs/GAPs can affect the interaction of Ras and its effector proteins in order to determine the intensity and duration of Ras signaling. These factors ultimately determine if the signal output will be proliferative, cytotoxic, or cytostatic.

Inhibition of farnesyltransferase

In tumorigenic cells, prenylation of Ras is necessary for its activation. Therefore farnesyltransferase inhibitors (FTIs) have been developed to block oncogenic Ras signaling. Farnesyltransferase (FTase) and geranylgeranyl transferase (GGTase) are the enzymes responsible for the addition of a 15-C or 20-C isoprenyl lipid, respectively, to the C-terminus of proteins with a CAAX motif. These two enzymes share a common α subunit and distinct β subunits (20). Substrate binding of FTase or GGTase occurs by binding to farnesyl pyrophosphate (FPP) or geranyl pyrophosphate (GPP), respectively, followed by binding to the CAAX peptide. As these enzymes have different β subunits, inhibitors or shRNAs can be produced to selectively inhibit FTase or GGTase. Normal cells are heavily dependent on GGTase activity, therefore therapies blocking GG'n are likely to be very toxic in the clinic (75).

Unlike chemotherapy, small molecule inhibitors are directed against specific enzyme targets and may be less toxic to non-cancerous cells. Tipifarnib and lonafarnib are small molecule inhibitors in clinical trials that inhibit FTase by competitively binding to its CAAX peptide binding site. Farnesyltransferase inhibitors (FTI) such as tipifarnib inhibit prenylation of multiple proteins including Ras, RhoB, Lamin A/C, and the centromere proteins (CENP-E

and CENP-F) (19, 76, 77). It is likely that inhibition of or alternate GG'n of many farnesylated proteins contribute to the antineoplastic effects of FTI.

Pre-clinical Data

FTIs have shown anti-proliferative activity and pro-apoptotic effects in a wide variety of tumor cell lines including blood, breast, and solid malignancies (19, 76, 78-81). Feldkamp et al. found Ras GTP levels predict efficacy of FTI in human astrocytomas regardless of Ras mutational status (79). This result supports the original hypothesis of Ras as a major therapeutic target of FTI's even in tumors lacking oncogenic Ras mutations. High levels of H-Ras GTP and low K and N-Ras activities were predictive of favorable Ic50 values. End et al. found tipifarnib to be effective *in vitro* and *in vivo* against tumors bearing WT and mutant H-Ras (82). Ras mutational status has not been identified as a predictor of patient response to FTI. Not all mutations in Ras are oncogenic and therefore mutational status of Ras is not likely to predict patient response to FTI as originally expected. Increased Ras signaling in tumors which are not dependent on Ras has been shown to have anti-proliferative effects (50, 52, 66, 83, 84). GG'd H-Ras(61L) transduced into NIH 3T3 cells and then treated with FTI B581 increased Jun and Elk transcription in luciferase assays; farnesylated Ras and Raf transductions decreased or had no effect on Jun or Elk transcription, respectively (85). This result suggests inducing expression of GG'd Ras results in increased ERK activity when FTase is inhibited. Most groups disregard Ras as a major intermediate in FTI signaling when decreases are not observed in Ras activity or downstream target proteins (19, 75, 76, 78, 81, 86-94). Human pancreatic cancer cell lines treated with tipifarnib resulted in an increase in prolonged ERK activation and inhibition of STAT3(Tyr705), followed by increased $p21^{cip1/waf1}$, which resulted in growth inhibition (95).

Lonafarnib treatment of cancer cells (lung, ovarian, colon, glioblastoma, breast, and renal) depletes CENP-E from metaphase kinetochores, resulting in aberrant chromosomal maintenance (81). Similar chromosomal alignment defects were seen in head and neck tumor samples, suggesting FTI disrupts chromosomal maintenance (81). FTI alters the association between CENP-E and microtubules altering the microtubule-centromere interaction during mitosis (96). Rho B has also been implicated as having anti-tumorigenic effects as a result of GG'n after FTI. However, when Rho B was homozygously deleted in murine fibroblast cells, FTI still inhibited anchorage independent growth, suggesting that RhoB is not the only or major protein involved in this antineoplastic response to FTI (97). This data suggests FTI will inhibit

the localization and activity of many proteins that are likely to contribute to anti-proliferative effects of this treatment.

Clinical Trials

Lancet et al. found that FTIs represent a class of signaling inhibitors that are emerging in the clinic and they may inhibit critical growth and survival signals (76). They also found that Ras may be a rational target, but Ras-driven tumors are likely to exhibit signaling variability and susceptibity to FTIs, which may depend on pharmacologic properties of FTIs, and which Ras isoform is driving a specific tumors' growth.

In clinical trials, tipifarnib is normally administered orally twice daily for 21 days every 28 days for numerous cycles (98-103). It is normally given at 300 mg twice daily in adults and 150 mg twice daily in children. Side effects are most often myelosuppression, nausea, and vomiting. Monotherapy uses of tipifarnib have found limited effectiveness in the clinic. Tipifarnib has advanced to phase 3 clinical trials as monotherapy and shows indications for treatment of blood and breast cancers (76, 104). In phase 1 and 2 colorectal and pancreatic clinical trials with tipifarnib or lonafarnib, there was little clinical effectiveness obtained; these cancers have high incdence of K-Ras mutations which can be alternatively GG'd (19). As these cancers already have a dependence on K-Ras, increased Ras signaling is likely to not have an anti-proliferative effect on the cancer cells, which could explain their limited clinical effectiveness.

In a phase II trial, tipifarnib induced disease stabilization of more than 60% of patients with advanced myeloma (98). These patients had inhibited FTase activity and HDJ-2 farnesylation in peripheral blood mononuclear cells (PBMCs). They also determined GGTase activity after three weeks of tipifarnib treatment and 6 of the 8 samples analyzed had increased GGTase activity, however no correlation of this activity was found with patient response. They examined activation of AKT, ERK, and Stat3 in 4 samples and found a correlation with decreased pAKT with stable disease. To identify potential correlations between increased GGTase activity and Ras downstream effectors, a larger cohort with a complete data set would need to be analyzed.

Tipifarnib was administered orally 2X daily, 300mg, in 21 patients with myelodysplastic syndrome (MDS) for three weeks on followed by one week off for 8 weeks (105). Patient PBMCs were collected and analyzed for HDJ-2 inhibition, AKT / ERK activation status by immunoblot, and FTase 1 / GGTase 1 enzyme activities. Unfortunately not

enough samples could be completely analyzed for all of these substrates. The investigators did find in 9 of the samples tested for GGTase activity, 4 had increased activity, 4 had no significant effect, and 1 patient had decreased GGTase activity (105). Of these samples where GGTase activity was measured, three patients also had accompanying phosphorylated AKT and ERK analysis. Only one of these was a partial responder; that patient had a slight increase of GGTase activity (20% after 7 days tipifarnib treatment), and an increase in phosphorylated AKT but no detectable phosphorylated ERK. Based on the low number of complete analysis of patient data, no implications between increased GGTase activity and tipifarnib response could be made.

Breast cancers are not known to contain Ras mutations, but often have activation of HER2 RTK, which is upstream of Ras signaling, and therefore may be sensitive to tipifarnib treatment (106, 107). In a phase 1 clinical trial, breast cancer patients were treated with the single agent tipifarnib. A correlation of response with tipifarnib treatment in HER2+ tumors was seen in 6 of 9 responders (106). Tipifarnib in combination with tamoxifen synergistically inhibits MCF-7 breast cancer cell proliferation and cell cycle progression *in vitro* and *in vivo* (108). Combinational therapy studies for breast cancer patients with tipifarnib and tamoxifen are underway.

Two Phase 1 trials have been conducted treating children with solid tumors with tipifarnib, including a phase 1 trial in children with refractory solid tumors or Neurofibromatosis type 1 (NF-1). Tipifarnib was administered 2X daily for 21 days repeated every 28 days starting at 150 mg up to 375 mg twice daily (103). PBMCs were collected and FTase activity and HDJ-2 farnesylation were determined. Tipifarnib plasma concentration peaked in 2 hours; after 12 hours tipifarnib concentration was 3.3% of the maximum concentration, suggesting drug accumulation would be minimal. Due to disease progression many patients left the trial. Phase 2 studies in NF1 patients are underway. Another Phase 1 trial with tipifarnib was done in newly diagnosed diffuse intrinsic brainstem gliomas (BSG) (101). External beam radiation therapy was administered concurrently with tipifarnib, followed by adjuvant tipifarnib for up to 24 months. One year survival and progression free survival were 36.4 and 9.4%, respectively (101). Phase 2 trials in BSG's indicated no clinical advantage over historical controls (109).

Potential Markers of Response

Raponi et al. found that expression of RASGRP1, a guanine nucleotide exchange factor (GEF) that activates Ras, predicted sensitivity to tipifarnib treatment in gene expression profiles of bone marrow (BM) samples from AML patients (110). They report that RASGRP1 normally activates N-Ras and H-Ras at the Golgi, but blockage of H-Ras by FTI may be responsible for some anti-tumor effects. The gene expression ratio of increased *RASGRP1* and decreased *APTX* (aprataxin) (involved in DNA excision repair) was found to predict response to tipifarnib in newly diagnosed AML patients. This observation was also seen in 3 AML and 3 T-cell ALL cell lines. The correlation between the growth inhibition mediated by tipifarnib (IC_{50}) and the *RASGRP1* and *APTX* expression ratio was found to be 0.94, confirming the microarray and expressional profiling analysis of patient samples. Additionally, a gene expression profiling of 58 relapsed or refractory AML patients identified that lymphoid blast crisis oncogene, *AKAP13*, which predicted response rate to tipifarnib. AKAP13 is a GEF which activates Rho proteins. This gene had a negative predictive value for response to tipifarnib and was over expressed in patients who were resistant to tipifarnib therapy (111). When AKAP13 was expressed in HL60 and THP1 cell lines, it increased resistance to tipifarnib by 5- or 7- fold respectively.

Targeted specific therapies are rapidly being developed for clinical use. Some therapies such as imatinib have produced great outcomes in the clinic, however patients develop resistance to this therapy. Mutations in BCR/ABL have been identified in patient samples which become resistant to imatinib therapy (112, 113). To determine if mutation of FTase could potentially contribute to resistance of FTI, a series of mutations were made to FTase β and transduced into BaF3 K-Ras61L expressing cells (114). WT and mutant FTase β cells were treated with increasing concentrations of lonafarnib. Six of the nine mutants were able to form colonies when treated with 1 μM lonafarnib, 4 of which still formed significant colonies after 10 μM. Clonogenic abilities correlated with immunoblot analysis of HDJ-2 farnesylation, in which HDJ-2 was farnesylated even with lonafarnib treatment in FTase mutant cells. This result suggests that lonafarnib is not able to block FTase activity and the FTase mutant cells have become drug resistant. FTase mutations were also identified in patient samples, but a correlation with drug resistance was not identified. Analysis of FTase β mutational status is important in clinical trial design and may identify patient cohorts who are likely to be resistant to FTI.

No correlation between response to FTI and Ras mutational status have been identified. It is important to note that all mutations in Ras genes do not always result in oncogenic Ras, as we show in OS187, which has a K-Ras mutation in codon 61, but has low endogenous Ras activity (Chapter 3). It is assumed that mutations in Ras result in over activation of Ras. However, this is not always true. This finding supports our hypothesis that low endogenous Ras activation, and not its mutational status, is what contributes to response to FTI. Combinational therapy studies for FTI are increasing, but the mechanism of action of these drugs need to be determined to identify which patients would benefit from FTIs in the clinic.

Goal of Dissertation

Ras is commonly over activated in cancer, and of the four Ras proteins K-Ras B has the highest frequency of mutations. The four highly homologous Ras proteins create distinct signaling outputs despite interacting with a common set of effectors. These different signaling outputs are based on the post-translational modifications associated with each Ras protein within their hypervariable region. N- and K-Ras B can alternatively be GG'd if farnesylation is inhibited. These post-translational modifications associated with Ras determine the localization of each individual Ras species within a cell. The four Ras proteins associate with different and specific GAPs/GEFs, scaffolding proteins, and effector proteins; these protein interactions are dependent on where each Ras species is localized within the cell and the interacting proteins which are available in that region. These four proteins have distinct signaling outputs associated with them which are due to differential localizations and protein interactions. Protein signaling interactions with each of these Ras proteins has been extensively studied. How post-translational modifications can determine the localization of the Ras proteins has also been studied. However, the effect on cellular signaling due to alternatively geranylgeranylating N- and K-Ras has not been studied.

K-Ras B is mutated in over 90% of pancreatic cancers and over 60% of colorectal cancers. Farnesyltransferase inhibitors (FTIs) were designed to inhibit Ras signaling. No clinical effectiveness was found in these cancer types with FTIs. Clinical effectiveness of FTIs as monotherapy has been identified in blood cancers which commonly have N-Ras mutations, breast cancers which commonly have WT Ras, and cancers which have mutated H-Ras. Patient response to FTIs has not been found to be correlative to Ras mutational status. The lack of response of tumor types with mutated K-Ras led to the discovery of alternate prenylation of N- and K-Ras. H-Ras is not alternatively GG'd and therefore its activity is completely blocked by

FTI. Without a correlation of response with Ras mutational status, many researchers then disregarded Ras as a major contributor of response to FTI. Clinical effectiveness has been identified in cancers which do not have mutant K-Ras mutations and may have mutant N- or H-Ras mutations. Therefore, in diseases with Ras mutations, Ras mutational status would not be correlative to patient response, as we predict only cancers that have high K-Ras signaling will not respond to FTI therapy. Although most patients with pancreatic and colorectal cancer have K-Ras mutations we predict that the patients who do not have high levels of K-Ras signaling would still respond to FTI treatment.

We wanted to identify what effect FTIs had on tumor cell lines with low levels of endogenous active Ras. Our results show FTI reduced cell yield and increased cell cycle arrest in tumor cell lines that have low levels of active Ras. Next, we wanted to determine if cell death and cell cycle arrest from FTIs was from inhibiting the farnesylation of proteins or from a gain of alternatively geranylgeranylating proteins, specifically K-Ras. We used 293T cells, which are easily transduced, to determine if reduced cell yield and viability from FTI was from inhibiting farnesylation or from a gain in GG'd proteins. Our results show FTI reduced cell yield and viability and that both of these responses are partially due to increased GG'd proteins.

Our results show FTI increased active Ras, increased downstream MAPK effector proteins, and N- and K-Ras are both alternatively GG'd in 293T and tumor cell lines. These results collectively demonstrate the activity of GG'd N- and K-Ras are increased with FTI. N-Ras preferentially activates AKT signaling to provide pro-survival signals to cells, while K-Ras normally activates ERK signaling. Activation of ERK signaling can provide either pro-survival or cell death signals and which outcome occurs depends on the strength of signal and the duration of activation of this MAPK pathway. We predict cells which have endogenously high levels of K-Ras and ERK signaling will not respond to FTI. Therefore, we predict that even if K-Ras is mutated in a cell line or patient if the endogenous protein levels of ERK signaling is low we predict this cell line or patient will respond to FTI.

Combining our results with current knowledge about Ras and FTI our hypothesis is: **FTI activates GG'd K-Ras which results in reduced cell viability and cell cycle arrest in cell lines that express low endogenous active Ras** (Figure 4)**.**

Figure 4

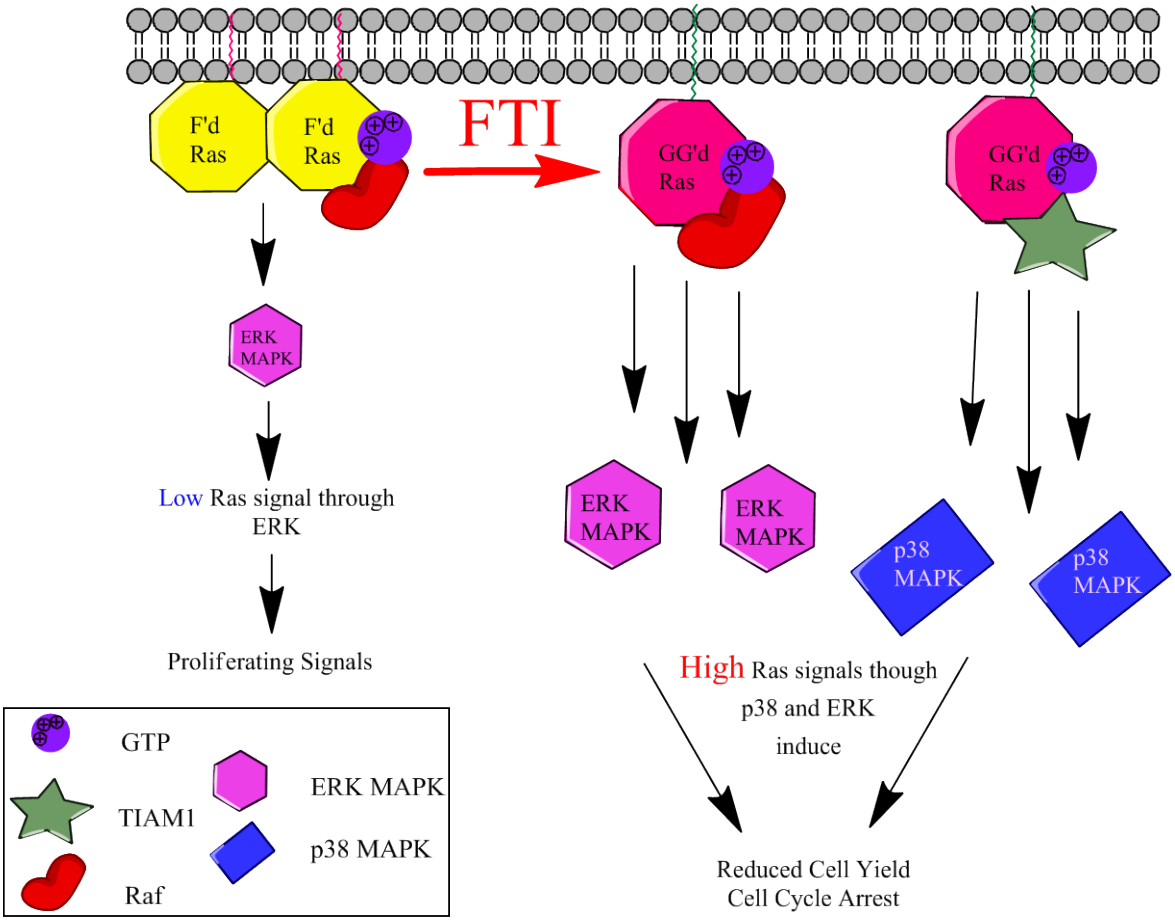

Figure 4. Hypothesis: FTI increases GG'd K-Ras to reduced cell yield and induce cell cycle arrest. FTI increases GG'd Ras which increases ERK and p38 MAPK signaling in tumorigenic cells with low endogenous active K-Ras to reduce cell yield and increase cell cycle arrest.

CHAPTER 2. Materials and Methods

Cell culture and experimental reagents.

Human osteosarcoma cell lines were maintained as follows: CCH-OS-M and CCH-OS-D cells were grown in Dulbecco's modified Eagle medium (DMEM) high-glucose 1X media (Invitrogen, Carlsbad, CA) with 10% fetal bovine serum (FBS) (HyClone, Logan, UT), 1% penicillin-streptomycin solution (Gemini Bio-Products, Woodland, CA), and 1% l-glutamine (Lonza, Walkersville, MD). Colorectal cell line OS187, neuroblastoma cell line COL, and normal kidney fibroblasts 293T (purchased from ATCC) were maintained the same as the human osteosarcoma cell lines. COL, CCH-OS-M, and CCH-OS-D cells were given additional 1% insulin transferrin selenium-A solution (Invitrogen) for initial growth of cell lines. SaOS2, LM7, and HOS osteosarcoma cell lines were grown in Minimal modified Eagle medium with 10% FBS, 1% penicillin-streptomycin, 1% l-glutamine, 1% MEM essential vitamins (Lonza), 1% sodium pyruvate (MP Biomedicals, Solon, OH), and 1% non-essential amino acids mixture (Cambrex Biosciences, East Rutherford, NJ). AML cell lines THP-1 and U937 (a kind gift from Dr. Patrick Zweidler-McKay, were maintained in RPMI high-glucose 1X media (Invitrogen), with 10% FBS and 1% penicillin-streptomycin. All cells were incubated in a humidified atmosphere at 37°C with 5% CO_2.

SaOS2, LM7, and HOS are long-term, established osteosarcoma cell lines. CCH-OS-M and CCH-OS-D are primary osteosarcoma cell lines derived from patients at the Children's Cancer Hospital at The University of Texas M. D. Anderson Cancer Center. CCH-OS-D was obtained from a core needle biopsy of a proximal femur lesion in an 18-year-old boy who also presented with pulmonary metastases. CCH-OS-M was obtained from a 15-year-old boy with recurrent pulmonary and pleural osteosarcoma 13 months after diagnosis of right proximal humerus osteosarcoma malignant effusion.

Chemicals: Tipifarnib (Johnson & Johnson, Langhorne, PA) and GGTI-298 (CALBIOCHEM, San Diego, California) were dissolved in dimethyl sulfoxide as 10 mM stock solutions.

Analysis of Downstream Ras targets: OS187, COL, SaOS2, and 293T cells were plated in 10-cm dishes, grown to 60% confluence, and then exposed to tipifarnib at the following concentrations for 24 hours: 0, 0.01, 0.1, and 1 μM. SaOS2 cells were additionally treated with 1 μM tipifarnib for 48, 72, and 96 hours.

N- and K-Ras alternate prenylation: OS187, COL, SaOS2, and 293T cells were plated in 10-cm dishes and grown to 60% confluence and then exposed to 1 μM tipifarnib, 4 μM GGTI-298, no drug, or both 1 μM tipifarnib and 4 μM GGTI-298 for 24 hours.

Western blot analysis

Lysates were collected as follows: The medium was removed, plates were washed with cold PBS, and 1 mL of lysis buffer [1% Triton X-100, 50 nmol/L Hepes (pH 7.4), 150 nmol/L NaCl, 1.5 nmol/L MgCl2, 1 mmol/L EGTA, 100 nmol/L NaF, 10 nmol/L NaPPi, 10% glycerol, 1 nmol/L phenylmethylsulfonyl fluoride, 1 nmol/L Na3VO4, whole protease inhibitor tablets (complete mini, Roche Diagnostics), and phosphatase inhibitor cocktail 2 (Sigma)], was added to each plate, and plates were incubated on ice for 35 minutes. The plates were then scraped with a cell scraper; lysates were collected into eppendorf tubes and centrifuged at 10,000 rpm for 10 minutes to precipitate DNA, RNA, and cell membranes. Protein concentrations were determined by bicinchoninic acid (BCA) analysis (Thermo Scientific, Pittsburgh, PA). Whole cell lysates were separated by SDS-PAGE on a 12% or 15% polyacrylamide gel and transferred to nitrocellulose membrane according to standard techniques. Membranes were probed with use of the following antibodies:

Rabbit Antibodies	Mouse Antibodies
1:4000, GE Healthcare Horseradish peroxidase–conjugated anti-rabbit IgG (NA934)	**1:5000, BD Biosciences, San Jose, CA** Horseradish peroxidase-labeled polyclonal anti-mouse IgG (554002)
1:1000, Cell Signaling, Danvers, MA phoshpo-44/42 MAPK Thr202/204 (9102) MEK1/2 (9122) phospho-MEK 1/2 Ser 217-221 (9121S) phospho-p38 MAPK Thr 180/Tyr182 (9211) p38 MAPK (9212) phospho-MKK3/6 Ser189/207 (9236) MKK3 (9232) phospho-MSK1 Thr581 (9595) phospho-ATF-2 Thr71 (5112) phopho-AKT Ser 473 (9271) AKT (9272) pan Ras (3965) phospho-p53 Ser6 (92845) p53 (7F5) (2527) p 21 Waf1/Cip1 (12D1) (2947)	**1:1000 Thermo Scientific** HDJ-2 (MS-225)
	1:200 Santa Cruz, Santa Cruz, CA K-Ras (sc-30) N-Ras (sc-31) Cyclin B (sc-245)
	1:1000, Cell Signaling, Danvers, MA Cyclin A (BF683) Cyclin D (DCS6) Cyclin E (HE12)
1:1000, Promega, Madison, WI MAPK/ERK (17925803)	**Goat Antibodies**
1:1000 Millipore, Billerica, MA Rap-1 (07-916)	**1:4000, Santa Cruz, Santa Cruz, CA** Horseradish peroxidase Donkey anti goat IgG (sc-2020)
1:1000, Sigma, TX Actin (A2066)	1:1000 GGTβ (sc-20)
Santa Cruz, Santa Cruz, CA FTβ (sc-137)	**Nuclear Stain for Immunofluorescence**
1:1000 GeneTex Inc, TX N-Ras (GTX108598) K-Ras (GTX100636)	**1:10,000 Invitrogen** SYTOX Green Nucleic Acid Stain (S7020)

Chemiluminescent signal was detected by the Immobilon Western Blotting detection system (Millipore).

Ras activity

OS187, COL, SaOS2, and 293T cells were plated in 10-cm dishes, grown to 80% confluence, and then exposed to 0.01 μM, 0.1 μM, or 1 μM tipifarnib or no drug. LM7, HOS, CCH-OS-M, CCH-OS-D, THP1, and U937 were treated with 0 μM and 1 μM. Lysates were collected and GTP-bound Ras was pulled down with Ras binding domain (RBD) bound to agarose beads. Lysates were resuspended in a 2X sample buffer and run on an immunoblot.

FTβ and GGTβ shRNA; K-Ras and N-Ras WT and Mutants

Stably transduced shRNA or N- and K-Ras constructs were plated in 10-cm dishes, grown to 80% confluence. Scrambled control and GGTβ shRNA were untreated or treated with 0.01 μM tipifarnib and lysates were produced.

Lysates were generated as mentioned above, and 1.5 mg/ml of protein was used for the Ras activity assay (Cell Biolabs Inc, San Diego, CA, STA-400). Immunoprecipitation and immunoblotting were conducted according to the manufacturer's directions.

Cell viability assay

OS187, COL, SaOS2, and 293T cells were plated in 6-well tissue culture plates at a density of 100,000 cells/well. The following day, tipifarnib was added to achieve the following concentrations: 0 μM, 0.01 μM, 0.1 μM, and 1 μM. Triplicate samples were treated at each concentration and time point. Untreated cells were analyzed on the day the drug was added as a starting point. Cell nuclei were counted at 96 hours or one week for SaOS2 cells as follows: the medium was removed from the plates and the cells washed with 2 ml of PBS. Cell nuclei were released from intact, nonapoptotic cells as follows: 0.5 ml of 0.01 M HEPES/0.015 M $MgCl_2$ buffer was added, and cells were shaken for 5 minutes at room temperature to equilibrate. After equilibration, 50 μl of 0.132 M Bretol with 0.525 M glacial acetic acid was added, and the cells were shaken for 10 minutes at room temperature, lysing the plasma membrane but leaving the nuclear membrane intact. A solution consisting of 3.5 ml of 0.9% NaCl and 0.5% formalin was added to fix the nuclear membranes, and 2 ml of the solution containing the nuclei was placed into an autosampler cup. Nuclei were counted by using an automated Vi-Cell Cell Viability Analyzer (Beckman Coulter, Fullerton, CA) which identified nuclei with a size between 5 and 25 μm.

To determine if duration of drug treatment affected growth of OS187, cells were plated as described above and treated with 1 μM tipifarnib for 24, 48, 72 or 96 hours. At earlier time points media with drug was removed and replaced with fresh DMEM media. After 96 hours nuclei were isolated and counted as described above. Additionally cells were treated for 96 hours where the media and drug was replaced with fresh media for 72 hours or continuously treated for one week, nuclei were isolated and counted.

Diameter of Cells

OS187 cells were treated with 0.01, 0.1, or 1 μM tipifarnib for 48 hours. Cells were trypsinized and the circumference of the untreated and treated cells were measured on an

automated Vi-cell Coulter cell counter. For this purpose we did want to use live cells in order to determine the size difference between FTI-treated and untreated OS187 cells. This cell counter automatically determines the diameter of each cell that it counts.

Cell cycle analysis

Tipifarnib treatment

OS187, COL, and SaOS2 cells were cultured and treated with tipifarnib as described above for 72 hours. Dead and live cells were collected and incubated overnight at 4ºC with 0.005% propidium iodide, 0.1% Triton X100, diluted in PBS. Cells were analyzed on a FACSCalibur flow cytometer (Becton Dickinson, Franklin Lakes, NJ).

Short hairpin RNA

Designing oligonucleotides for OS187 and SaOS2

Hairpin structures predicted to anneal to RNA of the β subunit of farnesyltransferase (FTβ; see Results for discussion of FTβ) were designed with use of software provided by Invitrogen). Two structures were used:

1011 predicted to anneal to the 5′ UTR

top strand

5′-gatctGCGATTTGAAGGAGGATTTCACGAATGAAATCCTCCTTCAAATCGCttttttC-3′,

Bottom strand

5′tcgagAAAAAAGCGATTTGAAGGAGGATTTCATTCGTGAAATCCTCCTTCAAATCGCa-3'

1927 predicted to anneal to the ORF

top strand

5′-gatctGGTCCCACCAAGATGAGTTCTCGAAAGAACTCATCTTGGTGGGACCttttttC-3′,

bottom strand 5′-

tcgagAAAAAAGGTCCCACCAAGATGAGTTCTTTCGAGAACTCATCTTGGTGGGACCa-3′

Oligonucleotide strands were from Sigma (St. Louis, MO).

Annealing oligonucleotides

Single-stranded oligonucleotides were self-annealed to generate a hairpin structure. The annealing buffer was 100 mM NaCL and 50 mM HEPES (pH 7.4). 1µl of 3 mg/ml stocks of top and bottom strand oligonucleotides were incubated with 48 µl of annealing buffer at the following temperatures for 4 minutes each: 94, 80, 75, 70, 65, 60, and 55°C. The mixture was incubated at room temperature for 1 hour and at 4°C for 20 minutes. To generate a retroviral expression system for short hairpin RNA (shRNA) expression, the MigR1 (MigR1 is a MSCV-

IRES-EGFP retroviral construct) (115), coexpressing GFP as a selection marker, was manipulated to contain a U6 promoter upstream of the hairpin sequence; this vector is now termed MigU6. Hairpins were ligated into retroviral vector MigU6 by using a standard T4 ligation reaction.

FTbeta and GGTbeta shRNA transduced into 293T cells

Scrambled control, FTβ (TRCN0000034624), and GGTβ (TRCN0000187927) shRNA pLK0.1-puro-CMV-TagCFP lentiviral constructs were purchased from Sigma.

p53 shRNA transduced into OS187

Scrambled and TP53 (TG320558) shRNA pGFP-V-RS retroviral plasmids were purchased from OriGene Technologies, Inc (Rockville, MD).

Retroviral transduction

MigU6 empty vector, scrambled control, 1011, or 1922 were used to make replication-incompetent retrovirus, which was then used to infect OS187 and SaOS2. pGFP-V-RS with scrambled or TP53 shRNA were used to make replication-incompetent retrovirus, which was used to infect OS187 cells.

To generate virus, 293T cells were seeded initially at a density of 140,000 cells/well in a 6-well dish. After 24 hours, the following were incubated for 5 minutes: Tube A, 2 µg of MigU6 or pGFP-V-RS vectors, 2 µg of VSVG, 2 µg of PCGP (kind gifts from Dr. Patrick Zweidler-McKay), and 250 µl Opti-MEM (Invitrogen); tube B, 12 µl of lipofectamine (Invitrogen); and 250 µl Opti-MEM. The contents of tubes A and B were then combined and incubated at room temperature for 30 minutes; 500 µl of the complex was then added to one well of 293T cells. After 8 hours, the complex was removed, fresh medium was added, and the plate was incubated in a humidified atmosphere at 32°C with 5% CO_2. Supernatant was collected at 24 hours and centrifuged at 2,500 RPM for 2 minutes. Next, 2.5 ml of viral supernatant and 8 µg/ml Polybrene (Sigma) were added to the OS187 and SaOS2 cells. These plates were centrifuged at 2,500 RPM for 1 hour and then incubated at 32°C for 24 hours. Next, the viral medium was removed and fresh medium added. By 48 hours after the initial virus exposure, infected cells had begun to express virally encoded genes and could be selected. Cells were sorted for GFP twice to generate a polyclonal population of transduced cells.

Lentiviral Transduction

Scrambled, FTβ, or GGTβ shRNA lentiviral particles had a titer of 1.6 X 10^7 TU/ml. 293T cells were plated at 60% densitiy, 12.5 µl of lentiviral particles were added to 1 ml

DMEM media with 10% FBS to a single well in a 6-well tissue culture plate. These plates were centrifuged at 2,500 RPM for 1 hour and then incubated at 32°C for 8 hours. Next, the viral medium was removed and fresh medium added.

Assays with Transduced shRNA Cells

Lysates were generated from FTβ shRNA retrovirally transduced in OS187 and SaOS2, lentiviral FTβ and GGTβ shRNA transduced into 293T cells, and TP53 shRNA transduced in OS187. Ras activity was assayed as described above. Parallel samples of lysates were tested by immunoblotting for FTβ, GGTβ, or p53 and respectively and knockdown was confirmed by densitometric analysis (Image J Processing software, NIH).

293T cells transduced with scrambled control, FTβ, GGTβ shRNA were plated in 6-well tissue culture plates at a density of 50,000 cells / well. The following day 0, 0.01, or 0.1 μM tipifarnib was added to triplicate wells for each of the transduced constructs. Cells were grow in normal tissue culture conditions for 3 days and counted on an automatic Coulter counter (described above).

293T cells transduced with scrambled control or GGTβ shRNA were plated in 6-well tissue culture plates. The following day triplicate wells were treated with 0, 0.01, or 0.1 μM tipifarnib. After 48 hours live and dead cells were collected and stained with propidium iodide and cell cycle was analyzed (described above).

Clonogenic Assays

Anchorage-dependent growth

1,000 OS187 and 4,000 SaOS2 cells were plated and grown in 0.01, 0.1, or 1 μM tipifarnib for 3 weeks. Fresh media and drug were refreshed weekly. After 3 weeks of growth media was removed and colonies were stained with 0.05% crystal violet. Colonies counted are representative of 50 or more cells.

Anchorage-independent growth

A 50/50 mixture of 1% soft agar and 2X DMEM with 20% FBS with the above concentrations of tipifarnib was solidified in 24 well plates. 10,000 COL and OS187 cells and 40,000 SaOS2 cells were mixed with a 1:1 mixture of 0.1% agar with corresponding concentrations of tipifarnib. Treatments were plated in triplicate. Fresh media with corresponding tipifarnib concentrations were refreshed to the top agar after one week. After 2 weeks topical media with tipifarnib was removed and colonies were stained with 0.05% crystal violet. Colonies were counted under 20X magnification using a light microscope.

Invasion assay

The invasiveness of SaOS2 cells with or without tipifarnib treatment was measured in a BD Matrigel invasion chamber. Cells were treated with 0.01, 0.1, or 1 μM tipifarnib for 48 hours before plating in chambers. 40,000 cells per well with SaOS2 and 20,000 OS187 cells per well were plated in the upper chambers in triplicate with the same concentration of drug added to the upper and lower chamber. Triplicate samples were averaged. Invasive cells were counted after 48 hours. Membranes from the Matrigel invasion chambers were stained according to the manufacturer's instructions, and invading cells were counted under 20X magnification.

BrDU

OS187 cells were plated at a density of 50,000 cells per well in 6-well tissue culture dishes. The following day 0, 0.001, or 0.1 μM tipifarnib was added to wells in triplicate. 48 hours later cells were stained according to the manufacturer's instructions using a BrdU flow kit (559619) purchased from BD Biosciences. Actively proliferating cells in S-phase of the cell cycle are stained in this process.

Images of OS187 cells

OS187 cells were treated with 0.01, 0.1, or 1 μM tipifarnib. Images were taken after 48 hours with a phase-contrast light microscope.

To determine if duration of tipifarnib treatment affected OS187, cells were treated with the above concentrations for 24 hours or continuously for 2 weeks. Cells that were treated for 24 hours had media with drug removed and replaced with fresh media. Continuous treated cells had fresh media and drug replaced every 4 days or when cultured. Cells were cultured when they became confluent. Images were taken from all treatment concentrations treated for 24 hours or continuously at days 3, 4, 5, and 6 and again after 2 weeks.

Cells that were treated with each concentration for 24 hours, one week, or two weeks were grown for three weeks and retreated with tipifarnib for one week or 4 days (indicated in Figure 18). Images were taken with a phase-contrast light microscope.

β-galactosidase Staining

OS187 cells were plated in 6-well dished and treated with 0.001, 0.01, or 1 μM tipifarnib continuously for 2 weeks. Fresh media and drug was replaced after one week. Media was removed and cells were fixed and stained according to the Senescence β-galactosidase staining kit purchased from Cell Signaling (9860).

Cloning of WT and mutant N-Ras and K-Ras

For WT N-Ras or K-Ras, two vectors were created. One with only a puromycin selection and another with puromycin and mKate fused to the N-terminus of WT N-Ras and K-Ras.

The MipR1-mKate2 was generated from MigR1, pPUR (6156-1, Clontech Laboratories, Inc.), and pCMV6-AC -mKate vector (ps100039, Origene). First, MigR1 vector was digested with NcoI and SalI for remove GFP coding sequence. The Puromycin resistance gene was PCR amplified by using the pPUR plasmid as template. A NcoI restriction site was added to the 5' prime end, an XhoI (compatible with SalI) site was added to the 3 prime end. The puromcyin-resistant insert was cloned downstream of internal ribosome entry site (IRES) to create MipR1. Then the MipR1 vector was digested with BglII and XhoI. mKate2 far-red fluorescent coding sequence was PCR amplified by using the pCMV6-AC-mKate as template, and BamH1(Compatible with BglII) was added to the 5 prime end, and XhoI was added to 3 prime end, this PCR amplified product was digested with BamH1 and XhoI. The mKate2 insert was ligated into the MipR1 vector to create the MipR1-mKate2-C vector. This vector has puromycin selection marker and expresses mKate2 far-red fluorescent in mammalian cells and generates of fusion protein to the mkate2 C-terminus. The multiple cloning sites are BglII, XhoI and EcoR1.

Mutant N- and K-Ras

Plasmid pCMV6-Entry-N-Ras and Plasmid pCMV6-Entry-K-Ras were purchased from Origene (RC202681, RC201958). The MipR1-mKate2 vector was digested with BglII and EcoR1. The N-Ras and K-Ras plasmids were digested with BglII and MfeI (compatible with EcoR1), and ligated into the mipR1-mKate2-C vector to create MipR1-mKate2-NRas-WT or MipR1-mKate2-KRas-WT. MipR1-mKate2-K-Ras or N-Ras reverse primers contain base pairs to create mutations in N-Ras and K-Ras. Primers for mutagenesis are listed below.

K-Ras-F-BglII: gcagccAGATCTatgactgaatataaacttgtggtagttg

K-RAS-R-mfeI: CGCGCCAATTGTTACATAATTACACACTTTGTCTTTGA

K-RAS-CAIL-R-mfeI: CGCGCCAATTGTTACAAAATTGCACACTTTGTCTTTGA

K-RAS-CVLS-R-mfeI: CGCGCCAATTGTTACGAAAGTACACACTTTGTCTTTGA

K-RAS-CYS-SER-R-mfeI: CGCGCCAATTGTTATTTAAGTACAGACTTTGTCTTTGA

N-Ras-F-BglII: gcagccAGATCTatgactgagtacaaactggtggtg

N-Ras-R-mfeI: CGCGCCAATTGTTACATCACCACACATGGCAATCC

N-Ras-CAIL-R-mfeI: CGCGCCAATTGTTACAATATCGCACATGGCAATCC

N-Ras-CVLS-R-mfeI: CGCGCCAATTGTTACGACAACACACATGGCAATCC

N-Ras-CYS-SER-R-mfeI: CGCGCCAATTGTTATTTCAACACAGATGGCAATCC

We used polymerase chain reaction (PCR) to create mutant constructs with PfuUltra High-fidelity DNA Polymerase (Agilent Technologies Inc.). PCR reaction conditions are indicated below.

1. 10× *PfuUltra* HF reaction buffer	5µl
2. 10mM dNTP Mix	1µl
3. Forward Primer (10µM)	1µl
4. Reverse Primer (10µM)	1µl
5. DNA template 80µg/µl	1µl
6. *PfuUltra* HF DNA polymerase (2.5 U/ µl)	1µl
7. DH2O	40µl
Total	50µl

Temperature	Time	
94º C	1 min	
94º C	30 sec	30 cycles
56º C	30 sec	
72º C	1 min	
72º C	10 min	
4º C	∞	

Transduction/ Selection

Retrovirus packaging GP2-293 cells (631530, Clontech) were cultured in DMEM (11995, Gibco) with 10% FBS (HyClone, ThermoScientific), at 37°C in 5% CO2. The incubating temperature reduced to 34°C after the packaging cells were transfected with MipR1-mKate-Ras expression plasmids and pVSV-G (Clontech) by using lipofectamin 2000 (6-well tissue culture plates, 4 µg expression vector, 0.8 µg pVSV-G, 10 µl lipofectamin for each well). Viral supernatants were collected after 40 hours incubation the supernatants were centrifuged at 1500 RPM for 10 minutes. The viral supernatant and 8 µg/ml of polybrene was added to 293T cells plated at a confluence of 60%. These plates were centrifuged at 2600 RPM for 1 hour and then incubated at 34°C for 24 hours. Viral supernatant was removed after 24 hours and cells were replated with regular media and incubate in 37°C for an additional 24 or 48 hours, then sorted for mKate expression with BD Influx Cell Sorter (South Campus Flow Cytometry Core).

Transfection

293T cells were transfected with MipR1-mKate2 empty vector (1) or N-Ras (4) or K-Ras (4) WT and mutant constructs (total of 9 constructs). 293T cells were seeded at a density of 140,000 cells/well in a 6-well dish. After 24 hours, the following were incubated for 5 minutes: Tube A, 3.5 µg of MipR1-mKate2 vectors and 250 µl Opti-MEM (Invitrogen); tube B, 7 µl of lipofectamine (Invitrogen) and 250 µl Opti-MEM. The contents of tubes A and B were then combined and incubated at room temperature for 30 minutes; 500 µl of the complex was then added to one well of 293T cells. After 8 hours, the complex was removed, fresh medium was added, and the plate was incubated in a humidified atmosphere at 32°C with 5% CO_2.

MipR1 verses MipR1-mKate2

293T cells transduced with an empty puromycin vector (MipR1), a puromycin and mKate empty vector (MipR1-mKate2), or both of these vectors fused to WT N-Ras or K-Ras (MipR1-Ras WT or MipR1-mKate2-Ras WT). Cells were selected in puromycin for 5 days as this was the length of time necessary to kill untransduced 293T cells. Cells then plated in 10 cm dishes, grown to 80% confluence, and lysates were made. Lysates were used for the Ras activity assay (described previously).

FACS sorting

MipR1-mKate N-Ras and K-Ras WT were transduced into 293T cells. Following 5 days of puromycin selection these cells were sorted and collected as three separate populations low, medium, and high mKate fluorescent signal. These sorted cells were treated with 3X gentamicin and penicillin / streptomycin media for 3 days to ensure they were not contaminated from the sorting machinery. These cells were then plated in a 10 cm tissue culture dish and allowed to grow to 80% confluence. Lysates were collected and used for a Ras pull down assay. Cells with low, medium, and high mKate fluorescent intensity were also plated in 6-well dishes and treated with 1 µM tipifarnib in combination with 4 µM GGTI-298 for 48 hours. Lysates were collected, run on an immunoblot, and probed with N- or K-Ras (GeneTex Abs), respectively.

WT and mutant N- and K-Ras constructs were cloned into MipR1-mKate2 and transduced as described above. Stably transduced cells were sorted with the BD Influx Cell Sorter and positive cells were treated with 3X gentamicin and penicillin / streptomycin media for 3 days to ensure they were not contaminated from the sorting machinery. Positively

transduced cells were then plated in 10 cm dishes or 6-well plates for a Ras activity assay or cell viability assay, respectively.

Percent mKate positive population

293T cells were transduced with MipR1-mKate2 N-Ras and K-Ras constructs and sorted 2, 5, 7, 9, and 14 days post transduction. Cells were not treated with puromycin. mKate fluorescence intensity was measured over time using Flowjo software.

Percent dead and/or dying population

Transduced/transfected MipR1-mKate2 N-Ras and K-Ras cells were analyzed using Forward Scatter (FSC) verse Side Scatter (SSC) allows for determination of two rough populations: a live population which normally represents the bulk of cells and a dead or dying population of cells. As a cell is dying, normally its granularity increases and then decreases and their size decrease. Granularity is measured by SSC and the relative size of the cell is measured by FSC. A dot plot with SSC on the y-axis and FSC on the x-axis allows for determining a live and dead and/or dying population.

Immunofluorescence

Stable transductions from the positive cells from the 48 hour post transduction sort were plated in 4 well chamber slides at a density of 30,000 cells per well in normal tissue culture conditions. Media was removed after 48 hours and cells were fixed with 4% paraformaldehyde (PFA) for 10 minutes. The cellular membranes were then permeablized with 0.2% TritonX100 for 5 minutes. Nuclei were stained with Sytox green (1:10,000) for 10 minutes. All reagents were dissolved in PBS. Slides were mounted with n-propyl gallate antifade solution and a cover slip. Images were taken on a confocal microscope.

Statistics

Significance was assessed by Student's t-test (Statistica Software) with an alpha error threshold of 0.05. All experiments were conducted at least three times unless otherwise stated.

CHAPTER 3: Reduced cell yield and cell cycle arrest from FTI are partially due to an increase of geranylgeranylated proteins.

Rationale

Farnesyltransferase inhibitors (FTIs) are effective at inhibiting the growth and metastasis of some tumors. However, the mechanism of how farnesyltransferase inhibitors reduce growth and metastasis of these tumors has yet to be discovered. Most groups researching FTIs analyze the effects of inhibiting farnesylation of proteins including Ras, RhoB, CENP-E, CENP-F, and the Lamins A/C. Cell cycle arrest in G2/M is one of many common effects seen as a response to FTI in multiple disease cell lines (including cancer) (19, 81). Inhibition of farnesylation of CENP-E has been implied to be associated with the arrest at G2/M (81, 96, 116). CENP-E needs to be farnesylated to associate with microtubules and the microtubule-kinetochore interaction is important for passage through the G2/M checkpoint. However inhibition of farnesylation did not affect CENP-E's association with the kinetochore. The consequences of inhibiting farnesylation of CENP proteins and the association with G2/M arrest remains controversial (19, 77, 90). It is highly possible that inhibiting farnesylation of many proteins contribute to the antineoplastic responses of FTI. All reports that identify specific anti-tumor functions associated with inhibiting farnesylation of specific proteins remains controversial (19, 75-77, 79, 104, 117).

When farnesylation is inhibited some proteins are alternatively GG'd. An alternative model for the anti-tumor mechanism of FTI would be if proteins that normally are farnesylated become GG'd in the presence of FTIs, altering the signaling characteristics of these proteins. If alternatively geranylgeranylating proteins is indeed the reason for FTI mediated affects such as reduced cell growth and cell cycle arrest, this would clarify the controversy about the mechanism of FTIs. Some anti-tumor effects have been attributed to alternate GG'n of RhoB, but these reports are only in Ras transformed cells, and RhoB is already preferentially GG'd (77, 87, 89). N- and K-Ras are also alternatively GG'd when farnesylation is blocked. The effect on cells after forcing endogenous GG'n of N- and K-Ras has not been extensively studied, and the cellular functions of GG'd N- and K-Ras have been assumed to mimic farnesylated N- and K-Ras.

We want to determine if antineoplastic effects of FTIs were from inhibiting the farnesylation of proteins and / or from alternatively geranylgeranylating proteins.

Results

We used 293T cells to analyze the mechanism of farnesyltransferase inhibition (FTI). 293T cells are commonly used because they grow quickly and are easily transformed / transduced. Therefore, we used this non-tumorigenic cell line as a model to determine the effects of FTI on cell survival and the cell cycle.

Tipifarnib decreases cell yield and induces cell cycle arrest.

To determine what effect FTI had on proliferation, non-tumorigenic 293T cells were treated with increasing tipifarnib concentrations for 96 hours. Cells were plated in 6 well dishes in triplicate. After 96 hours the plasma membrane was lysed, nuclei were fixed, and counted on an automated Coulter counter (Vi-Cell). Intact nuclei were counted in order to count only living cells, therefore any cells undergoing cell death were eliminated from this assay. 293T cells show a dose-dependent decrease in cell yield from tipifarnib treatment (Figure 5).

Figure 5

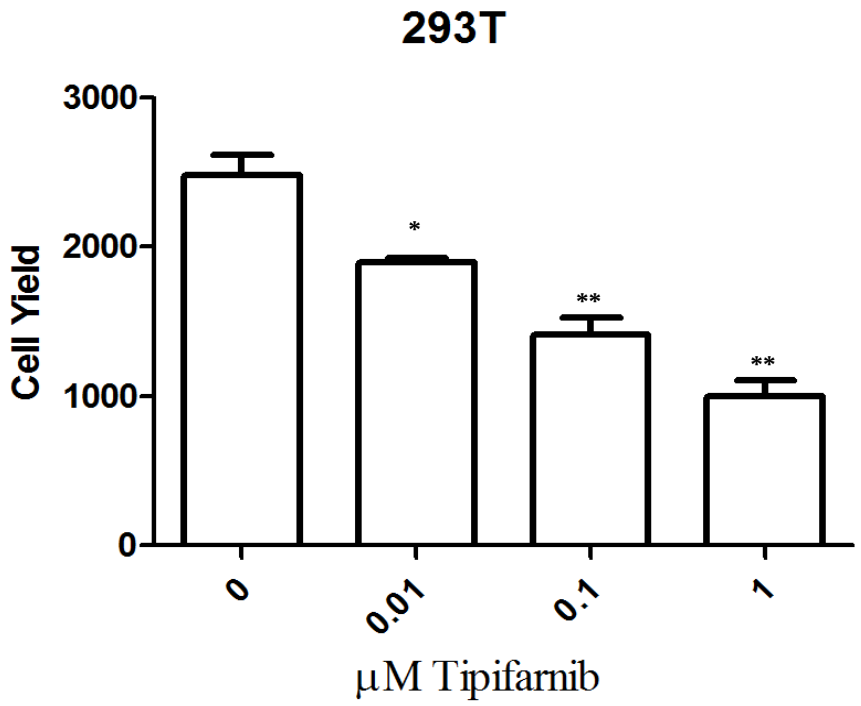

Figure 5. Tipifarnib reduces cell yield 293T cells. 293T cells were treated with increasing concentrations of tipifarnib for four days. Cell viability was assayed by counting nuclei after chemical lysis of the plasma membrane to avoid counting dead or dying cells. Cells were fixed and counted by an automated coulter counter. Data is representative of three independent experiments. Significance was assessed by Student's t-test (Statistica Software) *$p<0.05$, ** $p<0.001$.

Cell cycle was also assessed after tipifarnib treatment. After 72 hours of tipifarnib treatment there was a dose dependent increase in the percentage of cells in the sub G1 portion of the cell cycle (Figure 6). Increased sub-diploid DNA with higher doses of tipifarnib treatment suggests higher levels of stress induce a proportional increase of toxicity to these cells. 293T cells also underwent G2/M arrest with tipifarnib treatment (Figure 6).

Figure 6

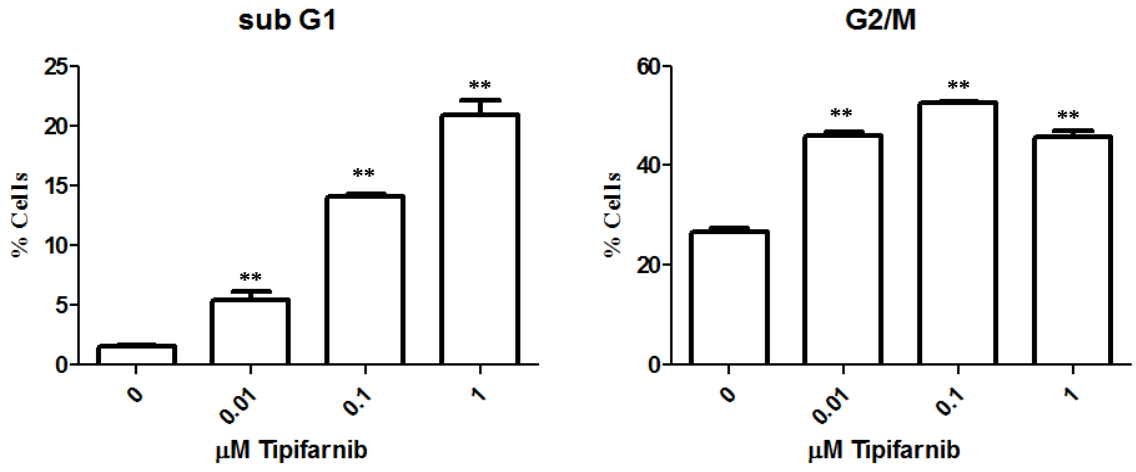

Figure 6. Tipifarnib increases the percentage of 293T cells in sub G1 & arrests cells in G2/M. 293T cells were treated with tipifarnib for 72 hours in triplicate. Detached and attached cells were collected and stained with a 0.005% propidium iodide solution as described in Materials and Methods. Cells were analyzed the following day on a flow cytometer. Cell cycle analysis is representative of three independent experiments. Significance was assessed by Student's t-test (Statistica Software) ** $p<0.001$.

Tipifarnib increases GG'd protein expression even after knocking down GGTase.

We then wanted to determine if increased Ras activity in GGTβ shRNA transduced cells correlates with increased GGTβ expression despite knocking down this gene with shRNA. Analysis of lysates from GGTβ shRNA show 75% decrease in GGTβ expression. However, when stably transduced GGTβ shRNA cells are treated with low dose 0.01 µM tipifarnib there is a 10% recovery of GGTβ expression (Figure 7). Increased GGTβ expression after tipifarnib treatment in GGTβ shRNA transduced cells suggests increasing GG'd proteins is important for the mechanism of how FTIs function.

Figure 7

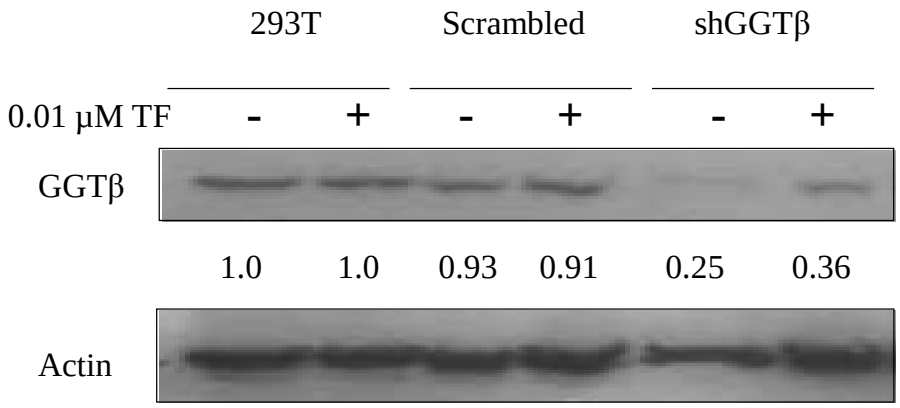

Figure 7. Tipifarnib treated GGTβ shRNA transduced 293T cells increases GGTβ expression. A. Parental 293T, scrambled, and GGTβ shRNA transduced cells were treated with 0.01 μM tipifarnib for 24 hours, lysates were collected, ran on an immunoblot, and probed with GGTβ and actin antibodies. Densitometry values are calculated by comparing GGTβ expression in transduced cells relative to untransduced cells and normalizing to actin. This is representative of two independent experiments.

Increased GG'd protein contributes to FTI mediated reduced cell yield and cell cycle arrest.

Cell viability in 293T cells was also assessed with FTβ and GGTβ shRNA. To determine if decreased cell viability from FTI was due to an increase of GG'd proteins, cells containing these stable shRNA constructs were treated with low concentrations of tipifarnib. There was a partial rescue of cell yield with 0.01 μM tipifarnib treatment in GGTβ shRNA (Figure 8). The increased GGTβ protein expression after tipifarnib treatment shown in figure 7 could explain why there is only a partial rescue of cell yield. Tipifarnib treatment results in GGTase alternatively geranylgeranylating proteins that are originally farnesylated. This is why GGTase protein expression is increased with tipifarnib treatment even with stably transduced GGTβ shRNA. It is likely 0.1 μM tipifarnib treatment, has even higher GGTβ protein expression despite initial knockdown of this gene in these cells.

Figure 8

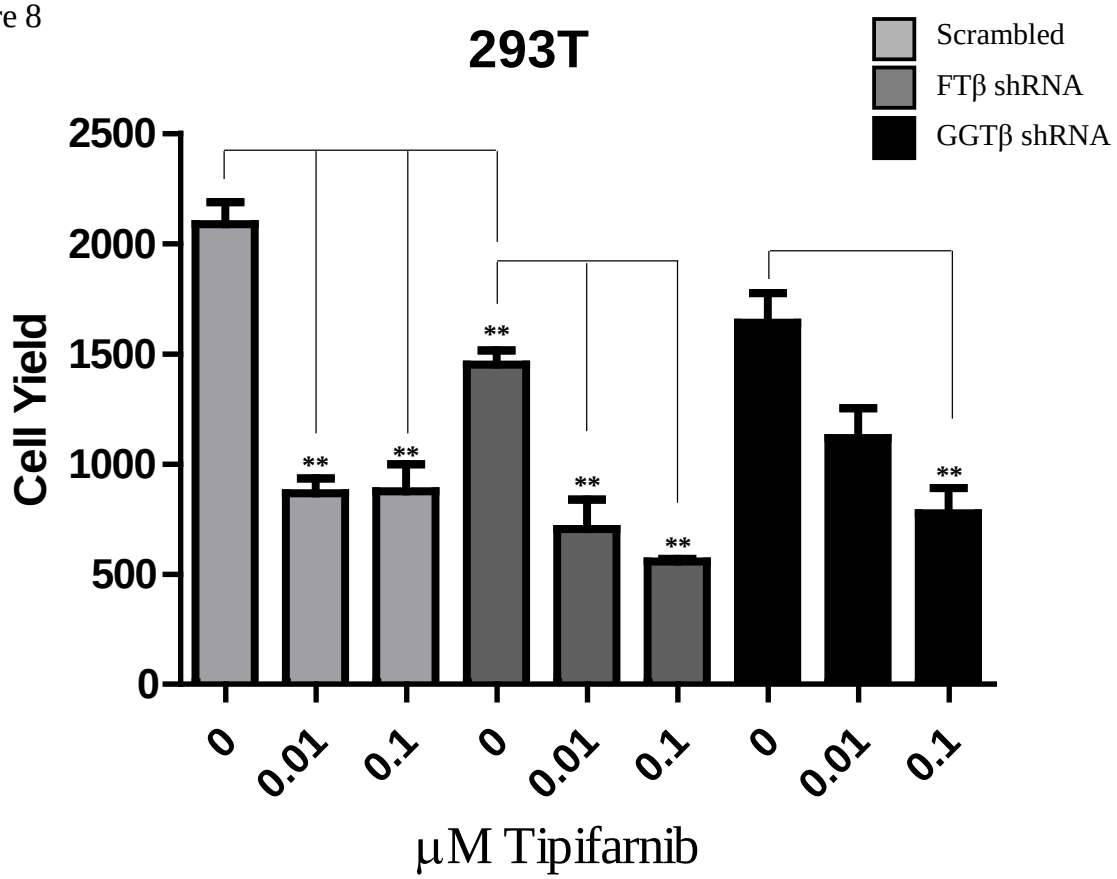

Figure 8. Knocking down GGTβ partially rescues tipifarnib effects on cell yield in 293T cells. Stable scrambled, FTβ, and GGTβ shRNA transduced cells were counted and plated in 6 well plates 30,000 cells per well. Two days after plating the media was treated with 0, 0.01, or 0.1 µM tipifarnib. Cells were grown for an additional 4 days. Cells were isolated and counted as described in Figure 5. Data is representative of two independent experiments.

To determine if increased GG'd protein was contributing to increases in sub G1 and G2/M in response to FTI, GGTβ shRNA was transduced into 293T cells. Stably transduced cells were plated at a density of 30,000 cells per well in triplicate and treated with 0.01 or 0.1 µM tipifarnib. After 48 hours of treatment all cells were collected, stained with PI overnight and cell cycle was assessed by running the samples on a flow cytometer. GGTβ shRNA cells have a partial rescue of cells in the sub G1 phase after 0.01 µM tipifarnib treatment. GGTβ shRNA stably transduced cells are also rescued from G2/M arrest with 0.01 and 0.1 µM tipifarnib concentrations when compared to scrambled control transduced cells treated with tipifarnib (Figure 9).

Figure 9

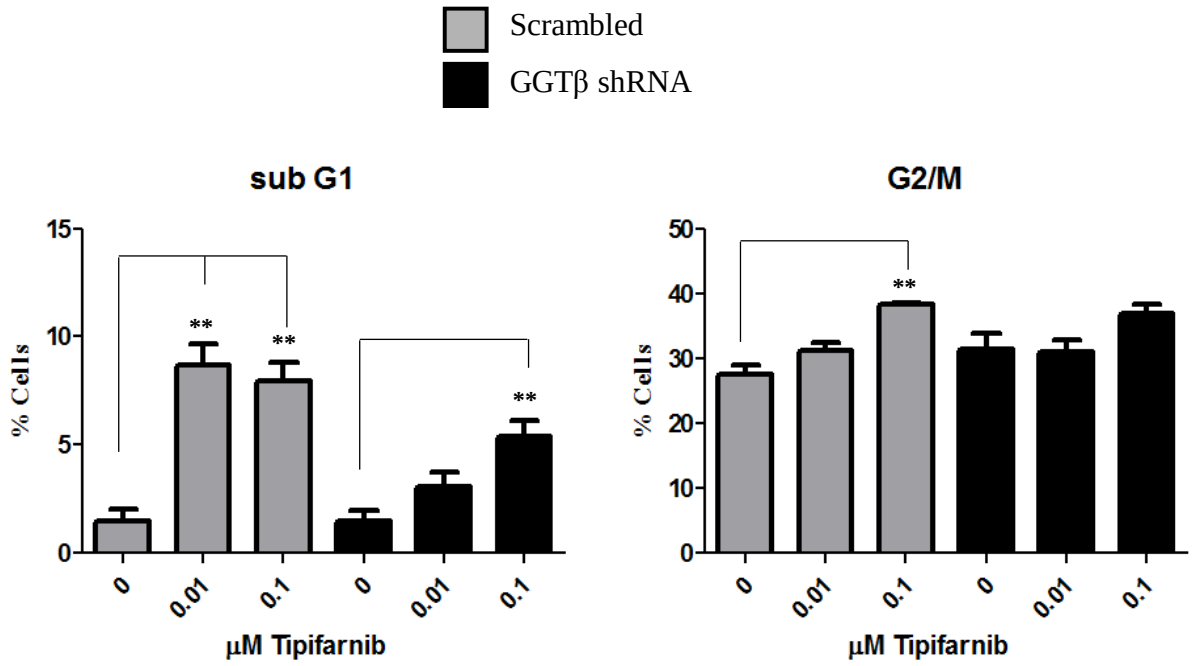

Figure 9. There is a partial rescue in the percentage of cells in sub G1 and G2/M in stable shGGTβ transduced 293T cells treated with tipifarnib. Scrambled and GGTβ shRNAs were transduced into 293T cells. 50,000 cells were plated in triplicate and treated with 0, 0.01, or 0.1 µM tipifarnib for 48 hours. Cells were collected and resuspended in PI and analyzed on a flow cytometer the following day. This is representative of two independent experiments.

Summary

To determine the mechanism for how FTIs function, we performed experiments to determine if anti-tumor effects of FTIs are from inhibiting the farnesylation of proteins and / or increasing GG'n of proteins. Inhibiting farnesylation by using the drug tipifarnib or FTβ shRNA in 293T cells reduced cell yield. Tipifarnib treatment also increased the percentage of 293T cells with sub-diploid DNA and the percentage of cells arrested in the G2/M phases of the cell cycle.

To determine if the protein expression of GGTase was altered by tipifarnib treatment, lysates were made from stable scrambled and GGTβ shRNA cells treated with 0.01 μM tipifarnib. GGTβ protein expression was increased after treatment with tipifarnib in GGTβ shRNA cells. This suggests increased GG'd proteins is an important affect of FTI.

We wanted to determine if alternatively geranylgeranylating proteins contributes to FTI mediated effects on cell yield. The differences in the β-subunits of FTase and GGTase allow for specific targeting of these genes. In 293T cells we created stable scrambled control, FTβ, and GGTβ knockdowns and treated them with low doses of tipifarnib. FTβ shRNA transduced cells had a slower proliferation rate than scrambled control transduced cells and tipifarnib further reduced the growth of these cells. The reduced cell growth after tipifarnib treatment is not surprising as shRNA does not completely abrogate FTase expression. Treatment with 0.01 μM tipifarnib in GGTβ shRNA transduced cells results in a partial recovery in cell yield. These results suggest increased GG'd proteins does contribute to reduced cell yield after FTI.

To determine if increasing GG'd proteins contributed to the tipifarnib induced cell cycle arrest, scrambled control and GGTβ knockdown cells were treated with tipifarnib and cell cycle was assessed. GGTβ shRNA cells had a reduced percentage of 293T cells with sub-diploid DNA and a reduced percentage of cells arrested in G2/M after tipifarnib treatment when compared to scrambled control transduced cells. These results suggest alternatively geranylgeranylating proteins after FTI is important for FTI mediated increase of cells with sub-diploid DNA and G2/M arrest.

Knocking down GGTβ in 293T cells and treating these cells with tipifarnib resulted in partial recoveries of cell yield, percentage of cells with sub-diploid DNA, and cells arrested in G2/M. GGTβ shRNA transduced cells also had up-regulated GGTβ protein expression after tipifarnib treatment. These results combined suggest increasing GG'd proteins are essential for how FTIs reduce cell viability and cell cycle arrest.

CHAPTER 4: K-CAIL (GG'd) reduces cell viability and results in increased cell cycle arrest.

Rationale

N- and K-Ras are both alternatively geranylgeranylated (GG'd) if farnesylation is blocked. Many researchers have identified how these two highly homologous Ras proteins can create distinct signal outputs depending on their localization within the cell and which downstream effectors are present in that localization (9, 27, 29, 35, 38, 53, 118). However, the cellular effects of alternatively GG'd N- or K-Ras are unknown. Since there has been no correlation made between the mutational status of Ras and anti-tumor effects of FTI, it has been assumed that alternatively GG'd N- or K-Ras would have no affect on cell survival. We analyzed what effects altered prenylation would have on N-Ras and K-Ras function. GG'd N-Ras and K-Ras are likely to have different effects on downstream signaling, cell viability, and cell cycle.

In the previous chapter we demonstrated FTI resulted in increased GG'd protein expression, contributing to reduced cell viability and cell cycle arrest from FTI. **The goal of this chapter is to determine if increased GG'd N-Ras or K-Ras B causes reduced cell viability and or cell cycle arrest from FTI treatment.**

Results

Tipifarnib increases the activity of GG'd N- and K-Ras.

To determine if N- and K-Ras were GG'd after tipifarnib treatment we used tipifarnib, a farnesyltransferase inhibitor (FTI), GGTI-298, a geranylgeranyl transferase inhibitor (GGTI), alone, and in combination. N- and K-Ras were only unprenylated in combination treatments, confirming both of these proteins are alternatively GG'd after tipifarnib treatment in 293T cells (Figure 10).

Figure 10

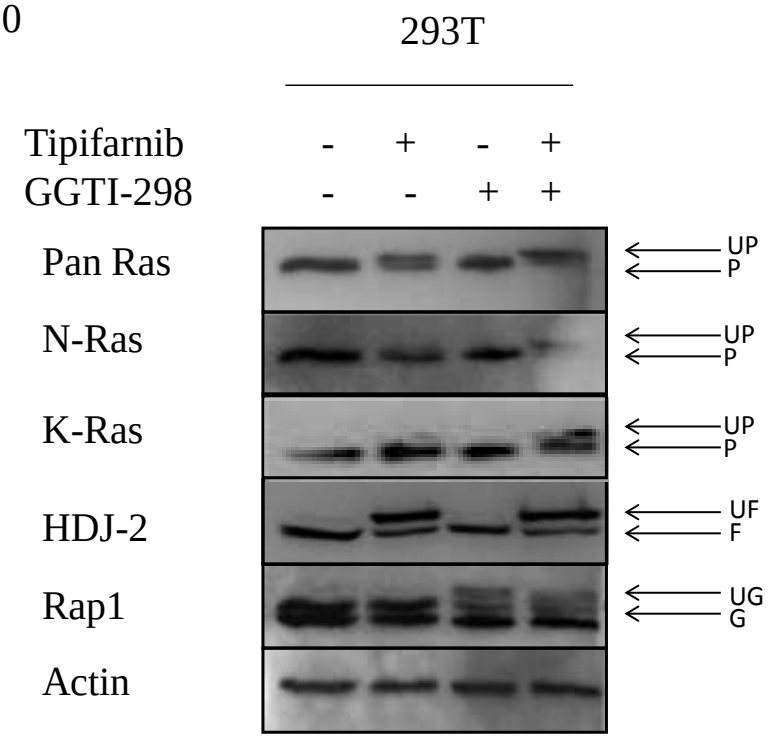

Figure 10. In 293T cells N- and K-Ras are geranylgeranylated (GG'd) with FTI treatment. To assess whether N and K-Ras B are alternatively GG'd we treated the cells with tipifarnib a farnesyltransferase inhibitor (FTI), GGTI-298, a geranylgeranyl transferase inhibitor (GGTI) alone or in combination and assessed the Ras family members. HDJ-2 is only farnesylated and therefore ensures FTI in tipifarnib-treated cells. Rap1 is only GG'd and therefore ensures GGTI in GGTI-298-treated cells. UP- unprenylated, P- prenylated, UF- unfarnesylated, F- Farnesylated, UG- ungeranylgeranylated, G- GG'd

To assess what effect alternatively GG'd N- and K-Ras after tipifarnib treatment would have on Ras activity we used a Ras activity assay from Cell Biolabs. This assay utilizes the Ras binding domain (RBD) bound to agarose beads. This binding domain binds to active GTP-bound Ras, which interacts with both Raf-1 and TIAM1 as both of these proteins bind to Ras

through their RBD. Surprisingly, tipifarnib treatment increased active GG'd Ras in 293T cells (Figure 11). We expected endogenous Ras protein to be GG'd but were surprised that tipifarnib increased protein levels of active GG'd N- and K-Ras.

Figure 11

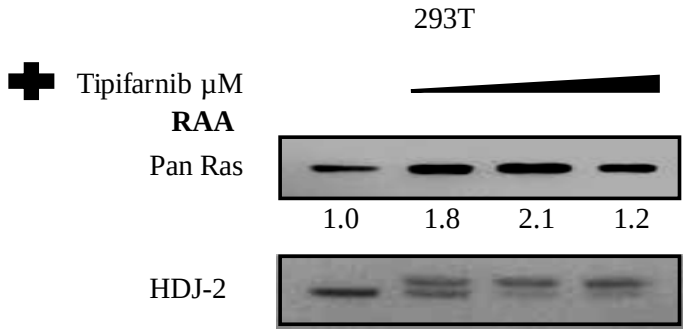

Figure 11. Ras activity is increased in response to tipifarnib treatment in 293T cells. A. Ras activation assay (RAA) in 293T cells. Cells were treated with 0, 0.01, 0.1 or 1 μM tipifarnib for 24 hours, lysates were collected, and Ras activation was assessed. Ras activity was assessed by pull-down with the Ras binding domain (RBD) bound to agarose beads, pulled down GTP-bound Ras was run on an immunoblot, and the membrane was probed with an anti-Ras antibody. HDJ-2 is used as a control to show farnesylation is inhibited. The upper band represents unprenylated protein while the lower band represents farnesylated protein. The same lysates used for the Ras pull-down were used to assess the prenylation status of HDJ-2 after 24 hours. Densitometry values were calculated by comparing tipifarnib treatment to untreated cells.

To ensure that the increased activity of Ras was from inhibiting farnesylation and not an effect from the drug tipifarnib, we used shRNA to inhibit FTase and GGTase. These two enzymes have common α subunits and different β subunits. To selectively inhibit the FTase and GGTase enzymes, lentiviral shRNA to FTβ and GGTβ were purchased from Sigma and transduced into 293T cells. Lysates were collected and 85% knockdown was achieved with FTβ shRNA and 92% knockdown was achieved with GGTβ shRNA (Figure 12 A). These lysates were used for the Ras activity assay and increased activation of Ras was found with FTβ shRNA compared to scrambled control transduced 293T cells (Figure 12 B). Ras activity appears completely abrogated in stably transduced GGTβ shRNA cells (Figure 12 B). Data from figures 10, 11, and 12 collectively demonstrate the activity of GG'd N- and K-Ras are increased after FTI.

Figure 12

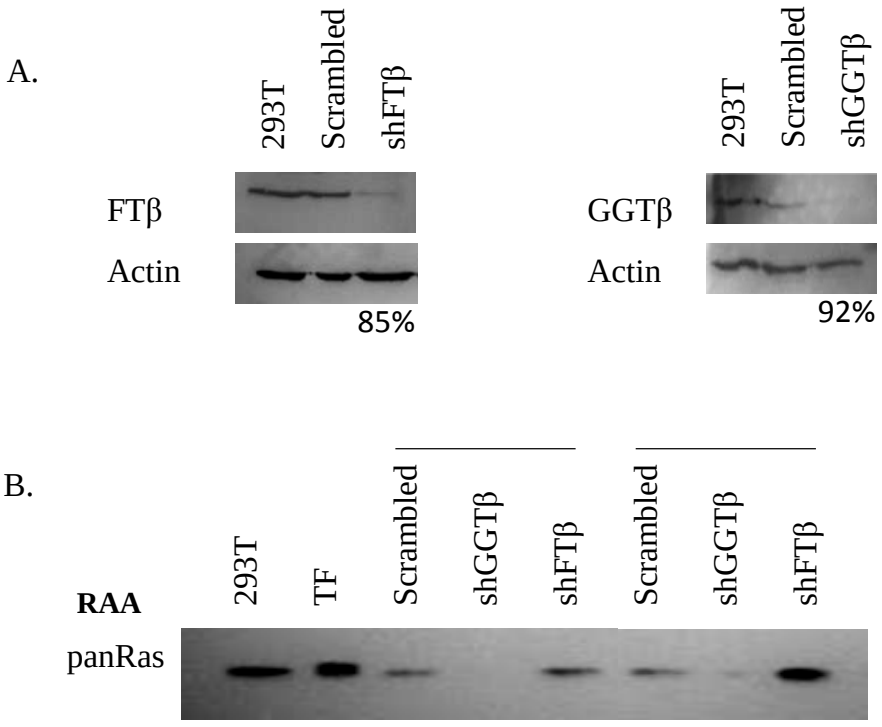

Figure 12. Knocking down FTβ increases Ras activity in 293T cells. Scrambled, FTβ, or GGTβ shRNA lentiviral particles were transduced into 293T cells. A. Stable knockdown was assessed in lysates collected. Densitometry values are the change in signal density of samples compared to control 293T cells relative to actin expression. B. Ras pull-down utilizing Ras binding domain bound to agarose beads to determine levels of active Ras in transduced cells. Immunoblot shows active levels of Ras in lysates from two independent transduction experiments.

Increased GG'd protein contributes increased Ras activation.

We then wanted to determine if Ras activity levels in GGTβ shRNA transduced cells correlates with increased GGTβ expression despite knocking down this gene with shRNA (shown in figure 7). Analysis of lysates from GGTβ shRNA show 75% decrease in GGTβ expression. However, when stably transduced GGTβ shRNA cells are treated with low dose 0.01 μM tipifarnib there is a 10% recovery of GGTβ expression (Figure 7, 13 A). GGTβ shRNA cells have increased Ras activity when treated with tipifarnib (Figure 13 B). Increased GGTβ expression and increased Ras activation after tipifarnib treatment in GGTβ shRNA transduced cells suggests increasing GG'd proteins are important for the mechanism of how FTIs function.

Figure 13

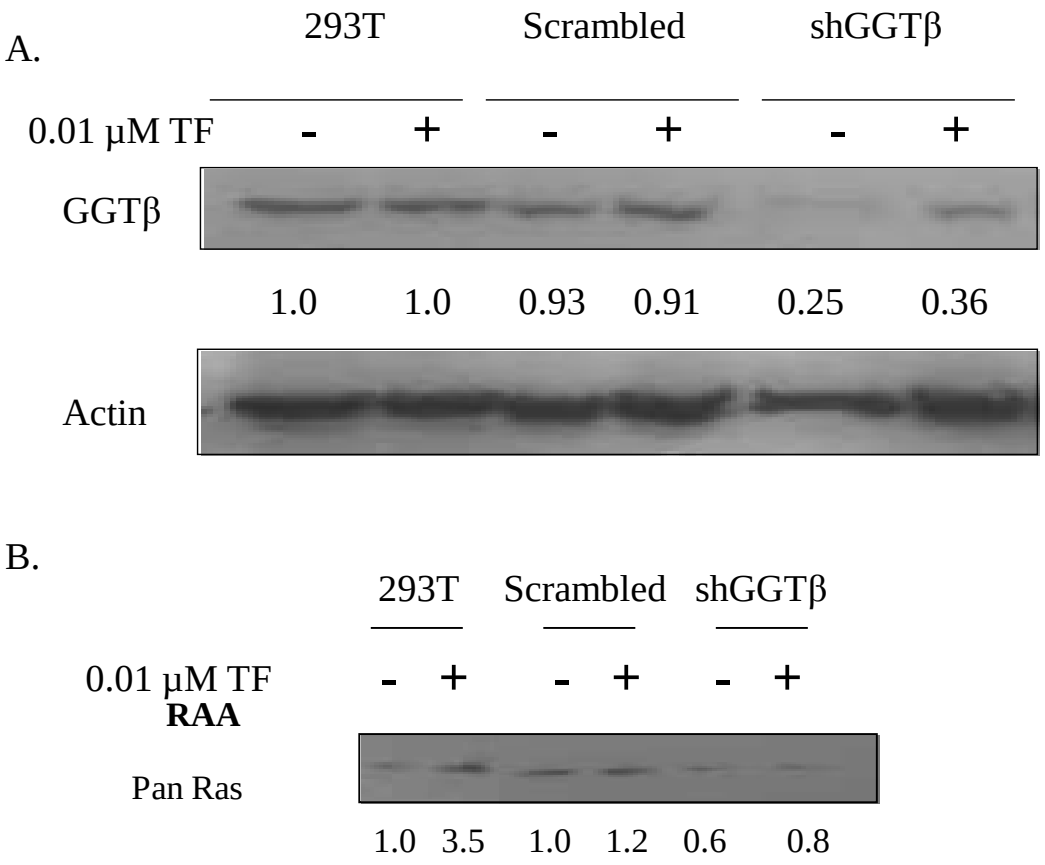

Figure 13. Tipifarnib treated 293T GGTβ shRNA cells increases GGTβ expression and Ras activity. A. Parental 293T, scrambled, and GGTβ shRNA transduced cells were treated with 0.01 μM tipifarnib for 24 hours, lysates were collected, ran on an immunoblot, and probed with GGTβ and actin. Densitometry values are calculated by comparing decreased GGTβ expression in transduced cells relative to untransduced cells and normalizing to actin. B. 293T, scrambled control, or GGTβ shRNA transduced 293T cells were treated with 0.01 μM tipifarnib, lysates were collected and Ras pull-down was performed. Densitometry for tipifarnib treated 293T cells are relative to untreated 293T cells. Densitometry values for transduced samples are calculated relative to scrambled shRNA transduced untreated 293T cells. This is representative of two independent experiments.

Model for creating N-Ras and K-Ras mutants

To assess the effects of increased activity of GG'd N- and K-Ras after tipifarnib treatments we made mutant constructs to determine if GG'd N- or K-Ras mimicked FTI mediated effects on cell viability and cell cycle. Point mutations that alter the prenylation group, which will associate with N-Ras and K-Ras have been previously published (15, 85). Point mutations in the CAAX motif of N-Ras and K-Ras were made in order for the Ras proteins to be WT (preferentially farnesylated (F'd)), CVLS (F'd only), cysteine mutated to serine (unprenylated), and CAIL (GG'd only) (Figure 14 A). These WT and mutant proteins were fused at the N-terminus to mKate a naturally fluorescent protein in a puromycin containing retroviral vector, MipR1mKate2 (Figure 14 B). These constructs were transduced into 293T cells to analyze the functional consequences in non-tumorigenic 293T cells.

Figure 14

A. Model for Mutations of N- and K-Ras B

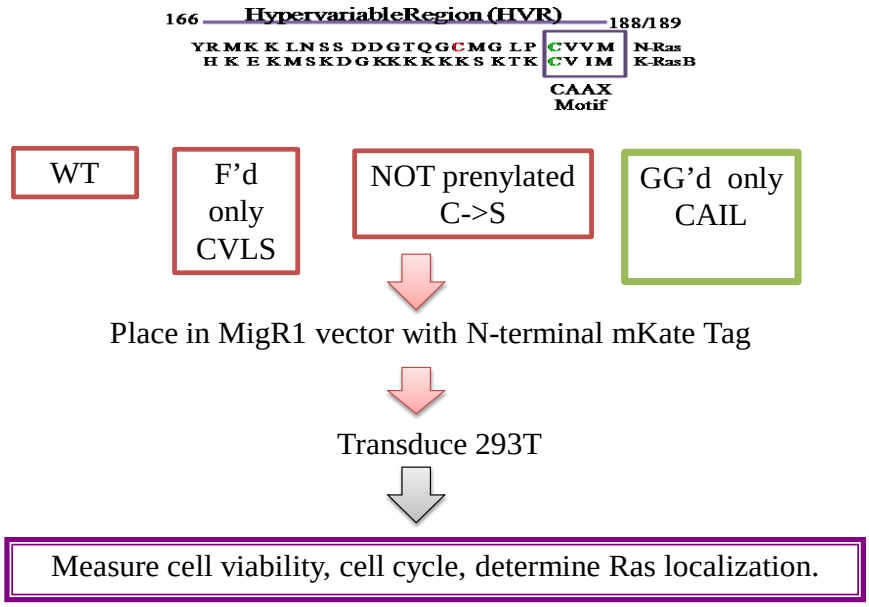

B.

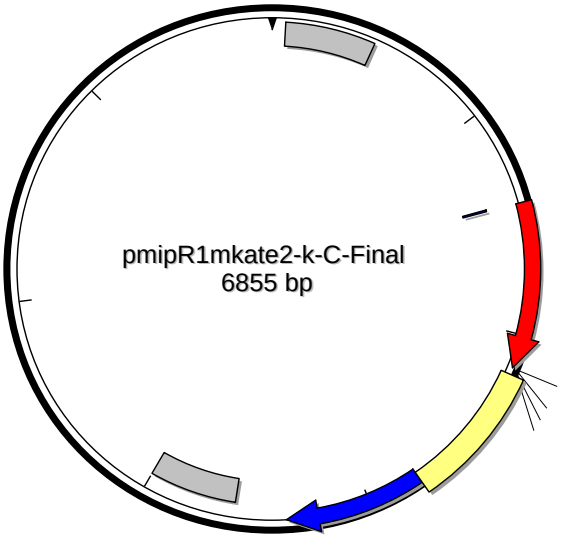

Figure 14. Experimental plan to incorporate mutant proteins into 293T cells. A. Point mutations were made to the CAAX motif of N- and K-Ras. Experimental plan once mutant constructs were made. B. Backbone of MipR1 vector with an N-terminal mKate fusion tag. 5' and 3' long terminal repeat sequences allow the retrovirus to insert their genetic sequences into the infected cells. IRES allows for transcription of the puromycin gene.

Expression of K-CAIL (GG'd) mutant increases cell death, sub-diploid DNA, and cell cycle arrest in G2/M.

N-Ras and K-Ras transduced cells were analyzed 48 hours post-transduction. We analyzed the size and granularity of transduced cells at this time point. Analyzing forward scatter (FSC) verse side scatter (SSC) allows for determination of two rough populations. A live population that normally represents the bulk of cells, which is enclosed by a black hexagon (inset Figure 15) and a dead or dying population of cells that are everything excluded from the hexagon. As a cell is dying, normally its granularity increases then decreases, while its size decreases. Granularity is measured by SSC and the relative size of the cell is measured by FSC. The ratio of dead and dying cells at 48 hours post transduction show K-Ras CAIL (GG'd) has a two fold increase of cells that are dead or dying compared to empty vector alone. This result supports our hypothesis that an increase in expression of K-CAIL (GG') Ras is toxic to cells which express low endogenous levels of activated Ras such as 293T cells.

Figure 15

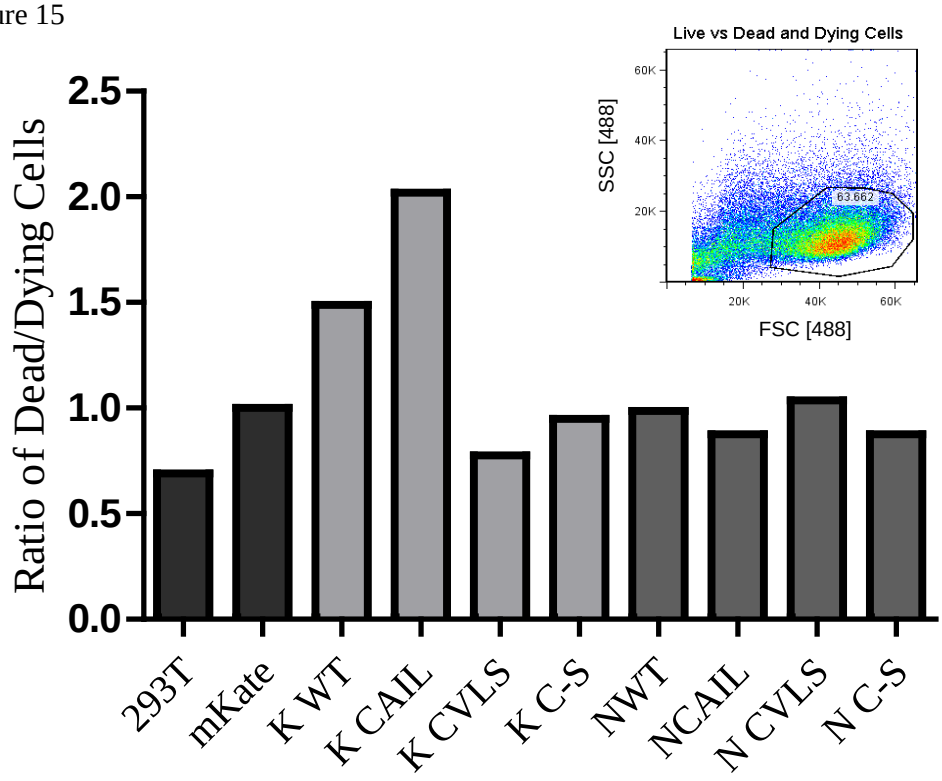

Figure 15. GG'd K Ras 29T cells are dying after 48 hrs. Cells were transduced with empty vector or K-Ras and N-Ras mutants, 48 hours later cells were analyzed for the percentage of live cells. The inset picture is a dot plot that represents how live from dead or dying cells were analyzed. This bar graph represents the ratio of dead and dying cells of the transduced cells relative to transduced empty vector. FSC correlates with the cell volume and SSC measures the inner complexity of the particles within the cell or granularity of the cell.

There was low transduction efficiency of the K-Ras constructs compared to N-Ras or mKate, which suggested a possible toxicity with increasing K-Ras expression (A I 10). The packaging cells used to produce virus in the transductions were GP2-293 a sub-line of 293T cells. If K-Ras is toxic to 293T cells then it is likely the virus produced from the sub-line will have a lower titer than the N-Ras and empty control. To bypass the possibility of toxicity of K-Ras in the packaging cell line, K-Ras plasmid constructs were transfected into 293T cells. The ratio of dead and dying cells was quantified; K-CAIL cells had 4 times more dead and dying cells compared to empty vector control and tipifarnib treated cells had 2 times more dead and dying cells than empty vector alone (Figure 16).

Figure 16

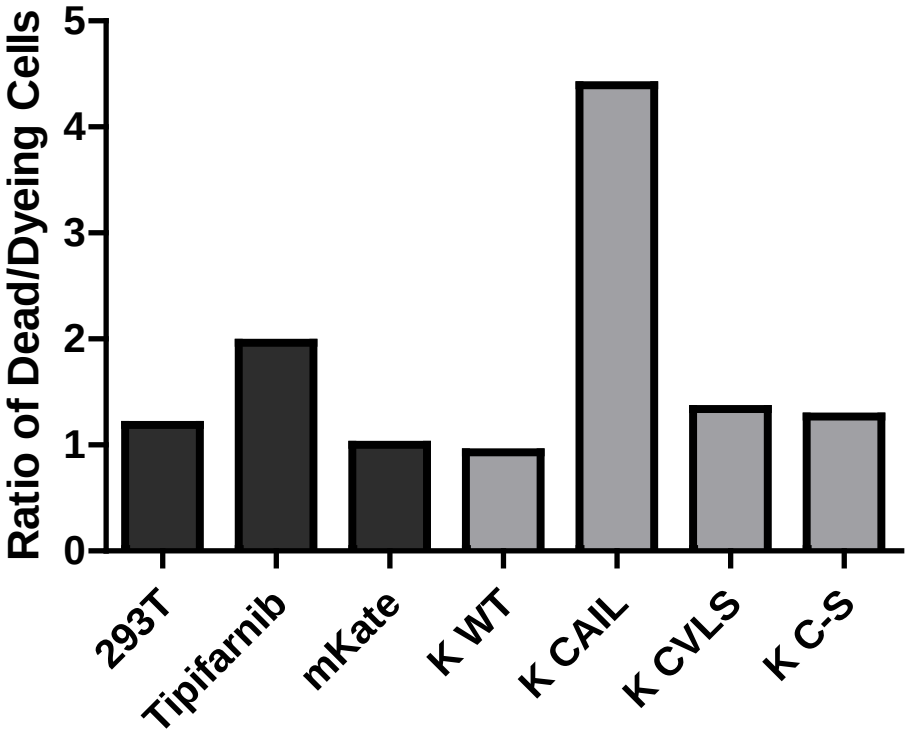

Figure 16. Transfection of K-CAIL is more toxic than 48 hr tipifarnib treatment in 293T cells. Empty vector and K-Ras wild type and mutants were transiently transfected into 293T cells. 48 hours after transfection cells were sorted and the percentage of dead and dying cells were determined as in figure 15. This experiment is representative of two transfections.

To determine the initial affects of K-CAIL (GG'd) on cell cycle, positive and negative mKate transfected cells were collected 24 hours post-transfection (Figure 17). The dead and dying cells normally excluded in cell sorting were also included. Both populations were

collected because some of the cells in the negative collected population are likely to have been transfected but lost mKate signal due to the pores forming in the plasma membrane while undergoing cell death.

Figure 17

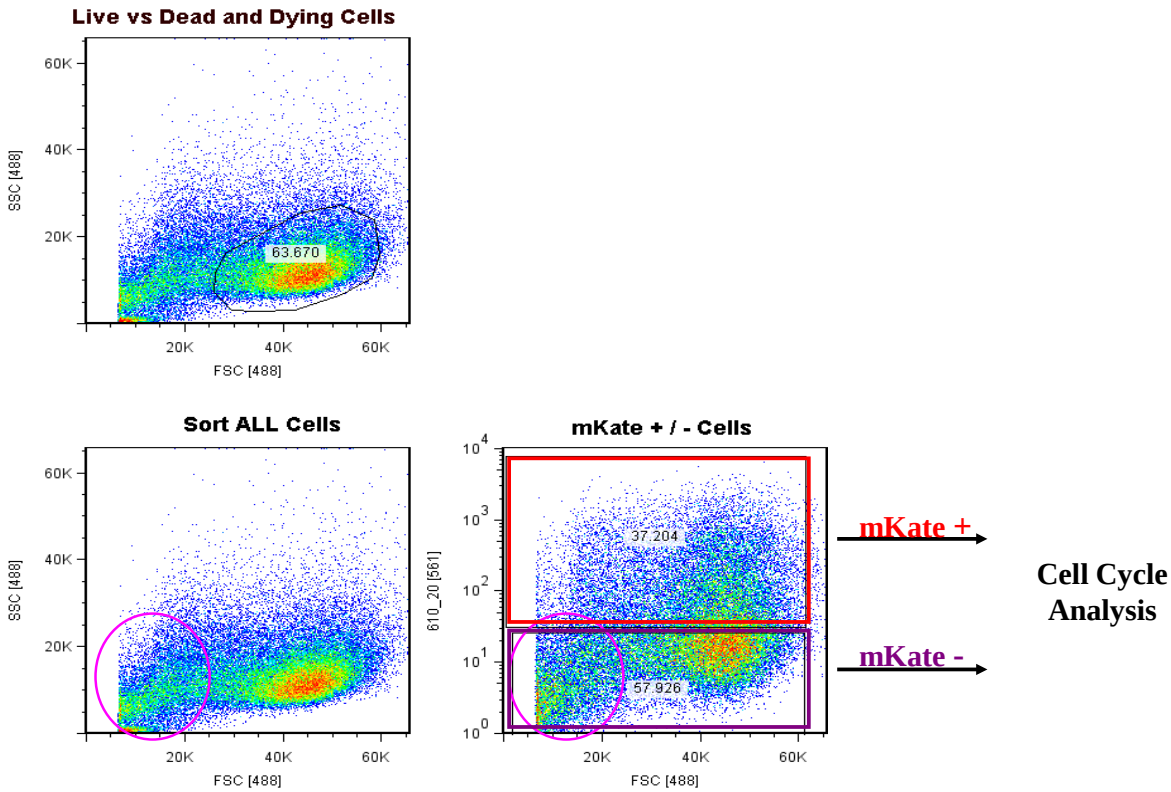

Figure 17. Graphical depiction of the experimental design to collect both negative and positive mKate fluorescing cells. All cells were collected to account for cells which are dead or dying due to expression of GG'd K-Ras. Pink circle represents cells which are dying that would be excluded from the positive mKate population as they have probably lost their membrane integrity. Both negative and positively expressing mKate cells were collected and subjected to cell cycle analysis 24 hours post transfection.

The sorted cells were centrifuged and resuspended in propidium iodide. The following day stained cells were run on a flow cytometer and cell cycle was assessed. The positive and negative K-CAIL-transfected cells had a three-fold increase of cells in sub G1 (Figure 18). The negative population is expected to have an increase of cells in sub G1 because dead and dying cells are collected in this population of sorted cells. During the process, dying cells will lose the mKate fluorescence signal as the cells membrane is disturbed. The positive K-CAIL population also had a two fold increase of cells in the G2/M phases of the cell cycle when compared to empty vector transfected cells.

Figure 18

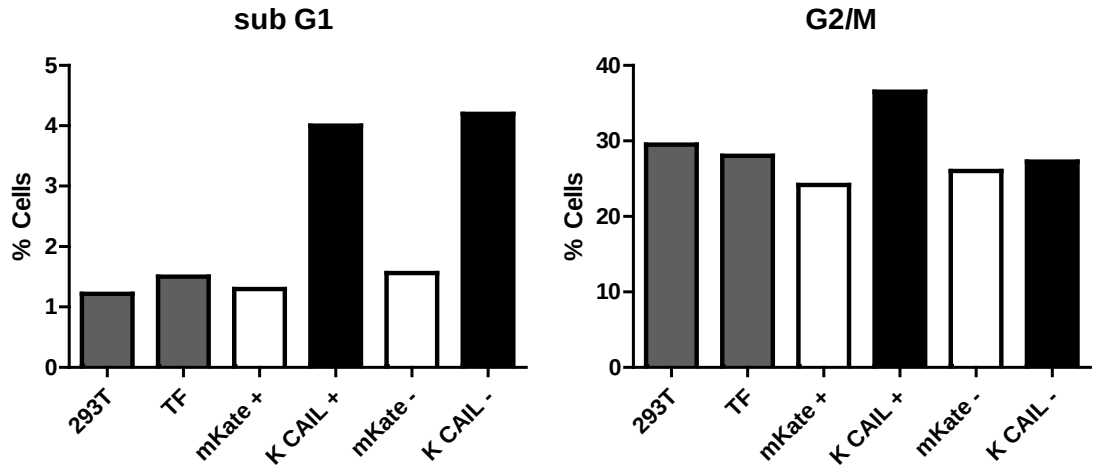

Figure 18. 293T cells are arrested in sub G1 and G2/M after 24 hours post transfection. Cells were transfected with empty vector or K-CAIL, 24 hours later cells were sorted. 20,000 cells from the sort were spun down and then incubated in a propidium iodine solution as described in figure 6. Cells were analyzed on a flow cytometer 24 hours after staining. Flowjo software was used to analyze the cell cycle results. This experiment is representative of three independent experiments (one transduction, two transfections).

Summary

Inhibiting farnesylation of select proteins with a methionine in the X position of their CAAX motif results in GG'n of these proteins. In 293T cells only combination treatment with tipifarnib and GGTI-298 (therefore inhibiting both prenylation enzymes) resulted in unprenylated N- and K-Ras on an immunoblot. This demonstrates both N- and K-Ras are alternatively GG'd after FTI in 293T cells.

To determine if the protein expression of GGTase was altered from tipifarnib treatment, lysates were made from stable scrambled and GGTβ shRNA cells treated with 0.01 μM tipifarnib. GGTase protein expression was increased after treatment with tipifarnib in GGTβ shRNA cells (Chapter 3). Furthermore, FTI increased the activity of GG'd N- and K-Ras in 293T cells after treatment with the drug tipifarnib and knockdown with FTβ shRNA. Increased Ras activity was surprising, as FTIs were created to specifically inhibit Ras signaling. Additionally, Ras activity was also increased after GGTβ shRNA transduced cells were treated with tipifarnib. These results combined suggest increasing GG'd proteins are essential for the mechanism of FTI, and indicate GG'd Ras may be mediating some antineoplastic affects of FTIs.

This chapter further analyzes the functional affects of expressing N-Ras and K-Ras mutants into 293T cells. Specifically we were interested in the functional consequences of expressing GG'd K-Ras. K-Ras preferentially activates ERK signaling and when over stimulated has been shown to result in cell death or growth arrest (50, 59). Expressing Ras proteins which are wild type (WT), farnesylated (F'd) only, GG'd only, or not able to be prenylated was done by creating Ras expression constructs with point mutations in the CAAX motif of both N-Ras and K-Ras. To determine initial affects these N-Ras and K-Ras mutants had on cell growth, 293T cells were transduced with empty vector, WT, or mutant constructs.

After transduction of these constructs into 293T cells the percentage of dead and dying cells induced by the expression of N- and K-Ras mutant proteins were quantified. The ratio of dead and dying cells for 293T cells transduced with the N-Ras and K-Ras mutants were determined by comparing them to the empty vector. K-CAIL had a 2 fold increase of dead and dying cells compared to empty vector alone, indicating that the presence of increased GG'd K-Ras by itself induces cell death. The toxicity induced by genetically engineered GG'd K-Ras suggests that the reduced cell viability observed in FTI-treated cells arises due to increase in

GG'd K-Ras in particular. K-Ras WT transduced cells also had a 1.5 fold increase of cells which are dead or dying compared to empty vector control. This increase in K-Ras WT cells could be due to the farnesylation machinery being overwhelmed by the increased Ras expression and forcing some of this WT Ras to be GG'd. No significant increases in the dead or dying population were seen in any other K-Ras or N-Ras transduced 293T cells. There was no increase in K- or N-CVLS (farnesylated only) suggesting specifically that increased activation of GG'd K-Ras is responsible for FTI mediated reduced cell growth.

Transfection of GG'd K-Ras resulted in a further increase of dead and dying cells. There was a 4 fold increase of dead and dying cells after expression of GG'd K-Ras compared to expression of the empty vector. There was a higher percentage of dead and dying cells in GG'd K-Ras transduced cells than with 24 hours of tipifarnib treatment. These findings demonstrate that forced expression of GG'd K-Ras is toxic to 293T cells and suggests increased expression of GG'd K-Ras from tipifarnib treatment is partially responsible for reduced cell viability.

Transfected cells were sorted for positive and negative mKate expression, not excluding the dead and dying population. It is possible that some of the negatively-sorted cells arise from transfected cells which have lost mKate expression due to loss of their cellular membrane integrity. Both the negative and positive K-CAIL (GG'd) sorted cells have an increase of cells in sub G1. Both had a 3-fold increase when compared to empty vector control. This result supports our theory that some of the transduced cells have lost their membrane integrity and have lost mKate signal. This result also implies cells that have increased GG'd K-Ras have sub-diploid DNA and are possibly becoming apoptotic. The positive population of K-CAIL (GG'd) also have an increase of cells arrested in G2/M phases of the cell cycle.

These data combined support the conclusion that GG's K-Ras is a stronger signaling molecule than farnesylated K-Ras, and that the unique signals from GG'd K-Ras, at high levels, induce growth arrest and cell death. Thus the growth arrest and cell death observed after FTI treatment of cells with intact K-Ras expression and low endogenous Ras signal results, at least in part, from the increase in GG'd K-Ras that follows FTI treatment.

CHAPTER 5: In tumor cell lines FTI reduces cell yield and increases the percentage of cells with sub-diploid DNA and arrests cells in G2/M. These affects could be mediated by increased GG'd K-Ras activity and activation of ERK and p38 MAPKs.

Rationale

For tumor cells, oncogenic (i.e., constitutively activating) mutations of Ras can provide mitogenic signals that are the functional equivalent of growth factor independence, one of the hallmark behaviors of cancer. Farnesyltransferase inhibitors (FTIs) were initially intended to block Ras signaling in cancers which contain over-activated Ras species. Initial clinical trials in patients with cancers known to contain K-Ras mutations such as pancreatic and colorectal cancer patients did not show much efficacy. No correlation between good clinical outcome and Ras mutational status was identified. Many groups attribute this lack of response to alternate prenylation of K-Ras and N-Ras, which would allow for continued Ras signaling when farnesylation is blocked. However, clinical benefit was seen in some patients that do not have over activating K-Ras mutations.

It was assumed that diseases / cancers with mutant Ras would react to FTI in the same way as wild type Ras does. More recent data, however, shows clear functional differences between oncogenic, mutated Ras signaling compared to wild type Ras signaling, as well as differences between the various Ras species. We hypothesize that the activity level of K-Ras, not the mutational status, will correlate with response to FTI. If the endogenous activity of Ras is low then the cell line / disease / cancer will respond to FTI. We hypothesize that an increase in GG'd K-Ras activity and signaling is key for response to this therapy. Most cell lines which have mutant K-Ras already have high levels of endogenous Ras activity so these cells will be unable to increase the activity of K-Ras to result in cell death.

Our goal was to determine what functional effects FTI would have on tumor cells lines that have low endogenous Ras activation. We also wanted to determine FTI effects on Ras signaling in tumor cell lines.

Results

To determine what affect FTI would have on tumor cell lines with endogenous levels of active Ras we did a Ras pull down on untreated cell lysates. We chose three tumor cell lines which had low endogenous active Ras (Figure 19). SaOS2 was derived from an osteosarcoma patient. COL was derived from a neuroblastoma patient. OS187 was derived from a colon cancer patient and has mutation in codon 13 of K-Ras and still maintains low levels of active Ras.

Figure 19

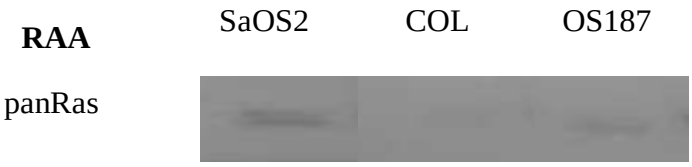

Figure 19. Low endogenous Ras activity in three tumor cell lines. Lysates were collected from three tumor cell lines and Ras pull down was performed as described in figure 11. Immunoblot shows active GTP-bound Ras levels in three tumor cell lines.

FTI affects on cell yield and cell cycle in tumor cell lines with low endogenous Ras activity.

To determine what effect inhibiting farnesylation would have on proliferation in cells with low endogenous Ras signaling, we used the farnesyltransferase inhibitor (FTI) tipifarnib. OS187 and COL cell lines were treated with increasing tipifarnib concentrations for 96 hours. SaOS2 has a doubling time of 72 hours whereas COL and OS187 have doubling times of approximately 24 hours. Therefore, SaOS2 cells were treated with tipifarnib for one week and then counted. Cells were plated in 6 well dishes in triplicate. After 96 hours the plasma membrane was lysed and nuclei were fixed and counted on an automated Coulter Counter (Vi-Cell). Intact nuclei were counted in order to count only living cells, therefore any cells undergoing cell death were eliminated from the assay as their nuclei would not be intact. Tumor cell lines with low endogenous Ras activity all show a dose-dependent decrease in cell yield after treatment with tipifarnib (Figure 20).

Figure 20

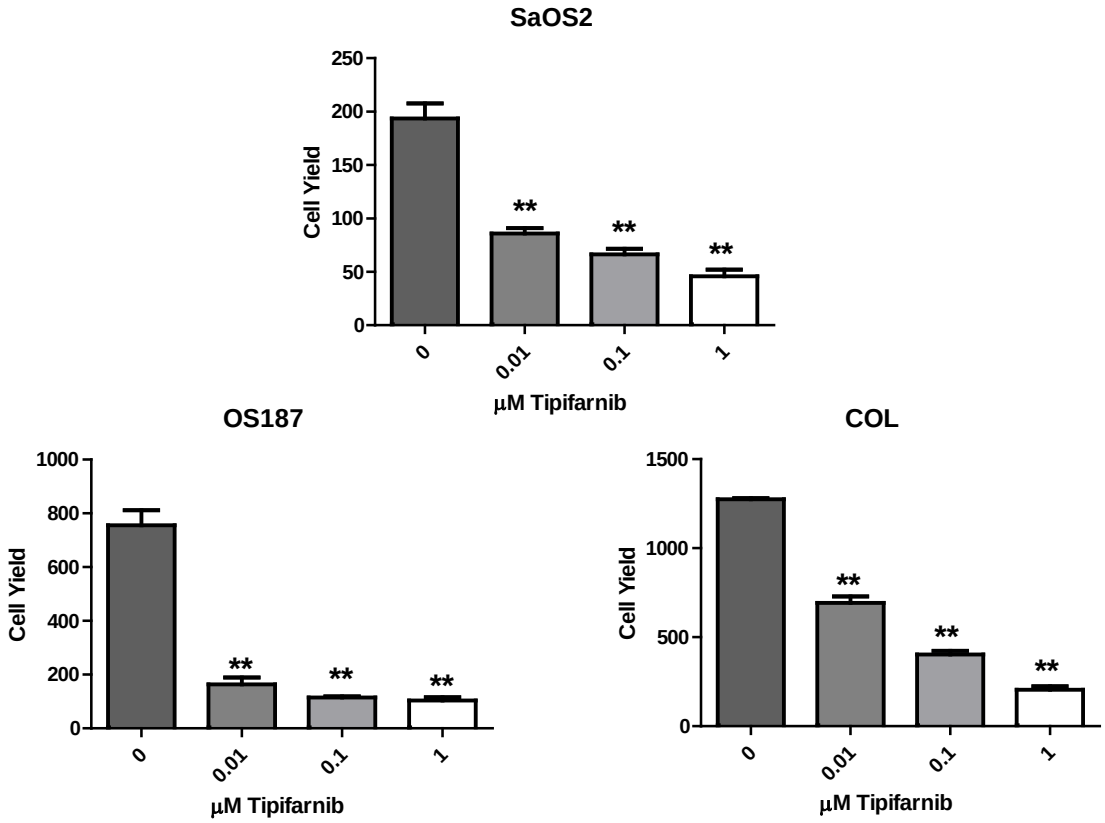

Figure 20. Tipifarnib reduces cell yield of tumor cell lines. OS187 and COL tumor cell lines were treated with increasing concentrations of tipifarnib for four days, SaOS2 was treated for one week. Cell viability was assayed by counting nuclei after chemical lysis of the plasma membrane to avoid counting dead or dying cells. Cells were fixed and counted by an automated coulter counter. Data is representative of three independent experiments. Significance was assessed by Student's t-test (Statistica Software) *$p<0.05$, ** $p<0.001$.

We next wanted to determine what effect FTI would have on the cell cycle of tumor cell lines with low endogenous active Ras. Cell cycle analysis of OS187 and SaOS2 tumor cell lines was also assessed. Both cell lines had a dose-dependent increase of cells with sub-diploid DNA and an increase of cells arrested in G2/M after tipifarnib treatment (Figure 21).

Figure 21

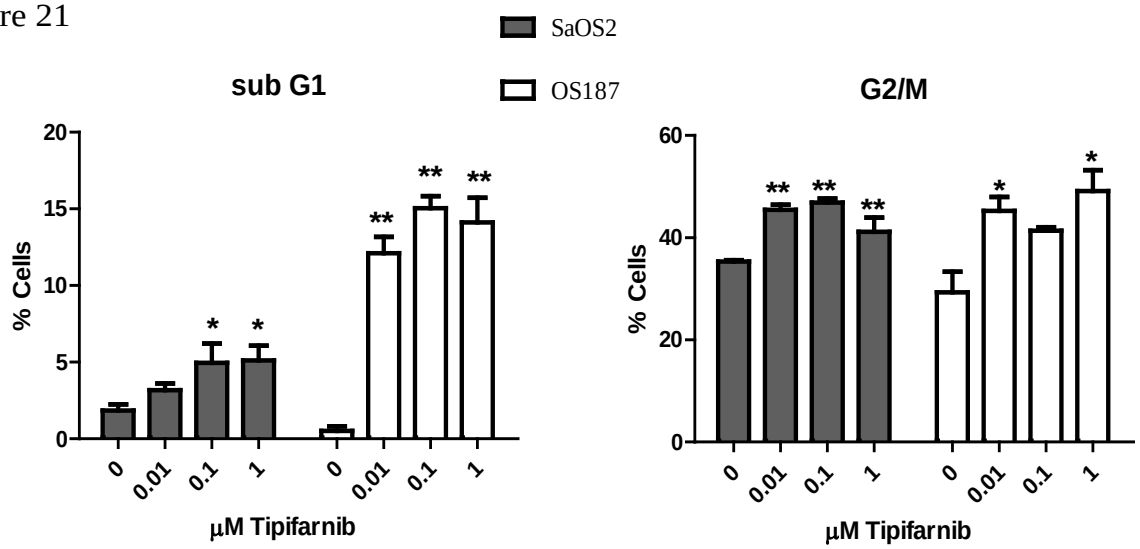

Figure 21. Tipifarnib increases the percentage of OS187 and SaOS2 tumor cells with sub-diploid DNA and arrests cells in G2/M. Tumor cell lines were treated with tipifarnib for 72 hours in triplicate. Detached and attached cells were collected and stained with a 0.005% propidium iodide solution as described in Materials and Methods. Cells were analyzed the following day on a flow cytometer. Cell cycle analysis is representative of three independent experiments. Significance was assessed by Student's t-test (Statistica Software) *$p<0.05$, ** $p<0.001$.

Farnesyltransferase inhibition (FTI) results in increased Ras activation in tumor cell lines with low endogenous expression of active Ras.

We next wanted to determine what effect inhibiting farnesylation would have on Ras activity in cells with low endogenous Ras signaling. We treated OS187, a colon cancer cell line with a mutation in codon 13 of K-Ras which maintains a low endogenous Ras activity, COL a neuroblastoma cell line, and SaOS2, an osteosarcoma cell line, with increasing concentrations of tipifarnib for 24 hours (Figure 22 A). In all three cells lines there was an increase in activated Ras with all three concentrations of tipifarnib treatment as determined by a Ras pull-down assay (Ras activity assay). Inhibition of farnesylation was confirmed by western blot analysis of HDJ-2, a protein which is only farnesylated and which has slower mobility on SDS-PAGE when farnesylation is blocked with tipifarnib treatment.

Additionally, Ras activation status was analyzed in a panel of osteosarcoma cell lines, a disease for which there are no known activating Ras mutations. LM7 is a metastatic subline of SaOS2 which was cycled through a xenograft mouse model 7 times for increased ability to form lung metastases. CCH-OS-M and CCH-OS-D are primary osteosarcoma cell lines which

were derived in our laboratory from patient samples. All four osteosarcoma cell lines had increased Ras activation when treated with tipifarnib (Figure 22 B).

To determine if this effect were true also in AML cell lines, THP1 and U937, which have been found previously to be sensitive to FTI, were treated with tipifarnib, and Ras activity was assessed with the Ras pull-down assay (110, 119). THP-1 has mutant N-Ras, while U937 does not have any Ras mutations. Both of these AML cell lines had high levels of endogenous activated Ras which were also both increased with tipifarnib treatment (Figure 22 C). These results from figure 20, 21, and 22 combined suggest tipifarnib will be effective in reducing cell viability and/or inducing cell cycle arrest in cells which have upregulated Ras activity in response to FTI regardless of mutational status.

Figure 22

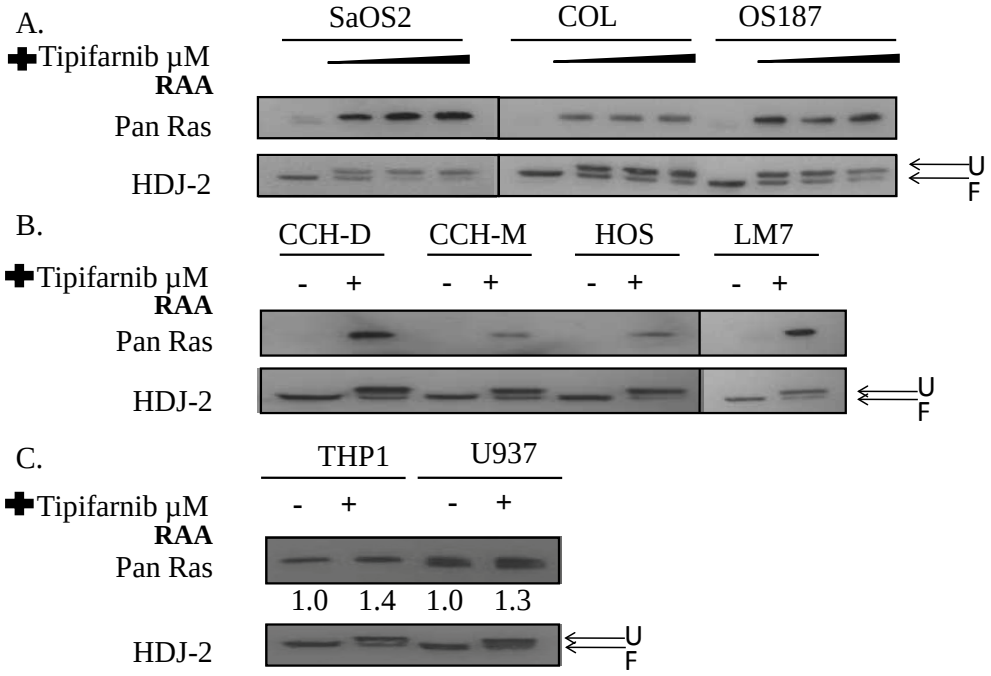

Figure 22. Ras activity is increased in response to tipifarnib treatment. A. Ras activation assay in SaOS2 (osteosarcoma), COL (neuroblastoma), and OS187 (colon cancer). Cells were treated with 0, 0.01, 0.1 or 1 µM tipifarnib for 24 hours, lysates were collected, and Ras activation was assessed. Ras activity was assessed by pull-down with Raf-Ras binding domain (RBD) bound to agarose beads, immunoblotting, then probing with an anti-Ras antibody. HDJ-2 is used as a control to show farnesylation is inhibited. The upper band represents unprenylated protein while the lower band represents farnesylated protein. The same lysates used for the Ras pull-down were used to assess the prenylation status of HDJ-2 after 24 hours. B. Four additional osteosarcoma cell lines and (C) two AML cell lines were treated with 1 µM tipifarnib for 24 hours and assayed as above. Adapted and reprinted by permission from the American Association for Cancer Research: Geryk-Hall, M., Y. Yang, et al. "Driven to Death: Inhibition of Farnesylation Increases Ras Activity in Osteosarcoma and Promotes Growth Arrest and Cell Death." Mol. Cancer Ther.: 1535-7163.MCT-09-0833.

To ensure that this increased Ras activation was due to blocking farnesylation and not an effect of the drug tipifarnib, shRNA was utilized to block the enzyme responsible for farnesylation. FTase is the enzyme that farnesylates specific proteins with a CAAX motif where the X residue is a methionine, glutamine, or serine. This enzyme has an alpha (α) and beta (β) subunit. The alpha subunit is the same for FTase and GGTase.

To selectively inhibit farnesylation, 2 shRNAs to the β subunit of FTase were used in OS187 and SaOS2. FTβ shRNA 1011 and 1922 both knocked down FTβ expression (Figure 23 A). An increase in Ras activation was found in both of these cell lines when expression of the β subunit of FTase was reduced (Figure 23 B).

Figure 23

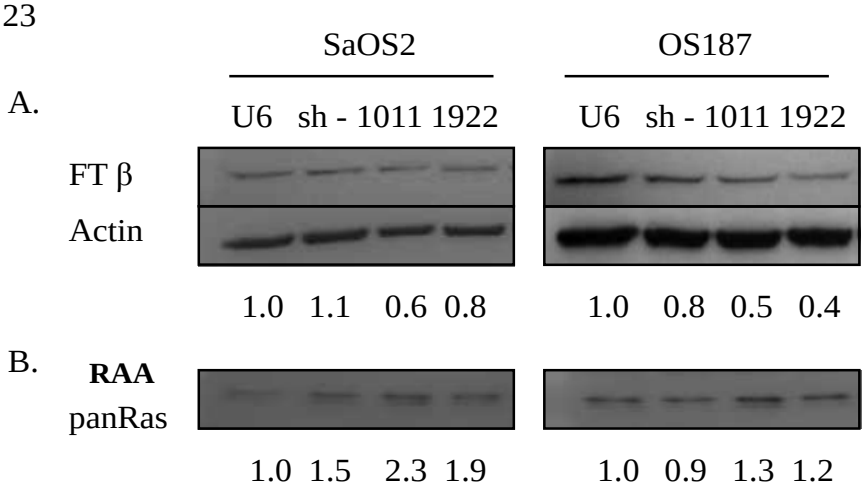

Figure 23. Ras activity is increased when FTβ is knocked down in SaOS2 and OS187 cells. FTβ shRNA was retrovirally transduced into SaOS2 and OS187. Cells were sorted with by a GFP tag encoded in the retrovirus. A. Immunoblots show knockdown of FTβ. B. Ras pull-down shows increased Ras activation with knockdown of FTβ. Numbers below represent densitometry analysis which shows the relative decrease in FTβ expression (A) and Ras activity (B). U6, empty vector; sh-, scrambled control; 1011 and 1922, two shRNAs specific to FTβ. Densitometry analysis was done as in Figure 2. Adapted and reprinted by permission from the American Association for Cancer Research: Geryk-Hall, M., Y. Yang, et al. "Driven to Death: Inhibition of Farnesylation Increases Ras Activity in Osteosarcoma and Promotes Growth Arrest and Cell Death." Mol. Cancer Ther.: 1535-7163.MCT-09-0833.

Inhibiting farnesylation results in alternate prenylation of N-Ras and K-Ras.

Increased activation of Ras with tipifarnib treatment suggests Ras is alternatively GG'd in these cells. To assess this, cells were treated with tipifarnib, GGTI-298, a geranylgeranyl transferase inhibitor (GGTI), alone or in combination for 24 hours. HDJ-2 is a control that is only farnesylated and has an increased mobility on an immunoblot when FTase is inhibited. Rap1 is a protein that is only GG'd and also has an increased shift in mobility on an

immunoblot when GG'n is inhibited. The upper band represents unprenylated protein while the lower band represents prenylated protein. In each individual treatment and in combination treatments, each respective protein shows an increased shift in mobility indicating that both enzymes' activities are partially inhibited in their respective treatments (Figure 24 A). Both enzymes FTase or GGTase are only partially inhibited as double bands are present in the control HDJ-2 and Rap1 probed immunoblots with tipifarnib and GGTI-298 treatments respectively. In the tumor cell lines N-Ras is unfarnesylated with tipifarnib treatment, and is further unprenylated with the combination treatment (Figure 24 A). K-Ras is only unprenylated in the combination treatment, suggesting K-Ras is GG'd with tipifarnib treatment alone. Ras activation is increased with tipifarnib treatment alone or in combination with GGTI -298 (Figure 24 B). The incomplete inhibition of these enzymes explains why there is still an upregulation of Ras activity in combination treatments and suggests N- and K-Ras are still becoming GG'd.

Figure 24

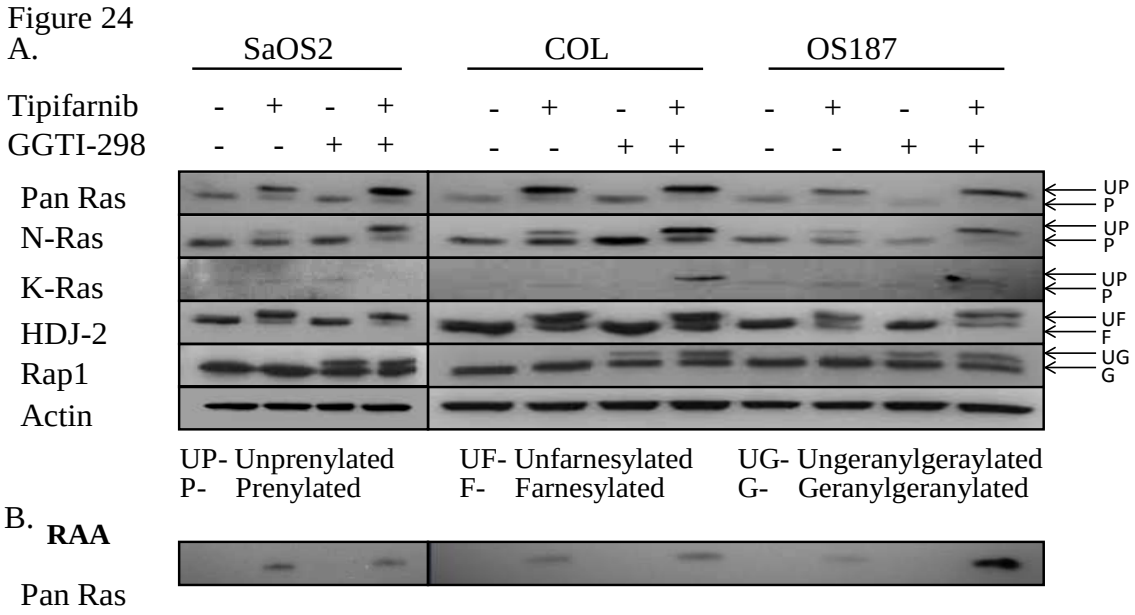

Figure 24. N- and K-Ras are geranylgeranylated (GG'd) in tumor cell lines with FTI treatment. A. To assess whether N and K-Ras B are alternatively GG'd we treated the cells with tipifarnib, a farnesyltransferase inhibitor (FTI), GGTI-298, a geranylgeranyl transferase inhibitor (GGTI) alone or in combination and assessed the Ras family members. HDJ-2 is only farnesylated and therefore ensures FTI in tipifarnib-treated cells. Rap1 is only GG'd and therefore ensures GGTI in GGTI-298-treated cells. B. Ras pull-down as described in figure 11 with the same treatments as stated in part A. Adapted and reprinted by permission from the American Association for Cancer Research: Geryk-Hall, M., Y. Yang, et al. "Driven to Death: Inhibition of Farnesylation Increases Ras Activity in Osteosarcoma and Promotes Growth Arrest and Cell Death." Mol. Cancer Ther.: 1535-7163.MCT-09-0833.

Activation of downstream effector proteins are increased in response to farnesyltransferase inhibition (FTI).

To ensure that the increased Ras activation seen in this Ras activation pull down assay was functionally active, expression of downstream effector molecules of Ras were assessed in tipifarnib treated samples. MAPK family members are known downstream effectors of Ras signaling. We chose to determine activation of specific pathways that were activated by binding to the Ras binding domain (RBD). ERK and p38 MAPKs are both activated by upstream effector proteins binding to Ras through their RBD (Figure 25).

Figure 25

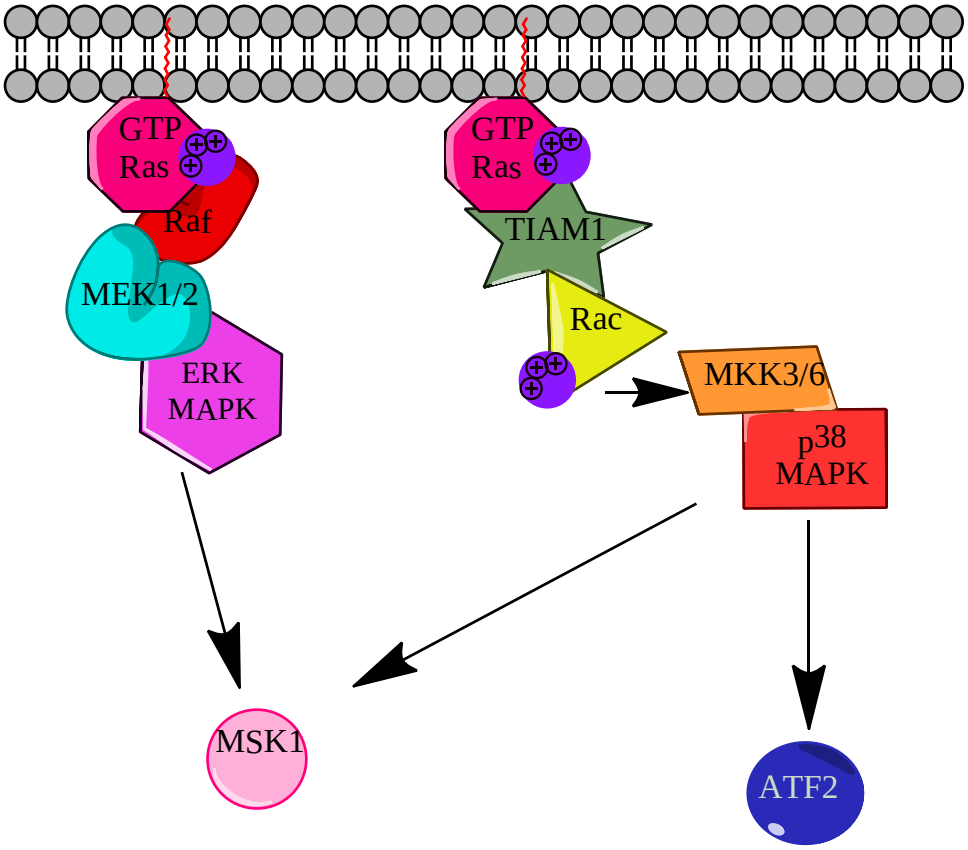

Figure 25. Graphical depiction of proteins in the ERK and p38 MAPK pathway. GTP-Ras activates Raf MAPKKK through its RBD. Raf then phosphorylates and therefore activates MEK 1/2 MAPKK, which finally phosphorylates and activates ERK MAPK. ERK activates MSK1. GTP-Ras associates with TIAM1 through its RBD. TIAM1 activates the GTPase Rac. GTP-Rac activates the MAPKK MKK 3/6, which then phosphorylates and activates p38 MAPK. p38 MAPK activates both MSK1 and ATF-2.

Activation of ERK and p38 were assessed first in our tumor cell lines SaOS2, COL, and OS187. These cell lines were treated with increasing concentrations of tipifarnib for 24 hours

and lysates were collected. SaOS2 proliferates almost three times slower than COL and OS187 therefore SaOS2 was treated with 1 µM tipifarnib for 48, 72, and 96 hours to assess upregulation of specific downstream effector molecules. After 24 hours of tipifarnib treatment both COL and OS187 had increased phosphorylation and therefore activation of ERK and p38 MAPKs (Figure 25). Longer treatments (48, 72, 96 hrs) with tipifarnib were required for SaOS2 to have increased ERK activation (Figure 26).

Figure 26

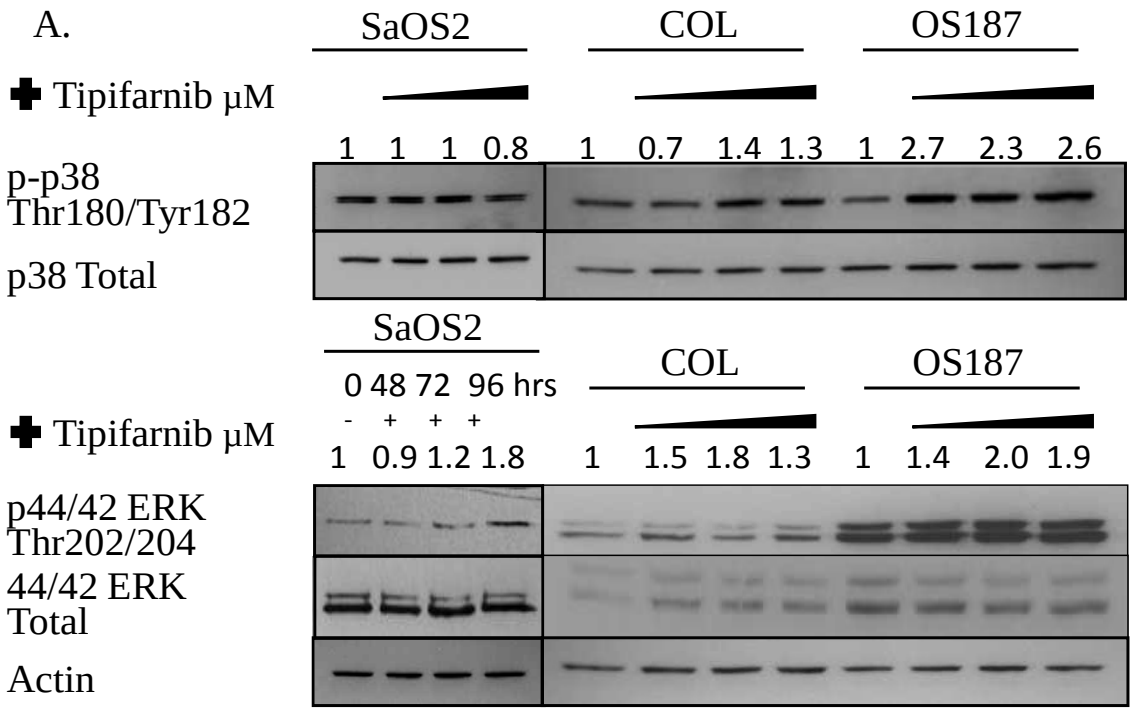

Figure 26. Downstream MAPK targets of Ras are increased in response to farnesyltransferase inhibition in tumor cell lilnes. Lysates were treated with increasing concentrations of tipifarnib for 24 hours, SaOS2 required longer treatment time points because of its slower growth. Immunoblots were probed with p38 and ERK MAPK antibodies. Numbers above each phosphorylated blot represent the relative change in signaling density compared to actin. Modified from manuscript: Geryk-Hall, M., Y. Yang, et al. "Driven to Death: Inhibition of Farnesylation Increases Ras Activity in Osteosarcoma and Promotes Growth Arrest and Cell Death." Mol. Cancer Ther.: 1535-7163.MCT-09-0833.

Proteins up and down-stream of these signaling pathways were also assessed (Figure 25). MKK3/6 are proteins upstream in the p38 MAPK pathway. MEK1/2 are upstream of the ERK MAPK pathway. MSK1 is activated downstream of p38 and ERK signaling, and ATF-2 is activated as a result of p38 signaling. All of these proteins have increased activation in

SaOS2, COL, and OS187 with tipifarnib treatment (pMSK1 was not tested at longer time points of tipifarnib treatment in SaOS2) (Figure 27). Densitometry values are indicated in table 2.

Figure 27

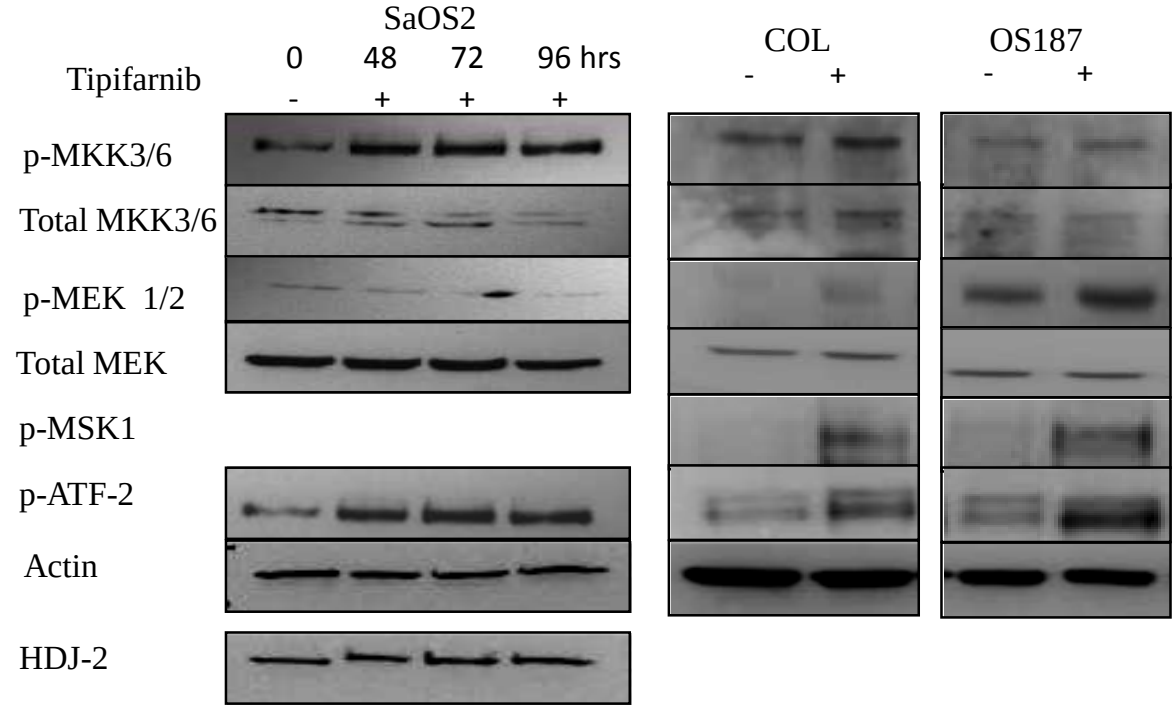

Figure 27. Up- and downstream effectors of MAPKs are increased in response to farnesyltransferase inhibition (FTI) in tumor cell lines. Cells were treated with 1 μM tipifarnib for 24 hours for COL and OS187 and up to 96 hours for SaOS2 then probed with antibodies for phosphorylated and total protein levels. Modified from manuscript: Geryk-Hall, M., Y. Yang, et al. "Driven to Death: Inhibition of Farnesylation Increases Ras Activity in Osteosarcoma and Promotes Growth Arrest and Cell Death." Mol. Cancer Ther.: 1535-7163.MCT-09-0833.

	SaOS2			COL	OS187
	48	72	96	1 μM	1 μM
p-MKK3/6	1.5	1.5	1.3	1.4	1.2
Total MKK3	1.1	1	0.8	1.5	0.9
p-MEK ½	0.6	1.4	0.4	2.8	1.4
Total MEK ½	1.1	1.2	1.4	1.6	0.8
p-MSK1				37.1	11.1
p-ATF-2	2.1	2.2	2.4	2.3	2.7

Table 2. Relative densitometry of proteins up- and downstream ERK and p38 MAPK in tipifarnib treated cells from figure 27. These numbers were determined comparing the changes in densitometry of treated lysates to untreated lysates relative to actin levels.

Summary

In this chapter the response to FTI in tumor cells with low endogenous active Ras was assessed. Tipifarnib treatment in tumor cells that have low endogenous Ras activity have reduced cell yield, an increase in the percentage of cells with sub-diploid DNA, and arrest cells in the G2/M phases of the cell cycle. These results are consistent with the 293T data presented in chapter 3, and suggests increased GG'd proteins are mediating FTI affects on tumor cell lines.

We next analyzed Ras activity in tumor cell lines using pharmacological and molecular techniques. For Ras to be active in tumor cells it has been reported that it must be associated with a cellular membrane. For Ras to associate with a membrane it must be prenylated. Tumor cell lines with low endogenous Ras activity have increased Ras activation when farnesylation is blocked as demonstrated with tipifarnib treatment. To ensure that the increased Ras activation was due to inhibiting farnesylation and not an effect of the drug tipifarnib, FTβ shRNA was transduced into two tumor cell lines. These tumor cells also showed an upregulation of activated Ras when FTβ was knocked down. This data is the first to show increased Ras activation in tumor cell lines as a result of inhibiting FTase.

Blocking farnesylation results in increased Ras activity and this strongly suggests that N- and K-Ras are GG'd. We analyzed the prenylation status in tumor cell lines by treatment with pharmacological inhibitors. K-Ras and N-Ras are both alternatively prenylated with tipifarnib treatment in tumor cell lines. Increased Ras activity was detected in tipifarnib treated cells and also in the tipifarnib and GGTI-298 combination treated tumor cell lines. In cells treated with both prenylation enzyme inhibitors not all detected N- or K-Ras is fully unprenylated, suggesting the remaining prenylated protein could be GG'd and more active in order to respond to the stresses induced by these inhibitors. We hypothesize the remaining protein is still GG'd in response to FTI, which would explain why there is still an increase in active Ras after combination treatments.

To ensure the increased Ras activation in response to FTI was functionally active, we assessed activated and total downstream effector protein levels. ERK and p38 MAPK pathways are upregulated in tumor cell lines in response to FTI. Increased activation of these two pathways has been associated with cell death and cell cycle arrest (50-52, 58, 59, 120, 121). We hypothesize increased activity of these two MAPK pathways in these tumor cell lines after FTI is responsible for the reduced cell yield, increase of cells with sub-diploid DNA, and

also G2/M arrest. Tumor cell lines which have low endogenous Ras activity have increased GG'd N- and K-Ras activation in response to FTI. The previous chapters suggest this reduced cell viability and cell cycle arrest are at least partially due to increased GG'd K-Ras. This chapter suggests GG'd K-Ras is mediating these anti-tumor affects by activating ERK and p38 MAPKs after FTI.

In summary this chapter demonstrates farnesyltransferase inhibition (FTI) increases Ras activation in tumor cell lines by increasing geranylgeranylated (GG'd) Ras signaling and activating ERK and p38 MAPK pathways.

CHAPTER 6: Discussion

When this project began the mechanism of how farnesyltransferase inhibitors (FTIs) reduce cell viability and induce cell cycle arrest still remained to be elucidated. FTIs block farnesylation of select proteins with specific CAAX motifs. Alternate geranylgeranylation (GG'n) of some of these proteins have been identified when FTase is inhibited. N- and K-Ras are among the few identified proteins that are alternatively GG'd when farnesylation is inhibited. The functional consequences of alternatively geranylgeranylating N- or K-Ras had not been studied. Our work focused on the functional effects of alternatively geranylgeranylating N- and K-Ras when FTase is inhibited and linked these effects to the cellular consequences of FTI treatment in cells.

Increased geranylgeranylated (GG'd) proteins mediate farnesyltransferase inhibitor (FTI) effects of reduced cell yield and cell cycle arrest.

Ras is a protein that sits at the convergence of many signaling cascades. Increased Ras signaling promotes tumorigenicity in many cancer cell types. FTIs were developed to inhibit Ras signaling. Alternate prenylation of N- and K-Ras when FTase is inhibited provided an explanation for why FTIs were ineffective in cancer types which specifically have over active K-Ras, as FTIs are still effective in cancer cells which have over active N-Ras signaling (i.e., Some leukemias). The mechanism of how FTIs reduce cell growth and induce cell cycle arrest is still largely undefined. The antineoplastic effects of FTIs have been previously linked to inhibiting farnesylation of various proteins. However, inhibiting farnesylation of these proteins and identifying specific antitumorigic properties associated with these proteins still remains controversial. Our work was designed to determine if FTI treatment increases GG'd proteins to inhibit tumor cell viability and growth.

To determine what effects FTI would have on cancer cell growth and survival, we first analyzed the effects of FTI on cell growth. As FTIs have been found ineffective in reducing cell growth in cells that have over active K-Ras signals, we selectively treated cell lines with low endogenous Ras signaling. Low levels of active Ras were confirmed by a Ras activity assay in each of the cell lines used. We found FTI decreased cell growth of all 3 tumor cell lines tested. FTI also reduced the cell growth of 293T cells. 293T cells are commonly used for analysis of what effects modifications or mutations have on non-tumorigenic cells. Cell lines with a low level of endogenously active Ras have reduced cell growth when FTase is inhibited.

The profound effect of FTI on the survival and proliferation of both tumorigenic and non-tumorigenic cells was also seen in cell cycle analysis by flow cytometry. All three cell

lines had an increased proportion of cells with sub-diploid DNA and an induced G2/M arrest after tipifarnib treatment. SaOS2 is p53 null, which could explain why there is only a slight increase of cells with sub-diploid DNA for this cell lines in our experiments. It is possible that longer treatment with tipifarnib in SaOS2 would allow for an increased proportion of cells in sub G1 and G2/M in a p53-independent manner. p53-independent pathways can result in cell cycle arrest; however, this process normally takes longer than in cells with functional p53 (122). FTI both inhibited cell growth and induced cell cycle arrest in tumorigenic and non-tumorigenic cell lines which have low endogenous Ras signaling.

To determine if the antineoplastic properties of FTIs resulted from increasing GG'n of proteins, we utilized GGTβ shRNA to selectively block GGTase. When 293T cells were transduced with GGTβ shRNA and treated with low dose 0.01 μM tipifarnib, there was a partial rescue of the reduced cell proliferation compared to non-transduced cells treated with tipifarnib, confirming the importance of GG'n in the FTI effect. Immunoblots showed induction of increased GGTβ expression following exposure to even this low dose of FTI, which was evident even in cells transduced with shRNA to GGTβ. This could provide an explanation as to why there is only partial rescue of cell proliferation, since the blockade of GG'n is incomplete and even less complete after FTI treatment. As an alternative explanation, the partial rescue could also be due to the effect of inhibiting farnesylated proteins other than Ras.

We next wanted to identify if the increase in GG'd proteins from inhibiting FTase contributed to cell cycle arrest. When 293T cells were transduced with GGTβ shRNA and treated with tipifarnib, there was again partial rescue of cell cycle arrest both in sub G1 and G2/M portions of the cell cycle. This data further suggests increased GG'd proteins are involved in cell cycle arrest from FTI.

These results collectively identify a mechanism of how FTIs induce antineoplastic effects. FTI increases GG'd proteins which contribute to reduced cell growth and also induces growth arrest in cells which have low Ras signaling.

Ras activity increases in cell lines which have reduced cell yield and cell cycle arrest in response to farnesyltransferase inhibition (FTI).

H-, N-, and K-Ras B (K-Ras) have distinct signaling outputs depending on their spatial localization within a cell. The signaling output and which cellular compartment these proteins associate with depends largely on the post translational modifications associated with these

three highly homologous proteins. Specific effectors of Ras have been identified as associating with H-, N-, or K-Ras at specific subcellular compartments. However, the signaling consequences of GG'd N- and K-Ras have not been extensively studied.

To identify what effect inhibiting farnesylation would have on Ras, we treated cell lines which have low endogenous Ras activity with the FTI, tipifarnib. We used a pull down assay which utilizes Raf-Ras binding domain (RBD) bound to agarose beads to determine the amount of active GTP-bound Ras in tumor cell lines and 293T cells treated with tipifarnib. Unexpectedly, all cell lines had increased Ras activity as a result of inhibiting FTase. This was surprising, since FTIs were expected to decrease Ras signaling. One other report identified increased ERK activation following tipifarnib treatment of pancreatic cells, but they did not identify Ras as for the source of increased ERK signaling (95). Other groups quickly dismissed Ras signaling as the source of FTI-induced effects, since they did not detect decreased signaling for Ras or any of the downstream effector proteins activated by Ras as a response to FTI. These investigators do not further comment on Ras as a mediator of response to FTI treatment (79, 86, 88, 90, 92, 94). Because of both the unexpected, radically counter-intuitive observations we made and the prevailing opinion that Ras had little to do with the cellular effects of FTIs, the burden was high for us to prove that Ras accounted for any effects seen after FTI treatment. To ensure that increased Ras activity arose directly from inhibiting farnesylation and not an off target drug effect, we used a molecular approach to specifically impede farnesylation: FTβ shRNA. The enzymes FTase and GGTase have homologous α subunits and different β subunits, so each enzyme can be preferentially targeted by creating a drug to bind to or by producing shRNA to the beta subunit of each enzyme. In our experiments, FTβ shRNA increased Ras activation in tumor cell lines and in non-tumorigenic 293T cells, indicating that inhibition of the enzyme resulted in increased Ras activity. This confirms our interpretation that increased Ras activation with FTI is a specific effect and not due to an indirect drug effect.

To demonstrate that Ras was increasingly GG'd in tumorigenic and normal cells as a result of FTI, we treated the same cell lines with pharmacological inhibitors of prenylation. Immunoblot analysis indicates both N- and K-Ras are alternatively GG'd with FTI treatment in both tumor and non-tumorigenic cell lines. These findings further suggest increased GG'd Ras may be responsible for antineoplastic effects of FTIs.

We were surprised that inhibition of both FTase and GGTase resulted in increased Ras activity. Although immunoblots of N- and K-Ras, when treated with pharmacological inhibitors, allowed us to assess that both are alternatively prenylated when FTase is inhibited, we are unable to determine the proportion of each respective protein which is alternatively GG'd. Small molecules are inhibitors that rarely provide complete inhibition of an enzymes' activity. We hypothesize with combination treatment GG'd Ras is still present, as we have found tipifarnib treatment increases GGTase expression. When 293T cells were transduced with GGTβ shRNA, GGTase expression was increased when the cells were treated with 0.01 μM tipifarnib. Likewise when a RBD pull-down was performed on these lysates, there was an increase in Ras activation when compared to GGTβ shRNA treatment alone. This would further explain why Ras activity is increased with the combination of tipifarnib and GGTI-298. Our data supports Ras as an important mediator of FTI effects, specifically by increasing endogenous levels of GG'd Ras.

To confirm that FTI-increased Ras activity identified in the pull-down assay represented active complexes, we analyzed activation of downstream effectors in response to tipifarnib treatment, with each tumorigenic cell line evaluated at the proper time, given their individual proliferation rates. ERK and p38 MAPK signaling pathways were both highly activated by FTI in all three tumorigenic cell lines. Strong activation of these pathways has been associated with growth arrest and cell death in tumorigenic cells. These results further suggest that increased GG'd Ras induced by FTI is responsible for both the growth arrest and reduced tumorigenic cell growth caused by FTI.

Geranylgeranylated (GG'd) K-Ras is toxic to 293T cells

There are many proteins which are farnesylated, and some of these proteins can be alternatively GG'd when farnesylation is blocked by FTI. The effects of FTI are likely a combination of inhibiting farnesylation of some proteins (i.e., H-Ras) and alternatively GG'd other proteins (i.e., K-Ras) which would otherwise be farnesylated in the absence of FTI. We show that when FTase is inhibited, GGTase expression is increased, even in cells expressing a shRNA targeting GGTβ. Increased Ras activity and increased GGTase protein expression with FTI demonstrates that GG'd Ras does contribute to some of the effects of FTI.

N- and K-Ras are alternatively GG'd when FTase is inhibited. We wanted to determine which of these Ras proteins was responsible for reduced cell viability and growth arrest. Fiordalisi et al, transfected NIH 3T3 cells with oncogenic H-, N-, and K-Ras (90). When

treated with a FTI, oncogenic K-Ras transfected cells had increased Elk activity observed with a luciferase reporter assay (90). Elk is a downstream transcription factor that is activated by both ERK and p38 MAPKs. They interpreted increased Elk activity as resistance to FTI. However, they did not test cell proliferation under these conditions. Our work suggests this increased Elk activity was a marker for the increased overall Ras signaling, which we have shown to be toxic. Their results support our findings in that forced expression of GG'd Ras increases MAPK signaling. These results further imply that K-Ras is specifically responsible for the increase in MAPK signaling which could be directly responsible for reduced cell viability.

Mutant constructs which allow Ras to be only farnesylated or only GG'd have been used previously. The functional consequences to cells have only been analyzed with H-Ras (123). This is the Ras protein which is only farnesylated. GG'd H-Ras is unlikely to represent the same functional consequences of GG'd N-Ras or K-Ras. GG'd H-Ras is unlikely to be representative of what would normally occur in a cell because H-Ras has a different HVR. Differences in the HVR have already been determined to change localization and activation of downstream targeting of Ras family members. Thus results obtained using mutated H-Ras should not be extrapolated to other Ras species and specific results for N- and K-Ras were needed.

We created N- and K-Ras constructs which could be specifically farnesylated, GG'd, or unprenylated by creating mutations in their CAAX motif. We transduced these constructs into 293T cells and our data combined show GG'd K-Ras decreases cell viability, increases the percentage of cells with sub-diploid DNA, and arrests cells in G2/M of the cell cycle. These data mimic results found from tipifarnib treatment. These results implicate GG'd K-Ras to be at least partially mediating these anti-proliferative effects induced by FTI.

Future Directions

FTI resulted in increased Ras activity and activated ERK and p38 MAPK pathways. Inhibiting GGTβ in 293T cells resulted in decreased Ras activity. This finding suggests that GG'd Ras has a higher affinity for activating Raf and other effectors which have Raf-like binding domains such as TIAM1. TIAM1 functions as a Ras-controlled GEF activator of Rac (56). Rac is an identified activator of Mirk which in turn can activate MKK3/6, the upstream activator of p38 MAPK (57). Raf and TIAM1 have similar Ras binding domains which explains why ERK and p38 MAPK can both be activated in tumor cells in response to increased Ras activation. Raf and/orTIAM1 specifically may be responsible for the growth-inhibiting and toxic effects of GG'd K-Ras. Future experiments, beyond the scope of this thesis, could elucidate these functions.

To confirm direct activation by Ras of Raf-1 and TIAM1, immunoprecipitations could be performed. MAPKs have intricate networks and are often activated in response to variable signals within a cell. Increased Ras activity could be activating either ERK or p38 MAPKs alone or both pathways. To determine whether the activity of these two MAPK pathways are responsible for the effects of increased GG'd Ras, cells could be treated with tipifarnib, and separate immunoprecipitations could be performed with either Raf-1 or TIAM1 conjugated to agarose beads. This experiment would allow for direct analysis of how much GG'd Ras is signaling though these respective pathways. This study would also determine if these two pathways are directly activated through increased Ras activation or if the activation of these MAPKs is through integrated signaling within the cells. Activation of downstream targets and immunoprecipitations could also be analyzed in FTβ shRNA transduced cells. We hypothesize that both of these pathways are directly contributing to reduced cell viability and cell cycle arrest from increased GG'd K-Ras activity induced by FTI.

Transduction of WT K-Ras also resulted in an increased percentage of dead and/or dying 293T cells. We hypothesize this is due to increased GG'd K-Ras from the FTase enzymatic activity being fully saturated in K-Ras WT cells. To determine the activity levels of each enzyme, positively transduced cells could be sorted, collected, and then made into lysates. The lysates could be run on an immunoblot and probed for GGTase, FTase, HDJ-2, and Rap-1. HDJ-2 would be a marker for FTase enzyme activity being saturated. If the FTase enzymatic activity is saturated, unprenylated HDJ-2 would be present. The same would be true for Rap-1 and GGTase. If GGTase were saturated, increased levels of Rap-1 would not be GG'd. We

predict that cells transduced with WT K-Ras would have increased GGTase expression and an increase in unfarnesylated HDJ-2. These findings would confirm that FTase is saturated and K-Ras is increasingly GG'd in WT K-Ras transduced cells. This would imply over expression of K-Ras in cells that are not already dependent on K-Ras signaling results in increased levels of active GG'd K-Ras even in the absence of an FTI.

To determine if the level of expression of GG'd K-Ras influences cell viability, cells transduced with the Ras-mKate fusion constructs could be sorted based on their fluorescence intensity, which would correspond directly with exogenous Ras activity. GG'd K-Ras cells could be separated by low, medium, and high-expressing GG'd K-Ras cells 48 hours post transduction to determine if lower expression of this protein would have the same cytotoxic effects observed in cells with high-level expression. As signal intensity is dependent on protein expression, we hypothesize cells with less GG'd K-Ras would be able to overcome the toxicities associated with increased GG'd K-Ras more quickly than cells with higher expression.

It would be important to confirm that GG'd K-Ras is resulting in reduced cell viability and cell cycle arrest in tumorigenic cells. Transductions and transfections of K-CAIL (GG'd) could be done in the tumor cell lines SaOS2, COL, and OS187. Transduced/transfected cells could be sorted into negative and positive populations. From these sorted populations lysates could be made and cell cycle analysis could be performed. From analysis during the sort, we predict inducing GG'd K-Ras in tumor cell lines will result in a high percentage of dead and/or dying cells. We also predict that inducing expression of GG'd K-Ras would result in increased ERK and p38 MAPK signaling, an increased percentage of cells with sub-diploid DNA, and an increase of cells arrested in the G2/M portions of the cell cycle.

The results of these experiments would confirm that over expression of active GG'd K-Ras is mediating cytotoxic and antiproliferative effects. These results would further support that FTI increases GG'd K-Ras to mediate these effects.

Translational Implications

This work collectively suggests FTI is effective in reducing cell viability and inducing cell cycle arrest in cell lines that upregulate GG'd K-Ras. We assayed the change in Ras activity in response to tipifarnib in two AML cell lines that have been shown by others to be sensitive to FTI and they both had increased Ras activity. THP-1 expresses mutant N-Ras. OS187 has mutant K-Ras although it maintains low endogenous active signal. Tipifarnib treatment resulted in increased Ras activity and reduced cell viability in these cell lines. These results imply that increased Ras activity, not Ras mutational status, may be the critical feature for FTIs to be able to inhibit tumor growth. In the tumor cell lines used, increased Ras activity induced by FTI activated ERK and p38 MAPKs. We hypothesize that activation of these two pathways induces anti-tumorigenic effects in response to FTI. Analysis of patient samples from FTI therapies is important to determine which patients will benefit from this treatment. Few potential markers of good therapeutic response have been identified. From our data we hypothesize that the following tests may distinguish responders from non-responders.

1) Determine Ras activity status. We predict that responders will have low endogenous K-Ras activity before treatment. Analysis of mutational status may not correlate with response as some Ras mutations are not oncogenic.

2) Determine p53 status. We predict that patients which have rapid tumor regression following FTI will have functional p53.

3) Analyze FTase and GGTase activity over the course of FTI treatment. We predict that responders will have increased GGTase activity with FTI treatment after the first round of therapy, which will be sustained throughout treatment.

4) Correlate increased ERK and p38 MAPK activity with increased GGTase activity. We predict that responders will have sustained increased ERK and p38 MAPK activation.

Further studies would need to be conducted to determine if other FTIs also increase Ras activity to increase ERK and p38 MAPKs signaling in order to verify if the analyses suggested would be applicable to all FTIs.

As ERK was activated in response to tipifarnib in non-tumorigenic and tumor cell lines, p38 MAPK activity may be predictive of response in specifically tumorigenic cells (Appendix I, Figure 13). This could be further investigated to determine if combinational therapy of FTI with p38 MAPK activators could be used to preferentially inhibit growth of tumorigenic cells.

Increased ERK activity may also be mediating anti-tumor response from FTIs. As the non-tumorigenic 293T cells had increased activation of ERK after tipifarnib treatment (A I 13), further studies would have to be conducted in non-immortalized cells to determine if ERK signaling is increased after tipifarnib treatment in these cells. If ERK signaling is effected in non-immortalized cells, combination therapy with tipifarnib that increases ERK signaling may be toxic to non-tumor cells in patients.

Combination therapies with tipifarnib and therapies that activate these two MAPK pathways may be good options for combination therapies. Current clinical trials are often focused on inhibiting Ras/ERK signaling; our data suggests activation of these pathways may be a good therapeutic approach. Research has shown that a strong increase in Ras/ERK activity can reduce tumor growth and metastasis; however this knowledge has not led to clinical trials or therapies. Understanding if increased Ras activity and increased ERK/p38 MAPK activation is universal among responders to tipifarnib treatment would allow for this therapy to be selected for specific patients who are likely to respond. Before combination therapy aimed at increasing ERK or p38 MAPKs with tipifarnib proceeds to clinical trials, initial studies in mice should be pursued to ensure that activation of these MAPKs would not result in spontaneous tumors. Increased ERK activation in non-tumorigenic cells may be the 2^{nd} or 3^{rd} "hit" transforming these cells into tumor cells.

Conclusion

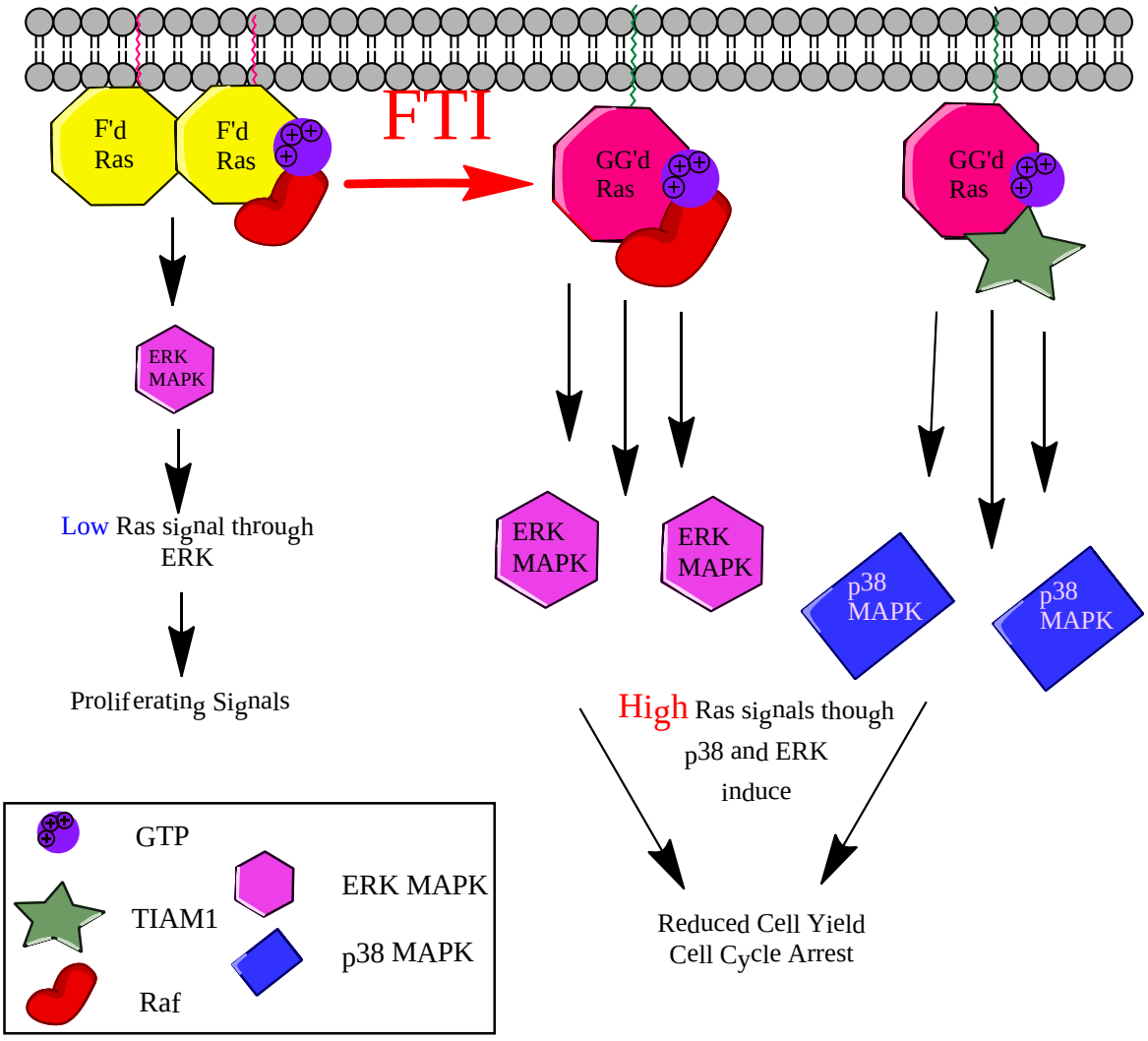

Figure 28. **Confirmed hypothesis: FTI increases GG'd K-Ras to reduced cell yield and induce cell cycle arrest.** FTI increases GG'd Ras which increases ERK and p38 MAPK signaling in tumorigenic cells with low endogenous active K-Ras to reduce cell yield and increase cell cycle arrest. Same figure as presented in figure 4.

Prior to our studies, the role of GG'd K-Ras in response to FTI was undefined. Most reports disregard K-Ras in the FTI response as it is alternatively GG'd, and thus would not be inhibited by FTI. These investigators assumed that GG'd K-Ras would function identically to farnesylated Ras. Our observations, therefore, provided a complete reversal from prevailing views, since we proved that FTI increases total Ras signaling. Increased Ras signaling in tumor types which are not dependent on Ras signaling can result in cell death, growth arrest, or senescence. This may be true whether the post translational modification is farnesylation or

GG'n. Alternatively, GG'd K-Ras may specifically induce in cell death, growth arrest or senescence in susceptible cells. Tumor cell lines that are forced to express Ras may saturate FTase, resulting in increased GG'd Ras. Since no report has determined which prenylation group is associated with Ras when its signaling results in cell death, increased GG'd K-Ras may be responsible for this alternate signaling. We used 293T cells to analyze the mechanism of farnesyltransferase inhibition. 293T cells are commonly used because they grow quickly and are easily transformed / transduced. We used 293T cells to determine if specifically GG'd K-Ras was resulting in cell death or growth arrest. We found GG'd K-Ras increased cell death and arrested cells in the G2/M portions of the cell cycle. Transduction with farnesylated-only K-Ras did not result in increased cell death in 293T cells. This result suggests that not only is increased Ras protein expression necessary to induce cell death and cell cycle arrest, but specifically increased GG'n of K-Ras is responsible for FTI mediated effects on cell proliferation and cell cycle arrest. In tumor cell lines we found ERK and p38 MAPKs were increased from FTI. Our data combined suggests FTI increases GG'd K-Ras activation which then activates ERK and p38 MAPKs to result in reduced cell viability and cell cycle arrest.

APPENDIX

Appendix I:
A: Functional Ras expressing an N-terminal mKate tag.
B: Long term affects of N- and K-Ras mutants transduced into 293T cells and K-CAIL associates with the PM.

Rationale

To assess if increased geranylgeranylated (GG'd) Ras was causing the increased cell cycle arrest and reduced cell yield from FTI, Ras constructs capable of only one type of prenylation, or unable to be prenylated were developed. This requires point mutations be made to the C-terminus of Ras in order to mutate its CAAX motif. N-Ras and K-Ras are the two Ras family members which can be alternatively GG'd when farnesylation is inhibited. To discriminate transduced from endogenous Ras protein a fluorescent tag could be added to the N-terminus of Ras, since tags added to the C-terminus would be cleaved after the protein was post-translationally modified. After Ras is prenylated, the AAX at the end is cleaved and the C-terminal cysteine is methylated. Furthermore a tag at the C-terminus might interfere with Ras prenylation. We created an N-terminal naturally fluorescent mKate tag fused to WT N-Ras and WT K-Ras. The goal of part A of this section is to ensure a N-terminal mKate fusion to Ras would be functional if transduced into 293T cells, in preparation for creating mutant Ras proteins which are only farnesylated, GG'd, or not able to be prenylated. The goal of part B is to determine long term consequences of transducing N- and K-Ras mutant constructs into 293T cells.

A: Functional Ras expressing an N-terminal mKate tag.

Results

mKate fluorescent tag fused to WT N-Ras and K-Ras is functionally active

A naturally fluorescent mKate was vector was purchased from Origene. The mKate coding region was cloned into a retroviral vector with a puromycin resistance gene under the direction of an internal ribosome entry site (IRES) element to allow for selection, MipR1 (Figure 24 A). mKate was added to the 5' end of the cloning site of this vector so it could fuse to the N-terminus of Ras. A Ras mutated to only express geranylgeranylated (GG'd) Ras was fused to N-terminally to mKate (further discussed in the next chapter) (A I 1). This image represents membrane associated Ras and demonstrates fluorescently N-terminally labeled Ras is able to associate with the membrane.

A I 1

A.

B.

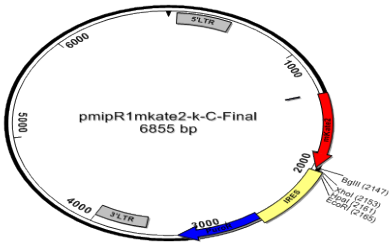

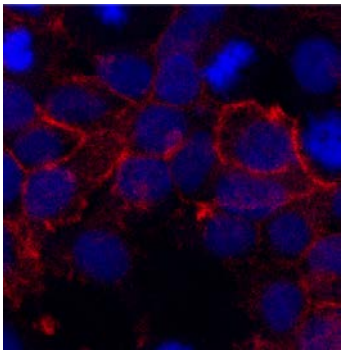

A I 1. N-terminal addition of a naturally fluorescent mKate vector. A. Backbone of the mKate vector where the naturally fluorescent marker is added to the N-terminus of a protein. 5' and 3' long terminal repeat sequences allow the retrovirus to insert their genetic sequences into the infected cells. IRES allows for transcription of the puromycin gene. B. Confocal image of mKate N-terminally fused to GG'd Ras protein.

For this tag to function, we wanted to ensure that the mKate fusion to Ras was GTP-bound. The following experiments were conducted in 293T cells as they are easily transduced

or transfected and would allow us to determine if this fusion to mKate results in functional Ras proteins. To determine if mKate would disrupt normal WT N-Ras or K-Ras, two vectors were created. One with only a puromycin selection and another with puromycin selection and mKate fused to WT N-Ras and K-Ras. 293T cells were transduced with an empty puromycin vector, a puromycin and mKate empty vector, or both of these vectors fused to WT N-Ras or K-Ras. Cells were selected in puromycin for 5 days as this was the length of time necessary to kill untransduced 293T cells. Cells were grown in normal culture conditions in a 10 cm dish. Lysates were collected when cells reached 80% confluence. Lysates were used in a Ras pull-down to isolate active Ras-Raf-RBD complexes. An immunoblot was run and the membrane was probed with a panRas antibody. The pull-down shows N-terminally fused N- Ras and K-Ras are both functionally active (A I 2). Since mKate fussed Ras constructs were functionally active and we could discriminate transduced / transfected Ras protein, from endogenous protein we chose to use this vector for further experiments. Two bands appear approximately at 43 and 45 kDa in mKate transduced N-Ras and K-Ras cells. The prenylation status of these bands will be discussed shortly.

A I 2

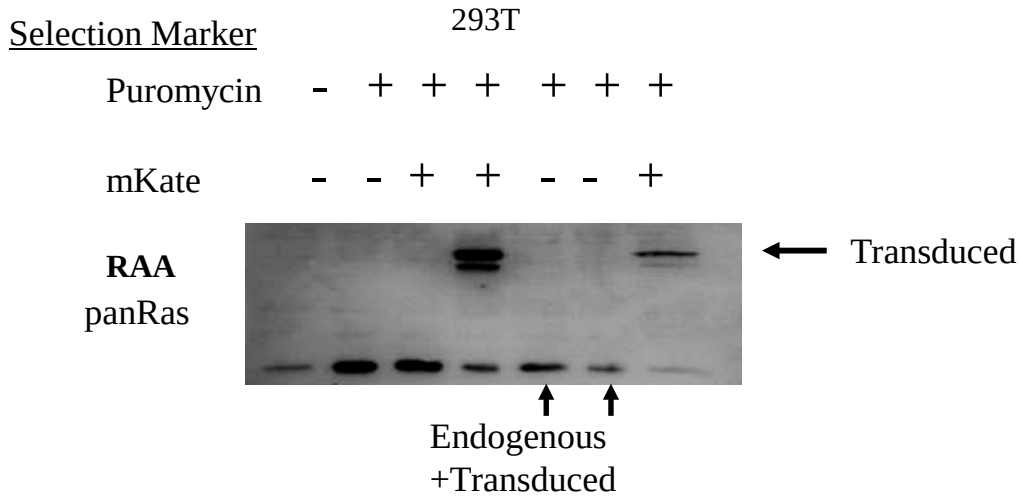

A I 2. In 293T cells the N-terminal mKate fusion to WT N- or K-Ras is active as shown by a Ras activity assay. To determine if the mKate tag would interfere with Ras function, WT N-Ras and K-Ras were transduced into 293T cells with a retroviral vector which had puromycin selection with and without an mKate tag. After puromycin selection lysates were collected and a Ras activity assay was performed as described in Figure 2. The 43 or 45 kDa band represents transduced protein when mKate is fused to Ras. When the transduced vector does not contain mKate then the Ras protein transduced into the cell will run at the same mobility as endogenous active Ras, 21 kDa.

Low, medium, and high sorted N-Ras and K-Ras transduced cells

To determine if different intensities of mKate fluorescent emission correlated or changed Ras expression, we sorted transduced WT N-Ras and K-Ras cells. Low, medium, and high mKate fluorescing cells were sorted and collected (A I 26 A). These sorted cells were treated with 3X gentamicin and penicillin/streptomycin DMEM media for 3 days to ensure they were not contaminated from the sorting machinery. These cells were then plated in a 10 cm tissue culture dish and allowed to grow to 80% confluence. Lysates were collected and used for a Ras pull down assay. As mKate expression increases Ras activation levels increase (A I 26 B). Endogenous levels of activated Ras increased in N-Ras transduced cells and decreased in K-Ras transduced cells.

A I 3

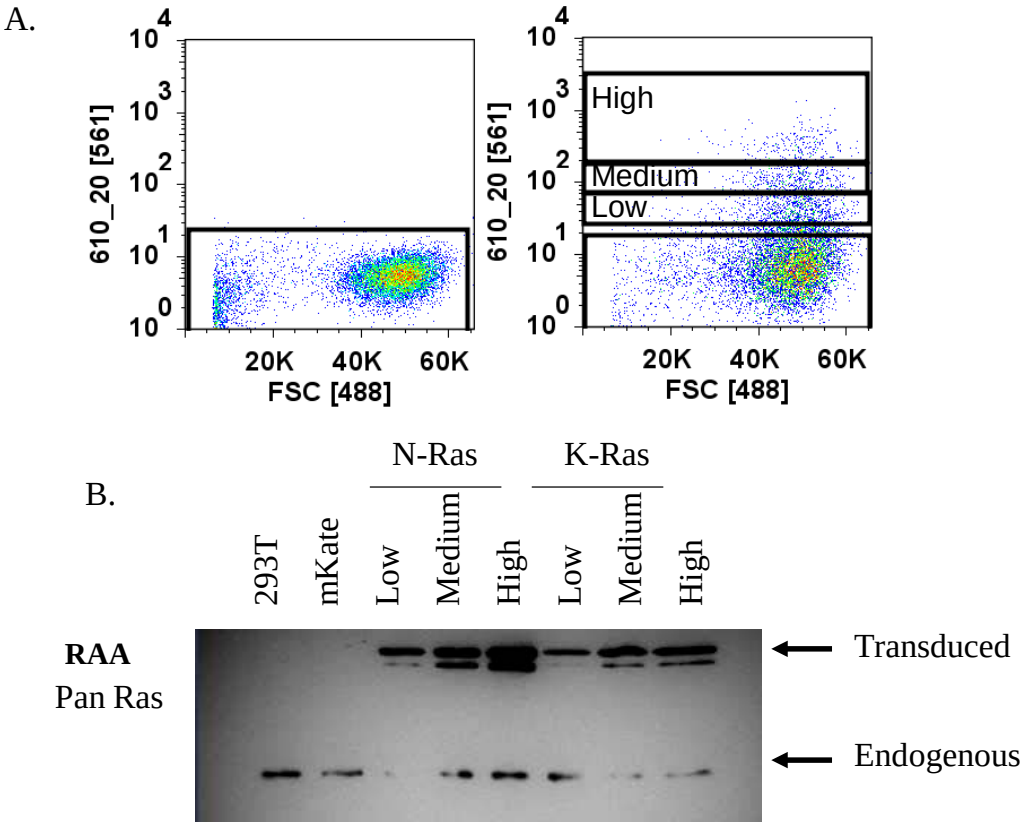

A I 2. Increased mKate fluorescence does increase Ras activation in 293T cells. A. 293T cells transduced with WT N-Ras or K-Ras underwent cell sorting based on the fluorescent intensity expressed. B. Sorted cells were grown, lysates were collected, and then used for the Ras pull down as described in Figure 2. As in Figure 25 the upper band on this blot represents transduced active Ras protein and the lower band represents endogenously expressed active Ras.

Sorted cells from figure 26 were also used to analyze the growth ability of these transduced cells. Cells were plated in triplicate in 6-well plates at a density of 30,000 cells per well and allowed to grow for 7 days. TF treatment was added one day after cells were plated. After growth for 7 days, nuclei were isolated were counted by an automatic Coulter counter as described in materials and methods. Two weeks after the initial transduction there was no difference in growth among the sorted WT N- and K-Ras cells compared to mKate transduced empty vector or 293T cells (A I 4). This demonstrates there is no effect on cell proliferation in 293T cells with different expression levels of stable N-Ras or K-Ras proteins.

A I 4

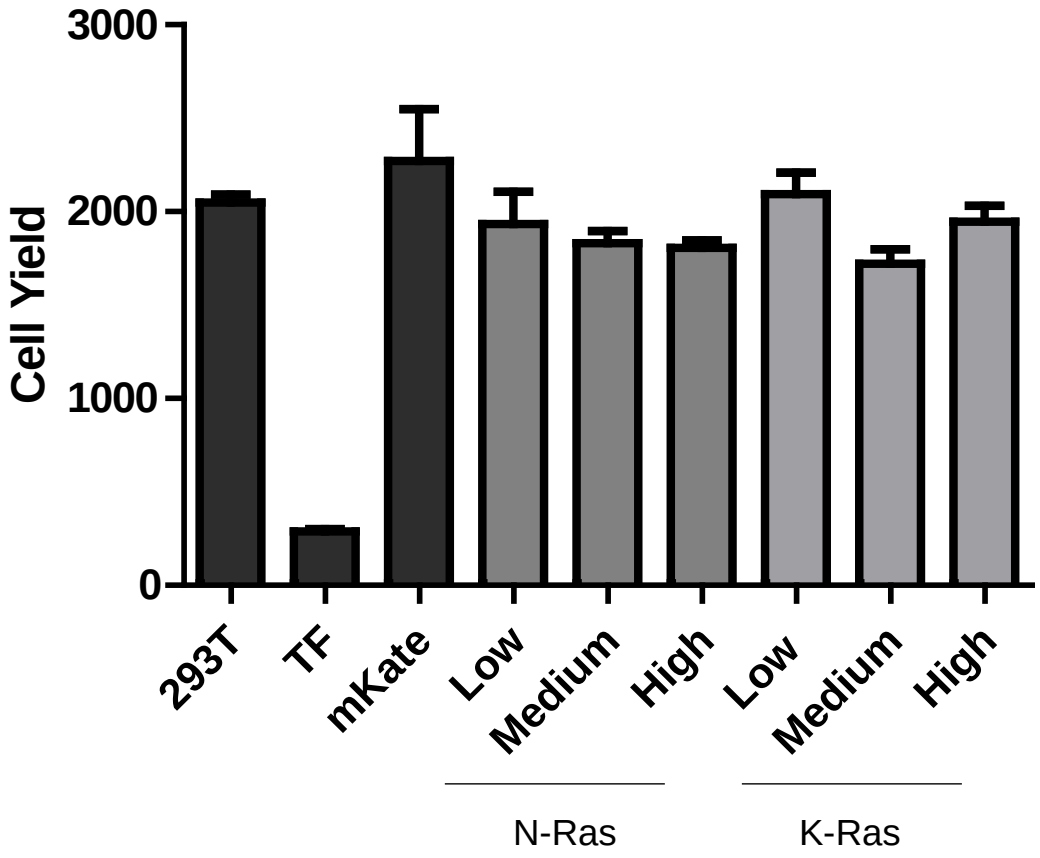

A I 4. No difference of cell growth in N or K-Ras WT transduced 293T cells when sorted with different fluorescence intensities. Sorted cells were plated in triplicate in 6-well dishes at 30,000 cells per well, grown for 7 days, and counted as described in Figure 7.

The initial Ras pull down experiment showed two upper bands in cells transduced with the N-terminal mKate tag fused to WT N- and K-Ras. To determine if one of these bands represented prenylated protein and the other represented unprenylated protein low, medium,

and high sorted cells were treated with a FTI and GGTI in combination for 48 hours. One the initial immunoblot is difficult to visualize the size difference between the two upper bands (A I 5 A). Two selected lysates were ran on a 35 mm gel apparatus and ran for 5 hours for better resolution of transduced protein. Running the lysates on a larger gel allows the increased mobility shift from prenylated (~45 kDa) to unprenylated (~46 kDa) transduced protein to be visualized (A I 5 B). The band that runs at a lower mobility in transduced Ras lysates is likely to be from a truncated mKate protein.

A I 5

UP- Unprenylated
P- Prenylated

T-Transduced
E-Endogenous

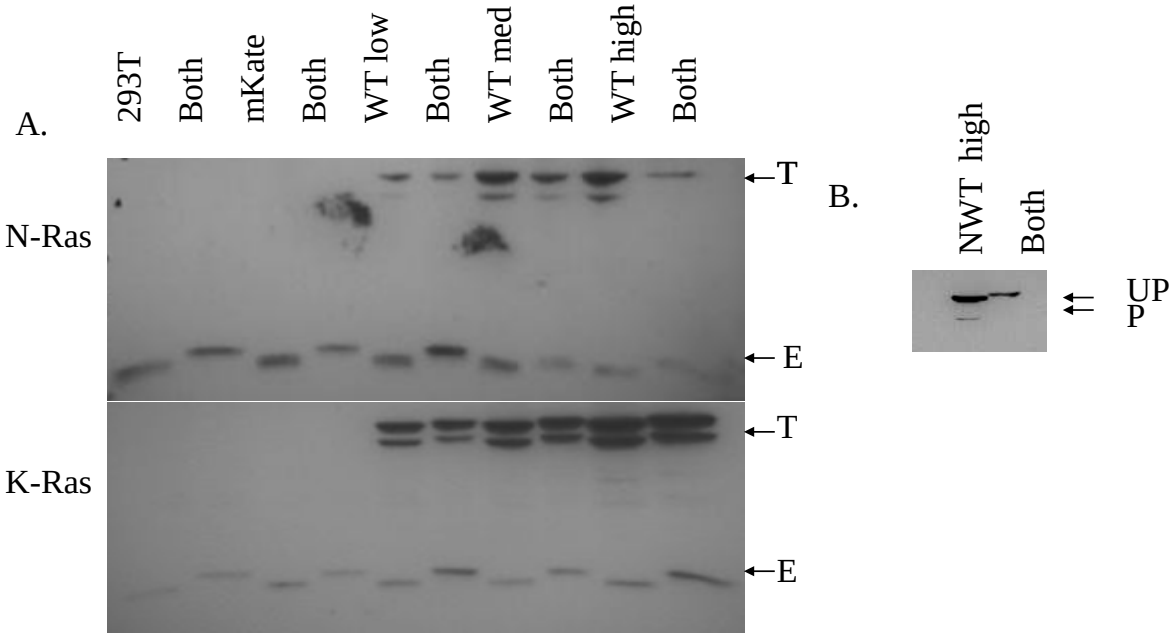

A I 5. 293T cells transduced with wild type N and K-Ras produce proteins that are prenylated. N-Ras and K-Ras sorted cells were untreated or treated with 1 µM tipifarnib in combination with 4 µM GGTI-298 to block both prenylation enzymes to ensure the protein being expressed is fully unprenylated. B. To better discriminate migration differences between the top bands the same lysates were ran on a 35mm gel for 5 hours. This allowed for a better separation of the top bands in A.

Immunofluorescence with mKate

To ensure that the mKate tag would allow visualization of transduced Ras proteins, WT K-Ras transduced cells were plated on 4 chamber tissue culture slides. Untransduced 293T

cells and mKate empty vector cells were plated as controls. K-Ras WT transduced cells were treated with 1 µM tipifarnib for 48 hours. Nuclei were stained with Sytox-green so they could be visualized by confocal microscopy. mKate is naturally fluorescent so no further staining was necessary. Untransduced 293T cells serve as a control. mKate stained cells have dispersed signal throughout the cytoplasm. WT K-Ras transduced cells have little membrane staining and have aggregated staining probably from degradation of K-Ras protein (A I 6). In WT K-Ras transduced cells treated with tipifarnib there is a more intense signal and it appears to have a higher affinity for the membrane. This suggests with tipifarnib treatment WT K-Ras protein is associating with the PM and is active.

A I 6

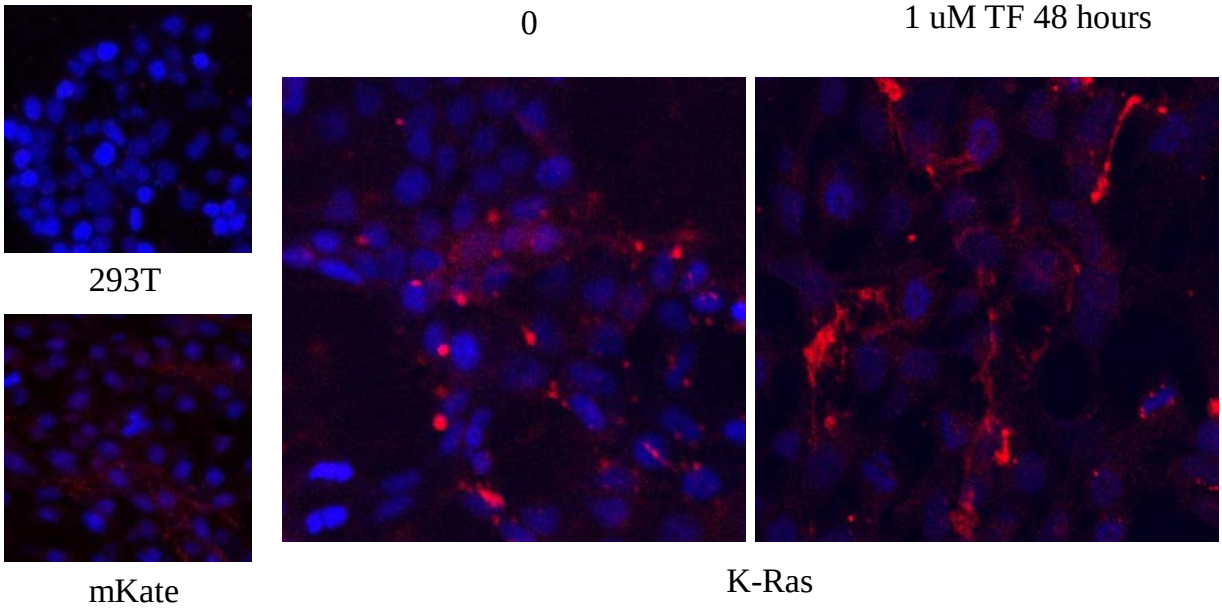

A I 6. Redistribution of Ras with tipifarnib treatment in 293T cells. mKate labeled K-Ras cells were mounted on a 4 well slide treated with tipifarnib (TF) for 48 hours, fixed using standard immunofluorescence techniques, nuclei were stained, and images were acquired on a confocal microscope. mKate and the nuclear stain were overlaid.

Summary part A

As Ras acquires several post-translational modifications on its C-terminus, an N-terminal tag was necessary to distinguish endogenous from transduced protein. We devised an N-terminal mKate tag which naturally fluoresces. Incorporating a fusion protein would also allow for separation of transduced and non-transduced (or transfected) cells for analysis. To verify the tag was not interfering with the ability of Ras to function, a Ras activation assay was performed. An N-terminal mKate fusion of Ras was functional as full length fusion proteins were detected at ~45 kDa. Two bands of transduced proteins were detected at ~45 and 42 kDa. To ensure the 42 kDa protein was not prenylated Ras and the 45 kDa protein was unprenylated Ras we used pharmalogical inhibitors to block both prenylation enzymes in order to detect only unprenylated protein. Unprenylated protein migrated slower than 45 kDa. Therefore we suspect the 42 kDa fusion protein detected is a truncated mKate-Ras fusion protein. Active Ras mKate fusion proteins are active as demonstrated by the Ras pull down showing an increase of active Ras-RBD complexes in WT N-Ras and K-Ras transduced 293T cells.

Stably transduced WT N-Ras and K-Ras cells were assayed for Ras activation status, cell proliferation, and immunofluorescence to detect localization of transduced protein. We determined fluorescence intensity is proportional to the amount of transduced N- or K-Ras protein. This transduced protein still appears functionally active as shown by a Ras pull down with low, medium, and high mKate fluorescing cells. Endogenous levels of Ras increased in WT N-Ras transduced cells and decreased in K-Ras transduced cells. This suggests forced expression of WT K-Ras might be toxic to 293T cells and the cells respond by decreasing the activity of endogenous Ras.

As mkate is naturally fluorescent, confocal imaging can detect where the fusion protein is located within a cell. When cells were sorted by low, medium, and high fluorescent intensity, the light emission from low and medium sorted mkate positive cells were not visible by confocal microscopy. However, high fluorescent sorted K-Ras cells did have detectable mKate signal. In untreated cells, K-Ras signal was located diffusely throughout the cell and high punctate signal was also detected in cells. This punctate signal is likely to be located in endosomes where Ras is being degraded to compensate for the higher rate of protein produced in the cells. It was evident that K-Ras transduced cells treated with tipifarnib for 48 hours relocalizes K-Ras to the membrane where it can be functionally active. These findings confirm with tipifarnib treatment Ras signaling is upregulated and localized to the PM to intensify Ras downstream signaling.

The mKate fluorescent tag was undetectable in low and medium N- and K-Ras sorted cells. An N-terminal truncated GFP fusion to H-Ras has been confirmed to have fluorescent signal and to not interfere with H-Ras localization (124). This fusion may allow for sorting low, medium, and high fluorescent populations for better microscopy images. This mKate fusion tag was created as it is supposed to overcome imaging limitations. This tag has been used for numerous applications including cell labeling and whole body *in vivo* imaging. However mKate expression did not allow for detectable imaging when sorted in low and medium fluorescent intensity when fused to N- or K-Ras. For *in vitro* purposes, a GFP tag may allow for better imaging of low and medium expressing N- and K-Ras fusion proteins. This would allow for us to determine if there are differences in the localization of N- and K-Ras with different levels of induced expression. We are also interested in determining if there is an increase and a shift to PM localized N- and K-Ras when low and medium fluorescent cells are treated with TF. We predict there will be increased Ras signal at the PM when cells with lower levels of Ras expression are treated with TF.

This section was a prerequisite to creating mutant Ras proteins. These mutant Ras proteins will allow us determine the functional consequences of N- and K-Ras proteins which can only be GG'd. **The work presented in this section confirms that N-terminally mKate-tagged Ras proteins are functionally active to use as a tool for identifying transduced protein.**

B: Long term affects of N- and K-Ras mutants transduced into 293T cells and K-CAIL associates with the PM.

Results

Point mutations in the CAAX motif of N-Ras and K-Ras were made in order for the Ras proteins to be WT (preferentially farnesylated (F'd)), CVLS (F'd only), cysteine mutated to serine (unprenylated), and CAIL (GG'd only) (Figure 14 A). To analyze the long term functional consequences of the constructs they were transduced into 293T cells and selected with puromycin for 3 days. These cells were then sorted in the FACScore facility based on mKate expression. To determine if increased mKate fluorescence correlated with increased active transduced Ras as in part A, CAIL and CVLS were sorted based on fluorescent intensity. We hypothesized CAIL to be toxic at high levels so sorting into these three expression levels may allow us to see toxicities associated with GG'd Ras. Stable transductions were plated in 10 cm dishes and lysates were collected once cells reached 80% confluence. As anticipated, increased intensities did correlate with increased Ras activation (A I 7 A). It was difficult to see separation of migration of unprenylated and prenylated proteins so remainders of the same lysates were ran on a 35 mm gel for 5 hours. The increased mobility of unprenylated protein from the C->S mutant protein runs at a higher mobility than prenylated proteins (A I 7 B).

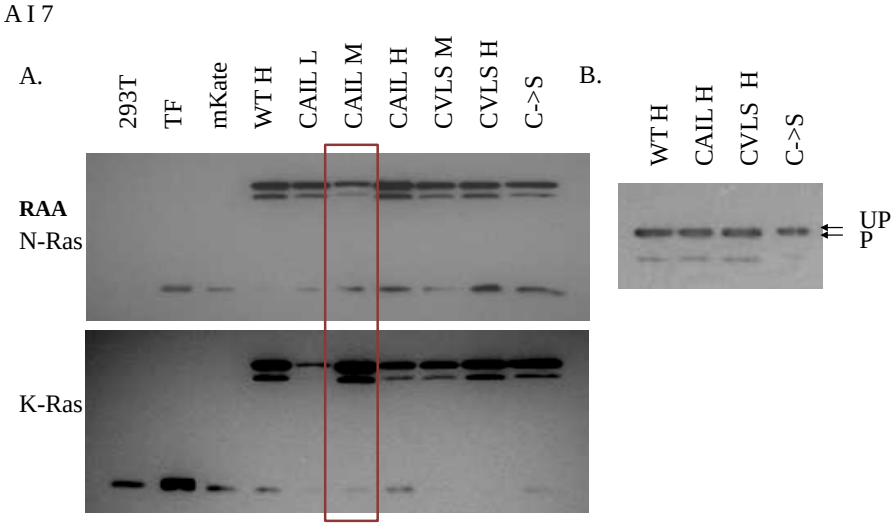

A I 7. Mutant N-Ras and K-Ras transduced 283T cells have increased activated Ras. A. Cells were transduced with mutant N or K-Ras. The mutant protein is created by mutations in the CAAX motif of both N-Ras and K-Ras. WT Ras is preferentially farnesylated. CAIL is a Ras mutant which can only be GG'd. CVLS can only be farnesylated. C->S can not be prenylated. Cells were sorted as the wild type cells in figure 26. Cells were plated and grown to 80% confluence, lysates were made and a Ras pull down was performed as described in figure 2. N-Ras and K-Ras CAIL medium expression lysates were swapped when loading the immunoblots. B. The remaining 10 µl from A. was run on 12% 35mm gel for 5 hours to get better separation of the prenylated and unprenylated bands represented by the mutants.

To ensure that these active Ras-RBD complexes were resulting in increased downstream signaling, immunoblots were run from the same lysates, and probed with phosphorylated MEK or AKT antibodies (p38 MAPK is not activated in 293T cells treated with tipifarnib) (A 1 13). K-Ras proteins preferentially increase MEK and ERK signaling (A I 8). Transduced N-Ras proteins activate both the AKT and ERK pathways.

A I 8

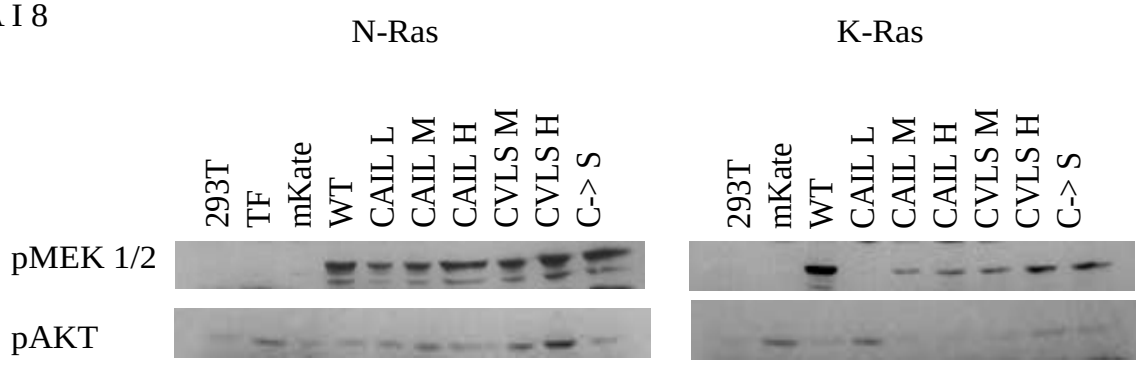

A I 8. pMEK1/2 and pAKT are increased in N-Ras and K-Ras transduced 293T cells. Lysates used from the Ras pull down were used to run on immunoblots to analyze downstream targets pMEK and pAKT.

Next we wanted to determine if GG'd N-Ras and K-Ras had an effect on cell proliferation. As stated previously, transduced cells were cultured for two weeks post transduction before experiments could be performed. This was partially due to the initial slow growth of K-CAIL after sorting positive cells. Transduced cells were plated at a density of 30,000 in triplicate in 6-well dishes. Cells were cultured in normal conditions for 4 days. After 4 days nuclei were isolated and counted with an automatic Coulter counter as described in materials and methods. K-CAIL (GG'd) was the only transduced construct that had decreased cell yield when grown for four days (A I 9). It is likely the initial affects (function, cytotoxic, or cytostatic) of the mutant transductions are overcome over time. Cells within a population often can manipulate other cellular pathways to compensate for signals which are originally cytotoxic. To exclude this possibility we designed an experiment which would allow us to see initial effects of these transduced mutant N-Ras and K-Ras proteins.

A I 9

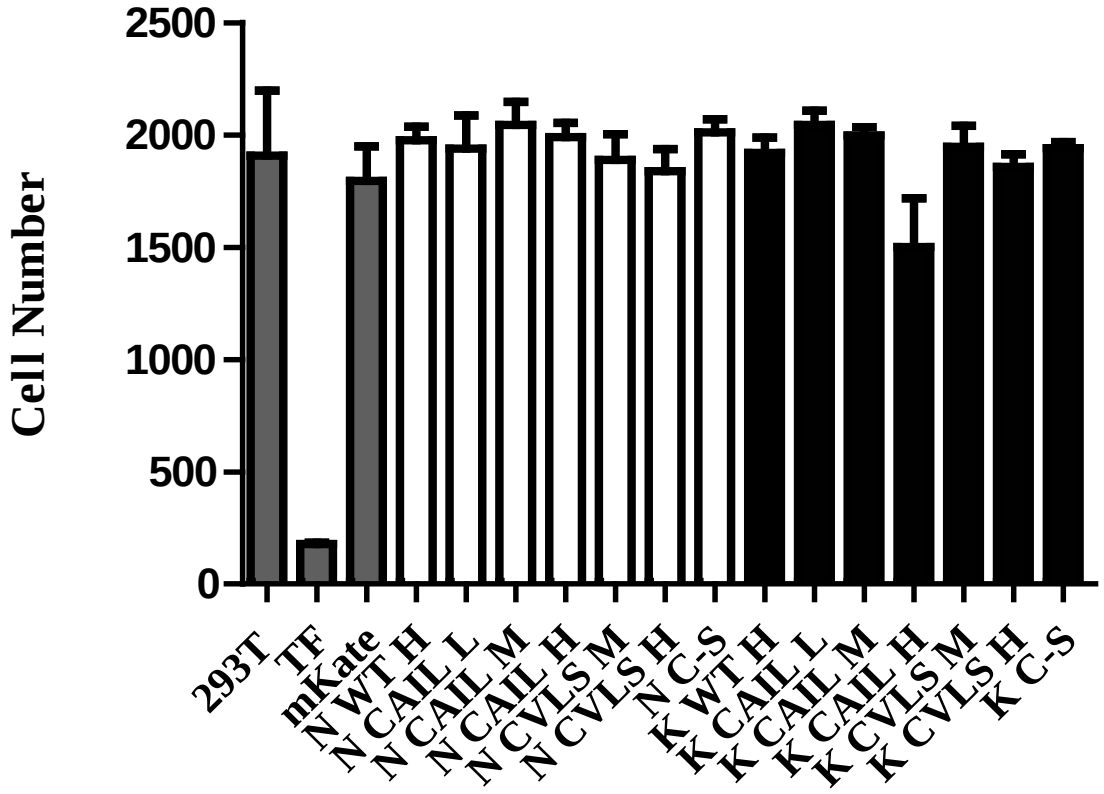

A I 9. K-CAIL high sorted 293T cells reduces cell yield. Stably transduced cells were sorted then plated at 30,000 cells per well in triplicate in 6-well plates. Cells were grown for 4 days then counted as described in Figure 7.

Initial effects of N-Ras and K-Ras mutants

In order to determine initial effects of these constructs, cells were transduced and sorted 48 hours post transduction. Unsorted transduced cells were continuously grown in culture to assess mKate expression in these cells over time. Transduced cells were sorted for mKate positive expressing cells on days 2, 5, 7, 9, and 14 post transduction. Expression of mKate in the sorted population was quantified for each of these days. N-Ras and mKate have similar transduction efficiency which range from 50-80% 5 days post transduction (A I 10). K-Ras is transduced at a much lower efficiency and is only 20-30% mKate positive 48 hours post transduction. After two weeks the percent of mKate positive N-Ras and mKate transduced cells are reduced to half of the percent positive cells 48 hours post transduction (20-32%). After two weeks post transduction, K-Ras constructs are only 1-4% of the population sorted.

These constructs are out grown by the untransduced portion of 293T cells. The reduced growth of mKate-positive cells also indicates these K-Ras constructs are toxic to 293T cells.

A I 10

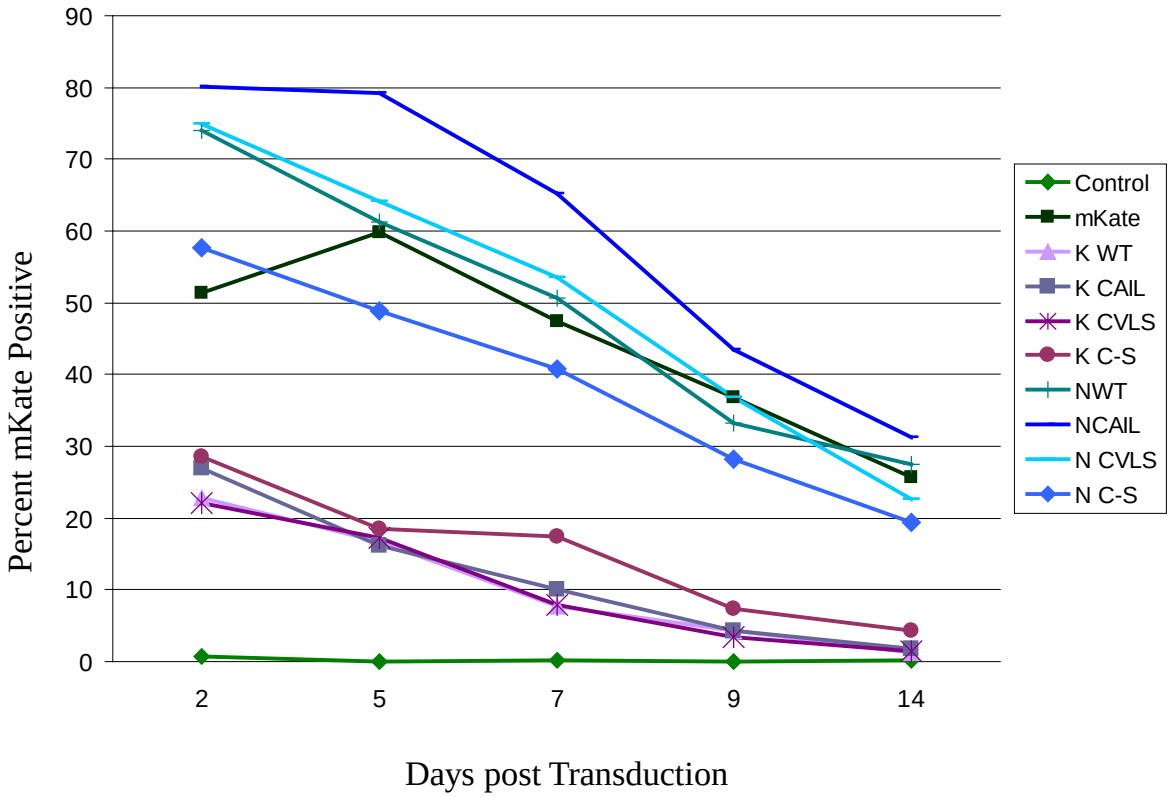

A I 10. mKate expression is lost in K and N Ras mutant constructs over time in 293T cells. Cells sorted 48 hours, 5, 7, 9 and 14 days after transduction were analyzed for mKate expression. The percent mKate positive cells were graphed over time.

CAIL (GG'd) mutant and tipifarnib treated WT cells localize to the membrane

Stable transductions from the positive cells from the 48 hour post transduction sort plated in 4 well chamber slides at a density of 30,000 cells per well in normal tissue culture conditions. Media was removed after 48 hours, cells were fixed, permeablized, and nuclei were stained with Sytox green. Images were taken on a confocal microscope. Although all cells plated were previously sorted positive for mKate signal, not all cells show mKate-positive Ras fusion proteins. mKate signal was not detectable for confocal microscopy in K-Ras constructs, therefore only N-Ras fusion proteins could be analyzed. WT and C-S mutant mKate-fused proteins are mostly cytoplasmic (A I 11). CAIL and CVLS both have cytoplasmic and membranous staining. CAIL (GG'd) fused protein has much more membranous staining than

WT and the other mutants. This suggests GG'd Ras associates with a higher affinity to the membrane. This was confirmed in two independent experiments.

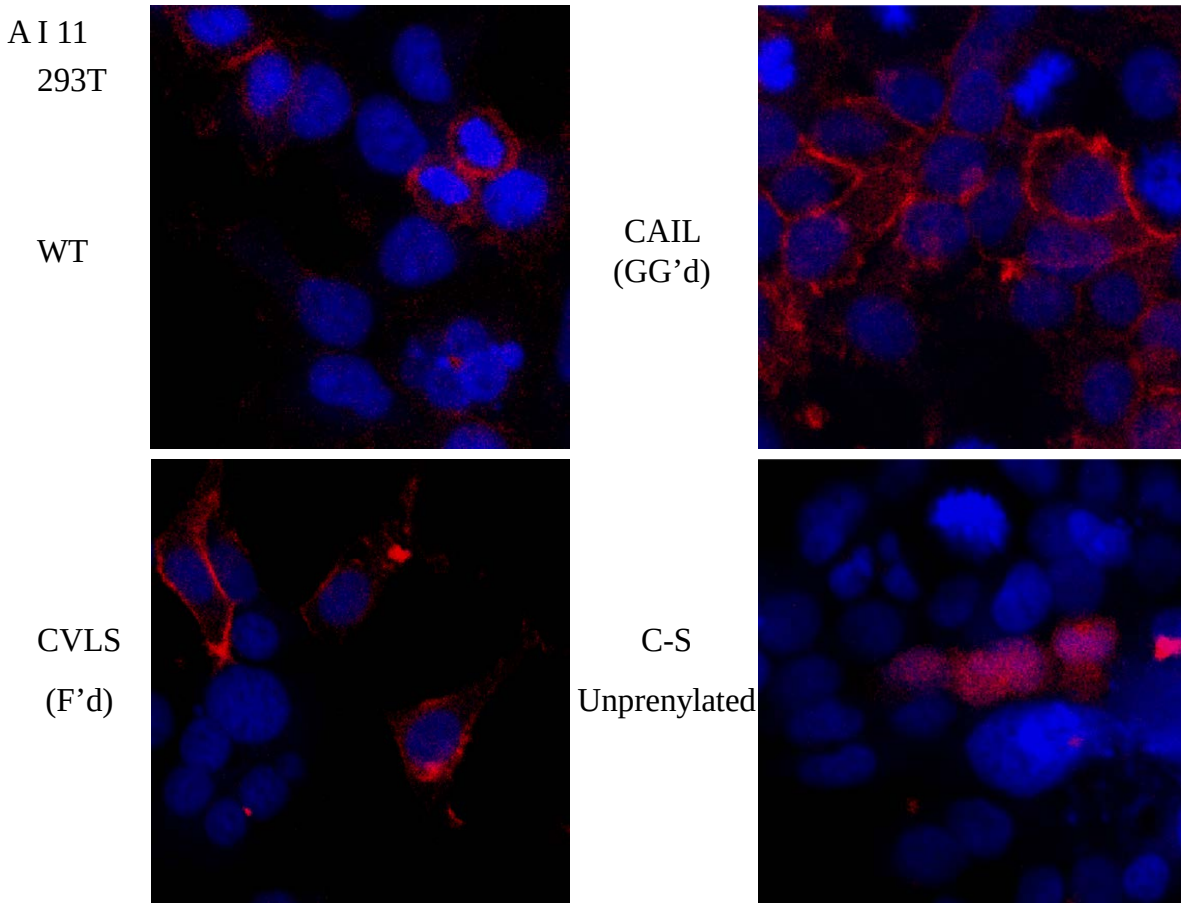

A I 11. 293T cells transduced with GG'd Ras associates with the membrane. Sorted cells were treated with antibiotics as indicated in figure 29 then plated in four well chamber slides 30,000 cells. Cells were fixed and nuclei were stained with Sytox green.

Comparison of tipifarnib-treated WT staining and CAIL (GG'd) staining show both have a greater affinity for the membrane than WT protein alone (A I 12). This suggests Ras proteins which are GG'd have a greater affinity for the membrane and are likely to have increased activation of downstream targets because of its localization.

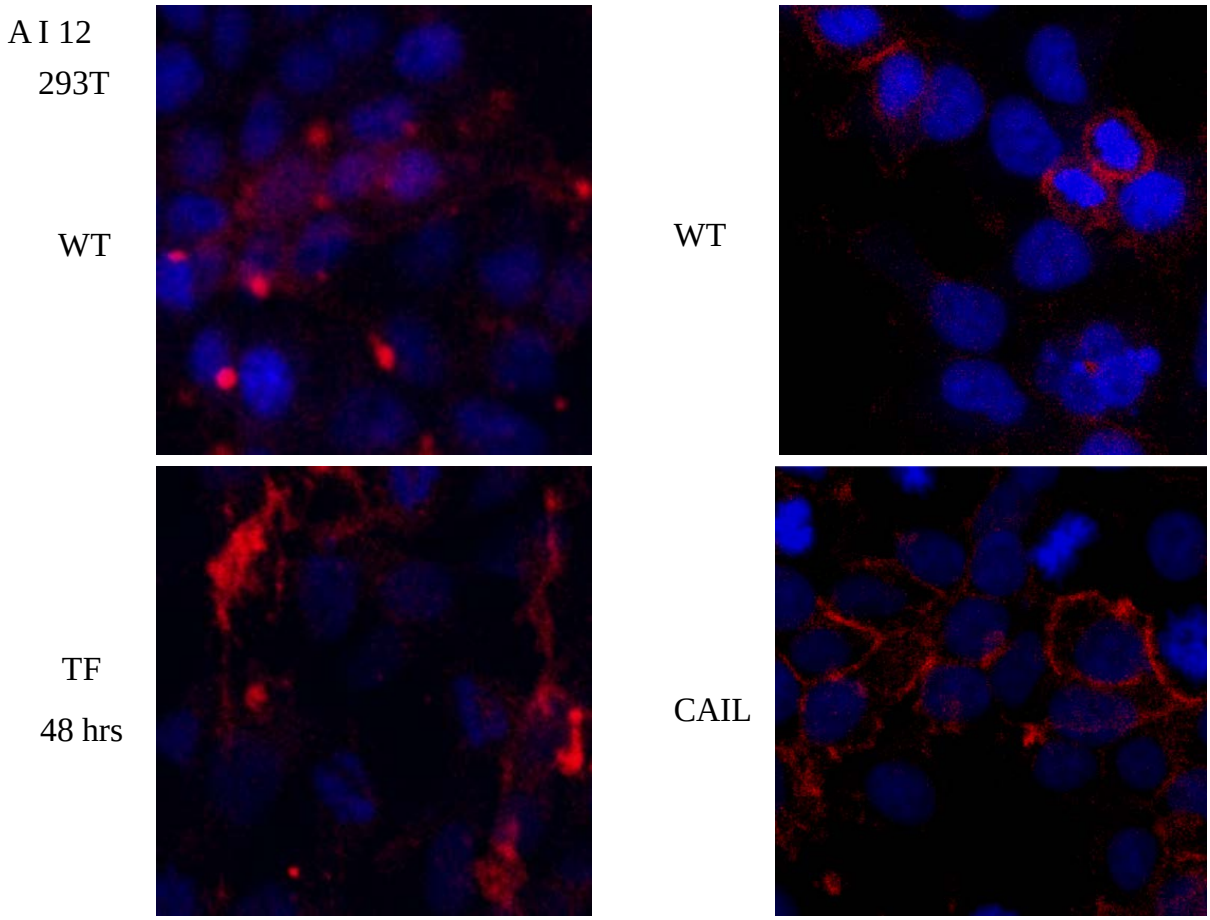

A I 12. Localization of GG'd Ras resembles tipifarnib (TF) treated 293T cells. Tipifarnib treated and GG'd only transduced cells show more membranous staining.

FTI results in differential signaling of Ras in non-tumorigenic 293T cells.

293T cells have up-regulated ERK signaling and AKT signaling (A I 13). p38 MAPK signaling is low in treated and untreated 293T cells. This demonstrates non-tumorigenic and tumorigenic cells have activation of different signaling pathways related to increased Ras activation with tipifarnib treatment.

A I 13

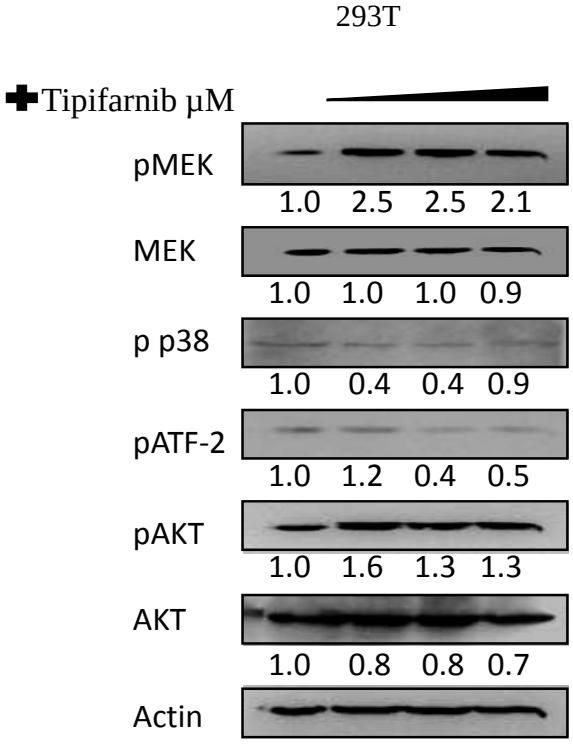

A I 13. ERK and AKT are activated in response to tipifarnib treatment in 293T cells. 293T cells were treated with increasing concentrations of tipifarnib for 24 hours. Lysates A were probed with listed phosphorylated and total protein antibodies to determine which downstream proteins of Ras were activated in response to blocking farnesyltransferase.

Summary

Stable transduced 293T cells produce active mKate-fused Ras constructs that are able to activate downstream effectors. Transfected GG'd K-Ras does transiently mimic FTI effects in 293T cells. The cells which escape cell death and cell cycle arrest possibly have acquired mutations to overcome the toxicity of GG'd K-Ras. It would be interesting to isolate colonies which are able to overcome GG'd K-Ras and do mutational studies on key cell cycle regulators such as p53 and p21. We would predict these genes are mutated in order to overcome the increased expression of GG'd K-Ras.

We hypothesize that the cells which are able to overcome increased expression of GG'd K-Ras have altered the levels of FTase and GGTase. We would predict initially GGTase is overworked and cannot geranylgeranylate all of the transduced GG'd K-Ras. These cells which have saturated GGTase probably have additional mutations which over time allow the cell to become dependent on over-expressed Ras. We predict that, to overcome increased Ras expression initially, GGTase is saturated and over time some cells survive increased GG'd Ras. Another possibility is that these transduced / transfected GG'd K-Ras cells have decreased GGTase expression, allowing them initially to overcome this transduced / transfected protein, and adapt to increased GG'd K-Ras over time.

The mutant (C->S) Ras in which the C-terminal cysteine is mutated to serine and unable to be prenylated was functionally active in 293T cells although it could not associate with the membranes. We would like to transduce these mutants into the tumorigenic cell lines OS187 and SaOS2. We could then test Ras activation status and ERK / p38 MAPK activity; this would allow us to determine if Ras has to be prenylated in order to be active in tumor cell lines.

Unlike the tumor cell lines, 293T did not have increased activation of p38 MAPK. This normal cell line had very low endogenous expression of p38 MAPK compared to our tumor cell lines. However, like the tumor cell lines, 293T cells did have increased MEK activity in response to FTI. Additionally, AKT activation was increased in 293T cells whereas only COL had increased AKT activation (data not shown) in response to FTI. This suggests tumor and normal cell lines have different signaling responses, as tumor cell lines tested here have increased ERK and p28 MAPK activation and the normal 293T cells have increased ERK and AKT activation when treated with tipifarnib.

Appendix II: Effects of FTI on clonogenicity and invasiveness in tumor cell lines.

Rationale

An increase in Ras activation is normally thought to result in proliferation signals, as Ras signaling has been shown to be involved in many aspects of tumor. Over the last decade increased Ras activity in cells which have low levels of endogenously active Ras have been shown to result in anti-proliferative signals. Specifically this increase of Ras activation has been linked to apoptosis, senescence, and/or cell cycle arrest. As shown previously, SaOS2, COL, and OS187 all have endogenously low Ras activation. We wanted to determine if blocking farnesylation and increasing Ras activation affects other aspects of tumorigenicity such as clonogenic cell growth and invasion. Clonogenicity is another hallmark of cancer, and there are two assays which can distinguish which proportion of cells in a given population have a propensity to form tumor *in vivo*. These two assays are distinct in that the proportion of cells which can form colonies in anchorage-dependent assays may be unable to form colonies in an anchorage-independent manner. We chose to perform both of these assays with our tumorigenic cells and assess if there were differences between anchorage-independent and –dependent growth of OS187, COL, and SaOS2 with tipifarnib treatment. The goal of this section is to assess the effects of farnesyltransferase inhibition on other functional hallmarks of cancer in OS187, COL, and SaOS2 tumor cell lines.

Results

Clonogenic Abilities of Tumorigenic Cells after FTI

To assess clonogenic abilities of these tumorigenic cell lines we performed anchorage-dependent and independent growth assays after treating these cell lines with tipifarnib. We plated COL, OS187, and SaOS2 in 6-well dishes at a low density in triplicate. We treated the cells with increasing concentrations of tipifarnib for three weeks. Fresh drug and media was replaced weekly to ensure farnesylation was continuously being inhibited. After three weeks, cells were stained with 0.05% crystal violet PBS solution. COL cells did not withstand the staining procedure and anchorage dependent growth could not be assessed on these cells. Colonies counted in this assay represent a group of cells greater than 50 and can be visualized without a microscope. Individual colonies were counted. In both OS187 and SaOS2 inhibiting farnesylation greatly reduced the cells ability to form anchorage dependent colonies (A II 1).

A II 1

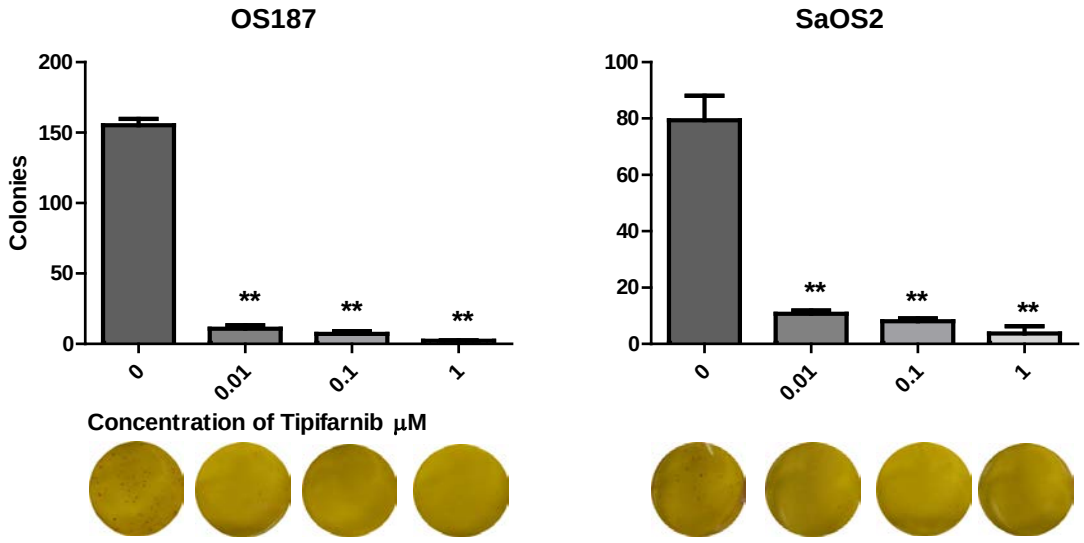

A II 1. OS187 and SaOS2 show sensitivity to tipifarnib by anchorage dependent clonogenic growth inhibition. 1,000 OS187 cells and 4,000 SaOS2 cells were plated for 3 weeks. Cells were treated with 0, 0.01, 0.1, or 1 μM tipifarnib. Fresh media with drug was refreshed weekly. After 3 weeks the media was removed and the cells were fixed and stained using standard techniques. Colonies were counted. These graphs are representative of three separate experiments. ** $p<0.001$.

Anchorage-independent growth was assayed by growth in soft agar. High concentration 1% agar 2X media and drug mixture were plated first and allowed to solidify. Then cells were plated with a lower concentration 0.1% agar 2X media and drug mixture. A top layer of 0.5 ml media with tipifarnib was added to the top of the agar. Media and drug were refreshed weekly to ensure inhibition of farnesylation for the duration of this experiment. There was a marked reduction of colony forming cells compared to the anchorage-dependent experiment. This is expected as this assay includes an additional barrier for clonogenic growth. In all three cells lines there is a dose dependent decrease of cells which can form colonies within this assay (A II 2).

A II 2

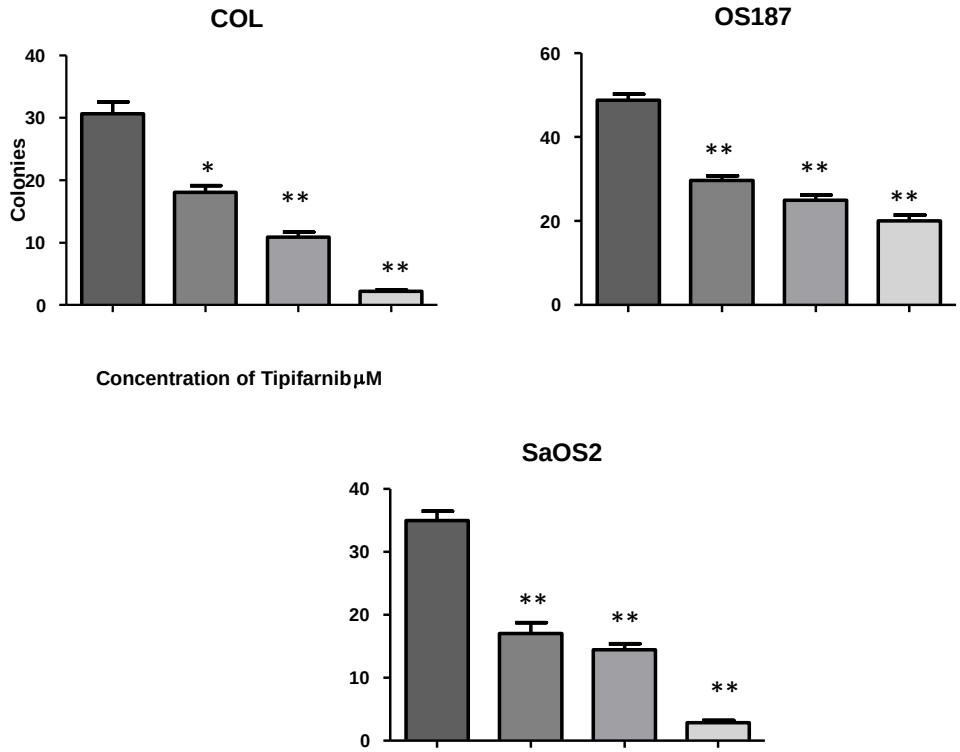

A II 2. All three tumor cell lines have reduced anchorage independent growth with tipifarnib treatment. Growth in soft agar with tipifarnib treatment reduced the number of individual cells to develop into cell clones that are identified as single colonies. For COL and OS187 10,000 cells were plated while 40,000 SaOS2 cells were plated. Tipifarnib was added to the bottom and top layers of the agar and 0.5 ml fresh media and drug was added on the top layer and refreshed after incubation of a week, to enable the cells to be exposed to tipifarnib for the duration of the experiment. After 2 weeks the cells were counted with 20X magnification using a light microscope. *$p<0.05$, ** $p<0.001$

Invasiveness of tumor cells with FTI

Invasiveness was another hallmark of tumorigenicity we wished to assess after FTI. SaOS2 and O187 cells were pretreated with increasing concentrations of tipifarnib for 48 hours prior to plating. 20,000 OS187 cells were plated in triplicate into matrigel. SaOS2 cells are much larger cells so to see an affect, 40,000 cells were plated in triplicate. Media with tipifarnib and 10% serum was added to the bottom of 24 well plates, while tipifarnib and serum starved media was used to plate pre-treated cells inside the Boyden chamber. Cells were incubated in the matrigel in a 37°C incubator for 48 hours. After 48 hours media was removed and cells were stained using standard techniques. Both SaOS2 and OS187 show a dose dependent decrease of invading cells with tipifarnib treatment (A II 3).

A II 3

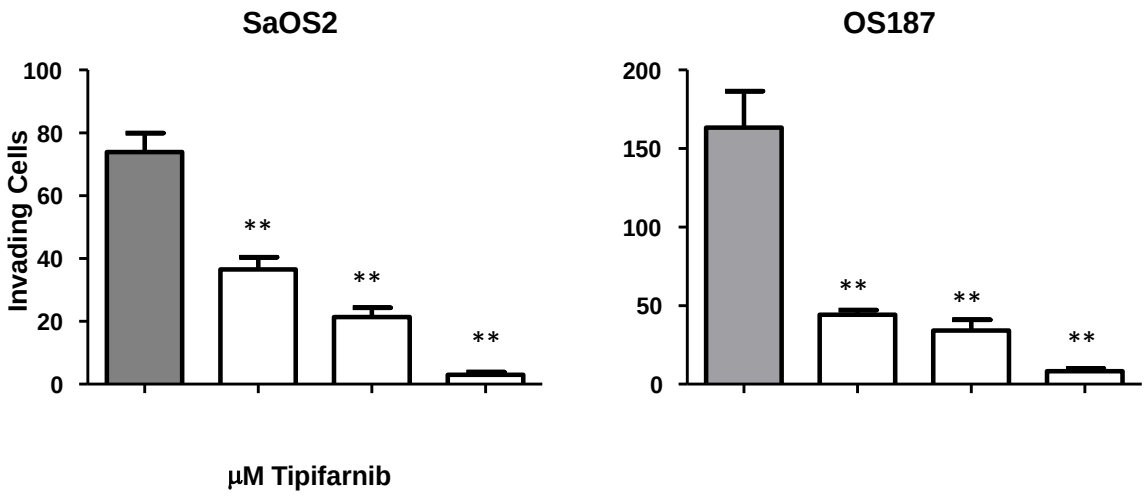

A II 3. SaOS2 and OS187 have a dose dependent decrease of invading cells with tipifarnib treatment. Cells were treated with tipifarnib for 48 hours then 40,000 SaOS2 cells and 20,000 OS187 cells were plated in triplicate into the upper chamber of the matrigel. Drug was added to the upper and lower chambers. Cells were cultured for an additional 48 hours then chambers were stained as previously described in the methods. ** $p<0.001$

Summary

In this section we show FTI inhibits tumor cell lines ability to form colonies and also reduces their invasiveness. Both anchorage-independent and anchorage-dependent growths were inhibited by FTI. There also appears to be decreased sensitivity to tipifarnib for the cells to grow within soft agar (anchorage-independent). This could be partially due to drug being refreshed topically and not completely being diffused throughout the soft agar due to the thickness of agar in this assay. Although tipifarnib was added initially to the agar, the cells in the bottom of this agar might have not been exposed to FTI for the duration of the experiment. The limitations to tipifarnib being distributed evenly in the anchorage-independent conditions may have stunted the effects that would otherwise be shown as this would allow for more cells to grow in the agar where they could form colonies without being exposed to tipifarnib.

To correct for drug distribution effects, this assay could be performed in a 6-well dish with a thinner layer of agar. If the same results were obtained then this difference could be due to the proportion of cells which would be more likely to develop tumor *in vivo* would have increased resistance to FTI, as anchorage-independent growth measures two tumorigenic properties. Anchorage-independent growth measures a cells ability to form a colony without attachment to chemically treated plates which are optimized for attachment by adherent cells. This assay measures a heterogeneous population of cells for those which have increased ability to form colonies which could form tumor *in vivo*. Both assays show a dose-dependent decrease of clonogenicity in response to FTI in all tumor cell lines tested.

Invasiveness was another characteristic of tumorigenicity we assessed. Both SaOS2 and OS187 had decreased invasiveness *in vitro* when treated with TF.

Inhibiting farnesylation in cells which have low endogenous Ras activation increases Ras activation and downstream MAPK signaling. FTI also increases GGTase expression, forcing K-Ras and N-Ras to be alternatively GG'd. Furthermore, **FTI inhibits tumorigenic cells proliferation, increases cell cycle arrest in sub G1 and G2/M cell cycles, decreases clonogenicity, and decreases invasiveness.**

Appendix III: FTI induced senescence

Background on Senescence

Senescence has been shown to be induced in normal cells by the expression of oncogenic Ras or overstimulation of Ras' downstream effectors (48, 84, 121, 125-129). Excess Ras signaling, as an overly-strong mitogenic signal, in itself can induce cell cycle arrest and/or senescence. Although tumorigenic cells can initially overcome a senescent barrier by expressing telomerase, they still maintain the ability to become senescent.

Senescence or terminal growth arrest can occur through alterations in telomeres or by different forms of cellular stress. Treatment-induced senescence in tumor cells is distinct from replicative senescence of normal cells and can have implications for tumor response to therapy *in vitro* and *in vivo*. Stressors include chemotherapeutic agents, ionizing radiation, or targeted agents such as small molecule inhibitors (130). Replicative senescence occurs in normal human cells due to a shortening of telomeres at the ends of chromosomes(131). Normal human somatic cells do not express telomerase, an enzyme necessary for extension of telomere ends and unlimited replicative growth of cells (132). Tumor cells often aberrantly express telomerase, thereby allowing them to maintain telomeres at a length that allows for continued proliferation (133). DNA damage-induced senescence is not associated with telomere shortening, as telomerase expression does not prevent senescence in tumor cells (134).

Senescence is a program that leads to irreversible cell cycle arrest and is a modulator of cell growth in cells which have damaged DNA (135). The amount of damage induced on a cell determines whether a cell will undergo apoptosis (cell death) or senescence. If the damage introduced to the cell is at a high level, this will normally result in apoptosis. Conversely, if the level of damage is low then senescence may be induced (84, 120, 126, 129, 136, 137). The dose of the stressor such as a drug (in our case tipifarnib) can be a determining factor for the fate of each cell. As the dose of a stressor increases, the proportion of cells that are likely to undergo apoptosis is likely to increase. Senescent growth arrest has been defined as irreversible and growth factors cannot re-stimulate proliferation in these cells. However, senescent cells remain metabolically active, and can still secrete factors to stimulate or inhibit tumor growth (135, 138, 139).

Markers of senescence

Although senescent cells are not proliferating, they are still metabolically active. By remaining metabolically active, these senescent cells may affect growth of nearby cells by

secreting growth factors. This has become a concern as this can result in stimulating the growth of a tumor with a bad prognosis for a patient. In prostate cancer increased expression of the senescence-associated proteins p16 and p21 expression were found to be markers of early relapse. However, the senescent markers Maspin and IGFBP-3 correlated with favorable patient outcome (130). Expression of multiple senescence-associated growth regulators may allow for analysis of which senescent markers represent favorable patient outcomes (130). Senescence is likely to occur in cells which have wild-type p53 and Rb functions. Common markers for senescence include a transient increases of p53 and p21 followed by a stable increase of p16 (140).

Most tumor cells have short telomeres and frequently express mutant forms of Ras or downstream effectors of Ras, overexpression of which leads to senescence in normal cells. Tumorigenicity overcomes these senescent events by activation of telomerase and inactivation of tumor suppressors such as p53, p16, and p21. Overexpression of many tumor suppressors has been identified as pushing tumor cells into a senescent phenotype. Tumor suppressors p53 and p21 promote damage-induced senescence in tumor cells. However, senescence has been shown to occur in the absence of p53, p21, or p16, suggesting other tumor suppressor genes are also important for promoting growth arrest (127, 130, 135, 141). Although senescence may occur in the absence of these genes, the induction is delayed (142).

There are markers that can be measured to indicate senescence within a given cell population. Measuring β-galactosidase activity at pH 6 is a universal way to measure senescence for i*n vitro* and *in vivo* experiments (143). β-galactosidase is a lysosomal hydrolase which is normally active at pH 4. This suggests an increase of lysosomal content in senescent cells occurs at a suboptimal pH (144). Replicative senescence is characterized by a G1 arrest (145). This growth arrest is due to repression of genes necessary for cell cycle progression and upregulation of growth inhibitory genes (48, 84, 121, 125-128, 139, 141, 146-149). This mechanism is likely to be evolutionarily conserved in order to protect cells from oncogenesis (135).

Ras induced senescence (A III 1)

Oncogenic H-RasV12 transforms immortal MEFs by activating ERK, however it induces senescence in primary fibroblasts by activating ERK, p53, and p16 (129). Knockouts of p53 or INK4a (includes p16 and p19ARF) allowed Ras-mediated tumorigenesis in primary MEFs (129). Oncogenic Ras resulted in senescence of normal cells and was able to transform immortal cells or primary fibroblasts with altered p53 or p16 expression.

A III 1

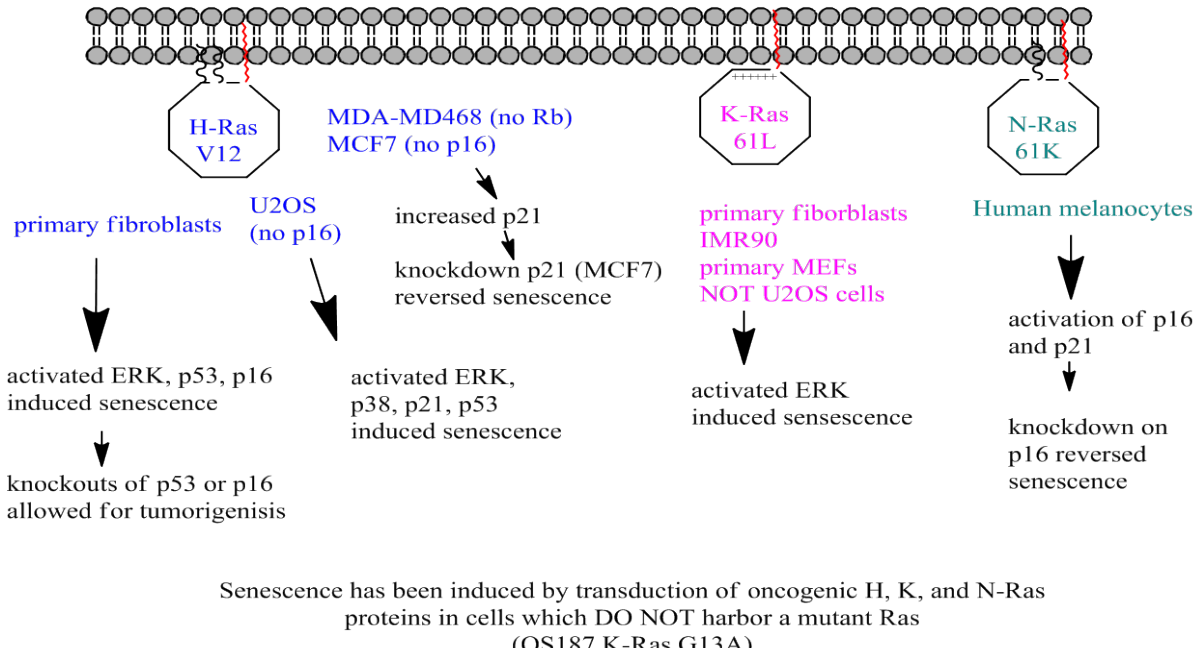

A III 1. Oncogenic Ras activates senescence. Mutants of all three Ras family members induce senescence. Different cell lines require activation of different cell cycle regulators to induce Ras mediated senescence.

In U2OS osteosarcoma cells, transduction of H-RasV12 activated ERK and p38 MAPK signaling which resulted in p21 activation (127). This induced a senescent-like phenotype in cells harboring WT Ras (127). This was only observed in osteosarcoma cells which did not originally harbor mutant Ras, and was independent of p16 and ARF as these cells do not express these proteins. With induction of H-RasV12 there was also a marked increased in p53, p21, and down-regulation of Rb. Oncogenic K-Ras61L also induced senescence in normal fibroblasts, IMR90 (fetal lung fibroblast), and in primary WT MEFs through activation of ERK, but did not in U2OS cells. It is possible the signaling pathway activated by oncogenic K-Ras is different than H-Ras, and the senescent pathway that can be activated by K-Ras is compromised in U2OS cells (127). This difference could also be due to the different mutational status of H-Ras and K-Ras, as it would have been a better comparison to mutate the same residue in both proteins.

Induction of senescence or a senescent-like phenotype by induction of H-RasV12 was analyzed in a panel of cancer cells with various mutations to determine which tumor suppressors were important for induction of this growth arrest. Two breast cancer cell lines were transduced with H-RasV12 and analyzed for senescence. MDA-MB468 lacks the

expression of Rb and MCF7 cells do not express p16, however transduction with oncogenic H-Ras induced senescence in both cell lines and increased p21 expression (126). Transduced activated MEK also resulted in permanent growth arrest of these two breast cancer cell lines. Three human cancer cell lines (T24, bladder H-RasV12; MDA-MD231, breast K-RasD13; HCT116, colon K-RasD13) which have activating mutations in *ras* genes were also transduced with H-RasV12. None of these cell lines with activating Ras mutations underwent a senescent phenotype, and continued to grow at a rate comparable to vector controls. When MDA-MB231 and T24 were transduced with activated MEK, they both had decreased growth and contained some cells which were phenotypically identical to senescence. Furthermore, knockdown of p21 in MCF7 transfected with oncogenic H-Ras reverses the senescent-like phenotype as shown by morphology changes back to normal MCF7 cells. Knockdown of p21 also increased the ability of MCF7 cells to form colonies in soft agar. This shows upregulation of p21 is important to induce senescence in cells transduced with H-Rasv12, which have no endogenous mutations in Ras.

In human melanocytes transduction with N-RasQ61K induced activation of p16 and p21, however only loss of p16 reversed senescence induced from oncogenic N-Ras (150). As most reports on senescence from oncogenic induced H- and K-Ras signaling rely on p21, this further implies differences in signaling requirements in different cell types and differential signaling of Ras species.

Rationale

Senescence is a modulator of cell growth in cells which have damaged DNA. The amount of damage induced on a cell determines a cells' fate. If the damage introduced to the cell is at a high level, this will normally result in apoptosis; conversely if the level of damage is low then senescence may be induced. The dose of the stressor or drug (in our case tipifarnib) can be a determining factor for the fate of each cell. As the dose of a stressor increases, the proportion of cells that are likely to undergo apoptosis is likely to increase. As we are using a pharmacological inhibitor, we were interested in assessing if FTI would result in a senescent or senescent-like phenotype with tipifarnib treatment. Senescent growth arrest has been defined as irreversible, indicating that growth factors cannot re-stimulate proliferation in these cells.

There are markers that can be measured to indicate senescence within a given cell population. Measuring β-galactosidase activity at pH 6 is a universal way to measure senescence during *in vitro* and *in vivo* experiments (143). Senescence is also characterized by a G1 arrest. Increased expression of p53 and p21 are transiently increased in senescent cells and these proteins often are detected as markers of senescence.

While culturing OS187 with tipifarnib it was evident these cells had an altered morphology and became swollen as a response to treatment. Senescent cells are described as having a flattened, swollen phenotype. Senescence is likely to occur in cells which have wild-type p53 and Rb function (139, 148, 150). Further analysis of p53 function was assessed in OS187. It was determined that p53 could be phosphorylated and therefore is functional in this cell line. As OS187 is a colon cancer cell line it is presumed that it would also have functional Rb protein (151). Therefore we wanted to determine if this cell line was undergoing senescence as a response to FTI.

Cells with functional p53 normally respond to therapies faster than cells without functional p53 (49, 83, 128, 129, 134, 139, 148). As OS187 was much more sensitive to FTI than SaOS2, which is p53-null, it is hypothesized that p53 is playing an important role in sensitizing OS187 to tipifarnib at low concentrations. We therefore wanted to investigate the possibility that tipifarnib acts through a p53 pathway to induce or contribute to senescence or a senescent-like phenotype in OS187 cells.

Results

Morphology changes and static growth characteristics of senescence

Initial observations with a light microscope at 20X magnification demonstrated a swollen, flattened morphology after 48 hours of tipifarnib treatment (Figure 15 A). In addition to photographing cells grown in a monolayer we also measured the circumference of untreated and treated cells. Cells were treated with tipifarnib for 48 hours, trypsinized, then counted and measured on an automated Coulter cell counter. For this purpose we did want to use live cells in order to determine the size difference between FTI-treated and untreated OS187 cells. This cell counter automatically determines the diameter of each cell that it counts. The results indicate an average size of cells per sample. After 48 hours of tipifarnib treatment, OS187 cells were 1.25 times larger than untreated cells (A III 2). Results depict the average cell size of three independent experiments.

A III 2

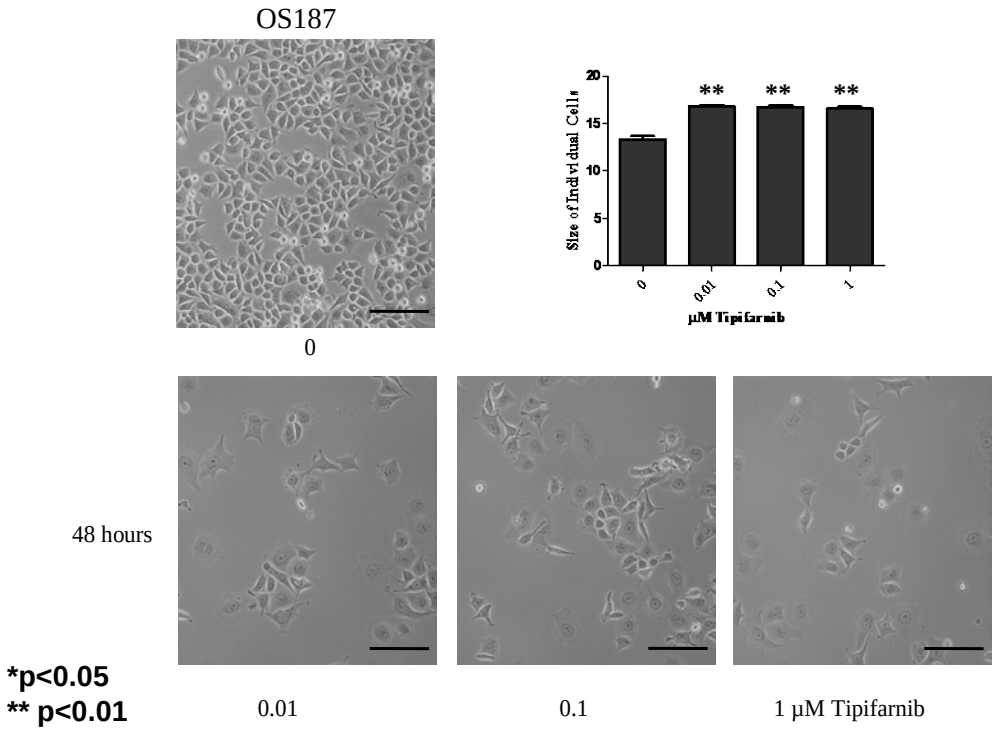

A III 2. OS187 cells have a swollen senescent-like appearance after tipifarnib treatment. OS187 cells were treated with 0.01, 0.1, or 1 µM tipifarnib for 48 hours. A. Pictures were taken on a phase-contrast light microscope. Scale bar represents 0.1 mm. B. Cells were treated for 48 hours with increasing concentrations of tipifarnib, trypsinized, and ran on an automated Coulter counter which calculates the size of individual cells. ** p values are < 0.001.

To determine if FTI was also acting as a cytostatic inhibitior, we conducted a time course experiment where we changed the duration of exposure of tipifarnib to OS187 cells. Cells were exposed to 1μM tipifarnib for 24, 48, 72, 96 hours, or one week. Fresh media was replaced after individual treatment times to allow cells to grow for a constant period of time. We found that, regardless of how long the cells were exposed to tipifarnib, the cells could not recover from FTI and regain the ability to grow (A III 3). The inset graph represents the same data with a smaller y-axis scale to focus on the similarities of reduced growth among tipifarnib-treated cells. This static growth is another indicator that senescence may be occurring in OS187 cells in response to tipifarnib treatment. The senescent or senescent-like cells captured in this assay still have intact nuclei, whereas cells undergoing apoptosis would not have intact nuclei, and are therefore excluded from this assay.

A III 3

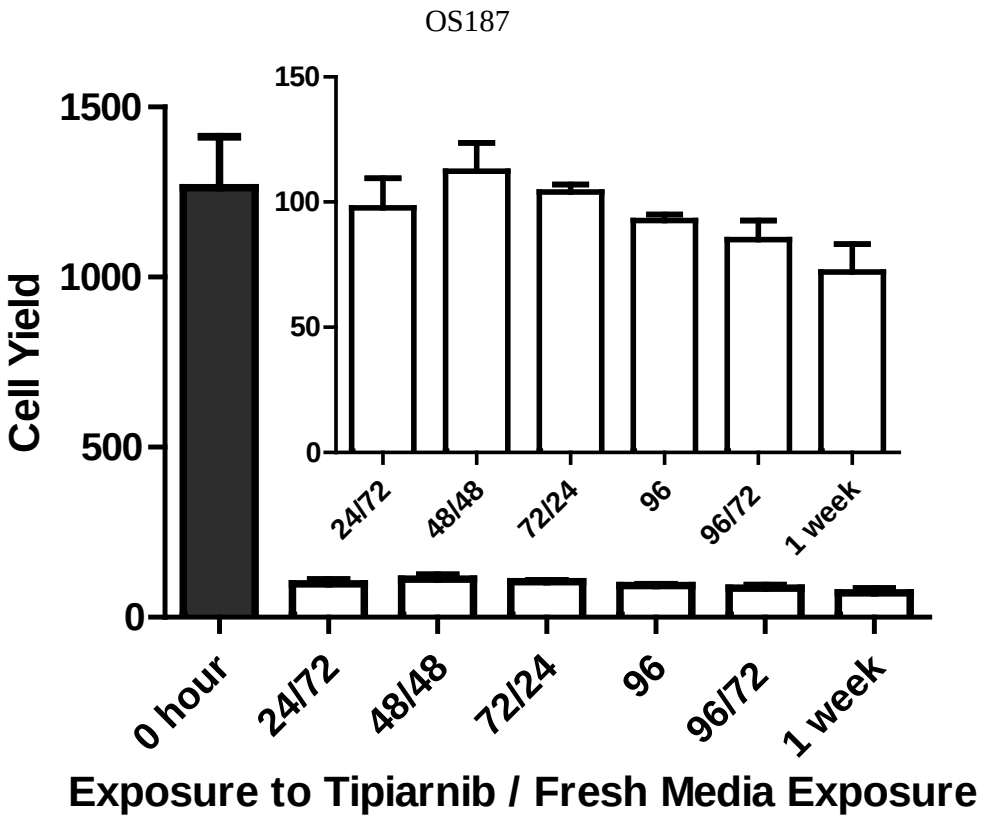

A III 3. OS187 cells display a senescent-like phenotype which is not dependent on duration of exposure to 1μM tipifarnib. OS187 cells were plated in 6 well dishes at 100,000 cells per well and treated with 1μM tipifarnib for 24, 48, 72, 96 hrs or one week. For example, after 24 hours of treatment media and drug was removed from the wells and replace with fresh media for 72 hours. Nuclei were collected and counted.

OS187 cells were treated with 0.01, 0.1, or 1 µM tipifarnib for 24 hours or continuously for 2 weeks. Pictures of treated cells were taken after 3, 4, 5, or 6 days and again after 2 weeks. Unaffected OS187 cells treated with 0.01 µM tipifarnib begin outcompeting tipifarnib sensitive cells by 4 days when only exposed to tipifarnib for 24 hours (A III 4). After 24 hours 0.1 µM tipifarnib treatment, unaffected cells take 5 days to begin to outgrow swollen, tipifarnib sensitive cells. Cells treated with high dose 1 µM tipifarnib take 2 weeks after initial 24 hours treatment for cells which appear to not respond to tipifarnib treatment to outcompete cells undergoing senescence or a senescent-like phenotype. Continuous treatment at all three concentrations contain mostly swollen and senescent or senescent-like cells. At lower concentrations there are still cells which do not respond to FTI as some cells still are the size of untreated OS187 cells after continuous treatment.

A III 4

A.

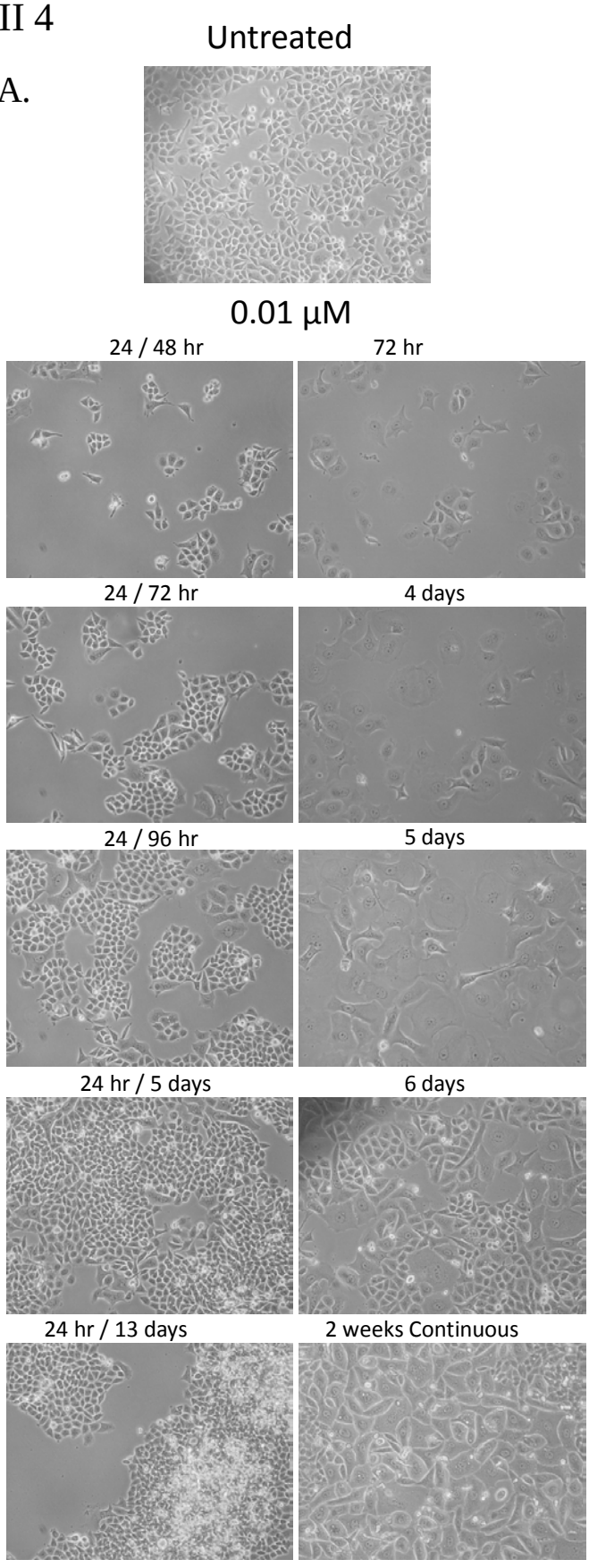
Untreated
0.01 µM
24 / 48 hr
72 hr
24 / 72 hr
4 days
24 / 96 hr
5 days
24 hr / 5 days
6 days
24 hr / 13 days
2 weeks Continuous

B.

Untreated

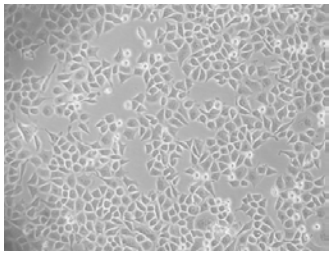

0.1 µM

24 / 48 hr

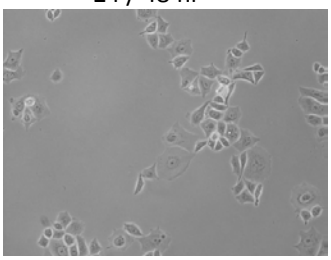

72 hr

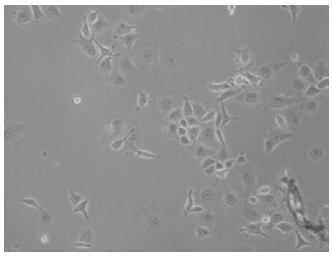

24 / 72 hr

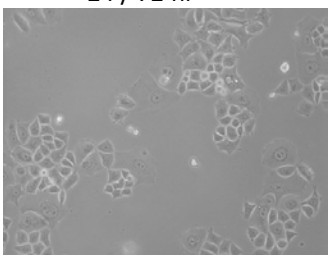

4 days

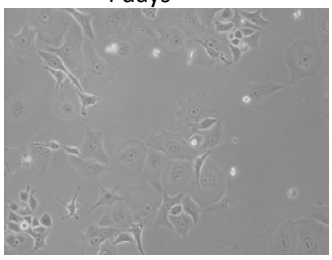

24 / 96 hr

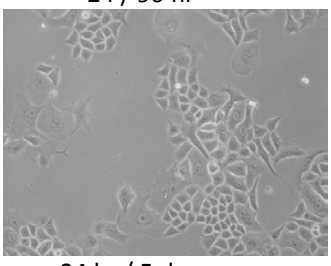

5 days

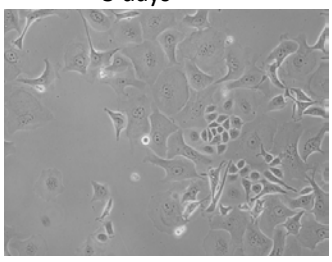

24 hr / 5 days

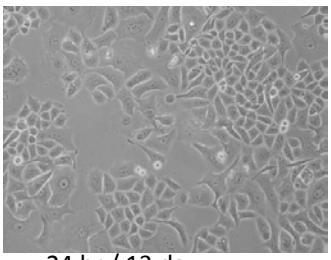

6 days

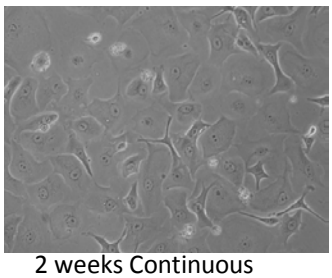

24 hr / 13 day

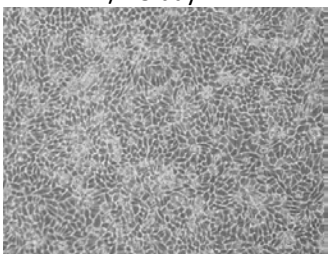

2 weeks Continuous

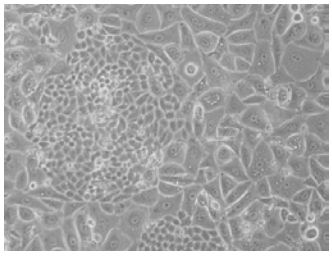

C.

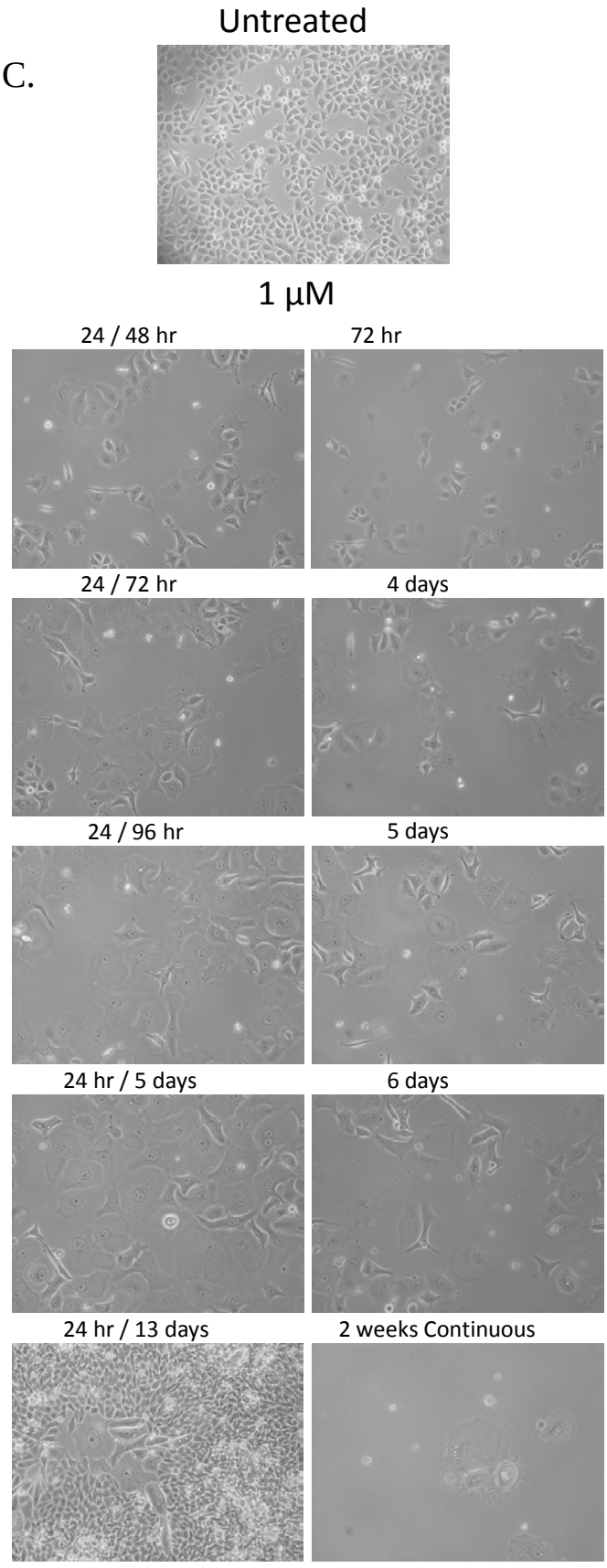

A III 4. Concentration and treatment duration do contribute to the proportion of OS187 cells which respond to FTI. OS187 cells were treated briefly for 24 hours or continuously with A) 0.01 B) 0.1 C) or 1 µM tipifarnib. Images were taken at days 3, 4, 5, and 6, or after 2 weeks.

To determine if these treated cells which were not sensitive to tipifarnib treatment initially had built a resistance to FTI, cells were retreated with tipifarnib. All cells were in culture for 3 weeks regardless of initial treatment time period. Cells treated for 24 hours had 3 weeks recovery. Cells treated for 1 week had a 2 weeks recovery. Cells treated for 2 weeks had a 1 week recovery. After 3 weeks, cells were treated with a second round of tipifarnib. All initial treatment durations and concentrations allow for some cells to be resensitized to tipifarnib, as cells which were unaffected by the initial treatment do respond to the second round of TF treatment (A III 5). After treatment with 1 µM for 2 weeks very few cells are alive and all have a swollen senescent or senescent-like morphology, therefore second round treatment had no additional benefit *in vitro*.

A III 5

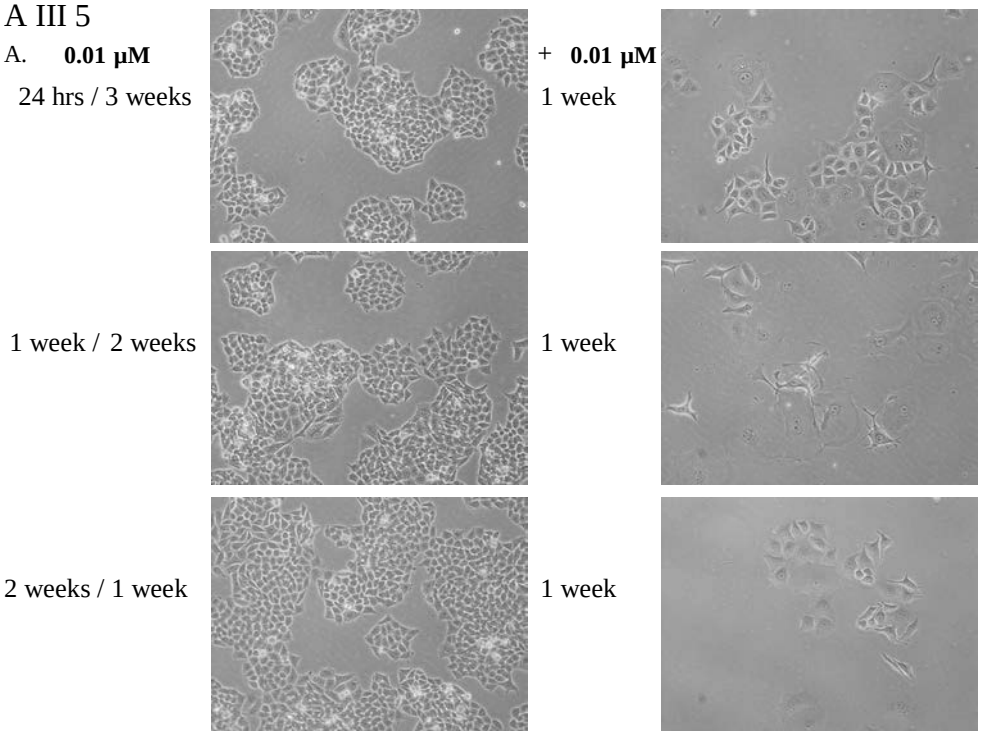

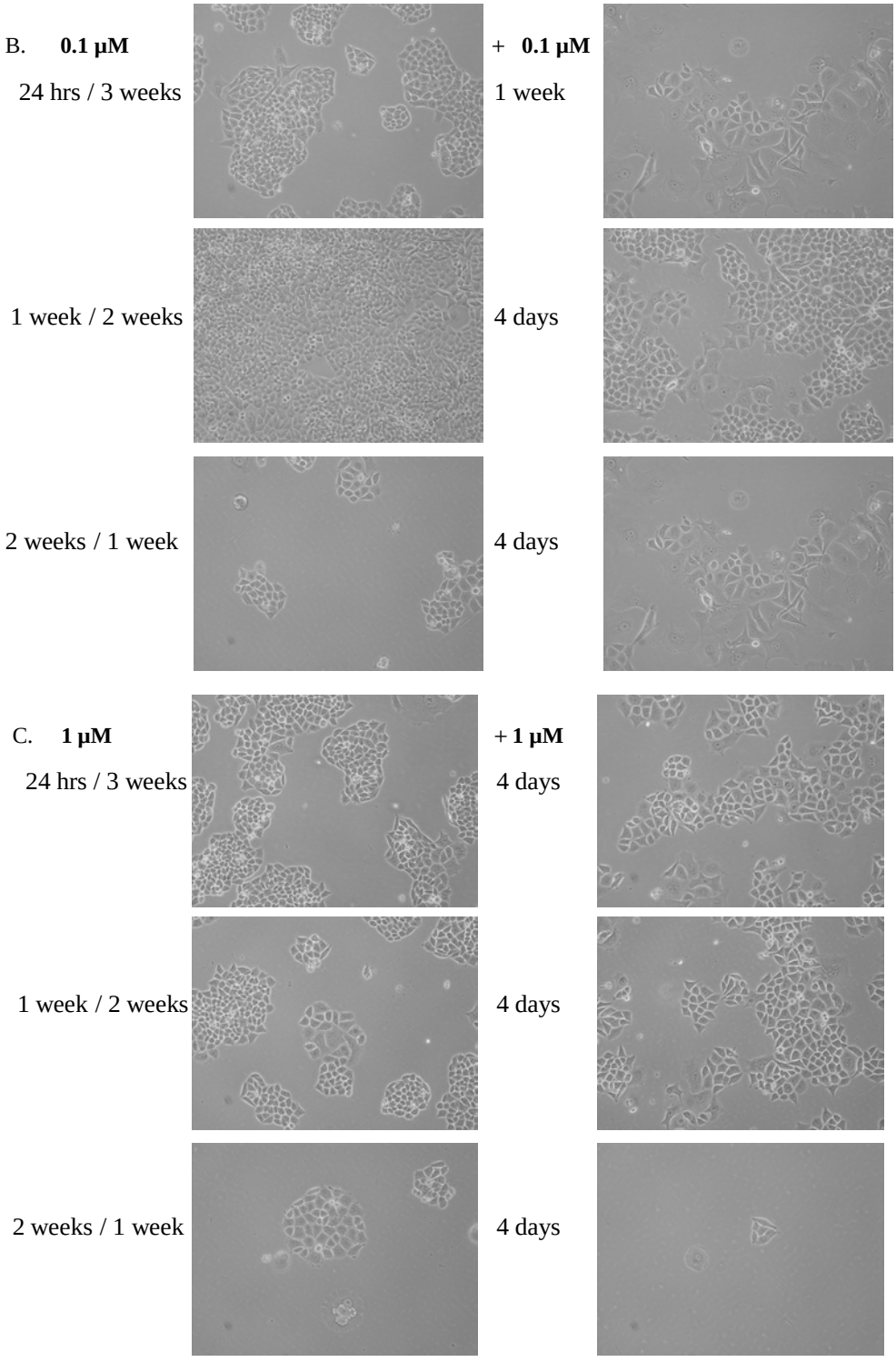

A III 5. Second round treatment with tipifarnib resensitizes original non-responding OS187cells regardless of initial treatment duration or concentration. Previously treated OS187 cells were treated with a second round of tipifarnib at the same initial concentrations used. A) 0.01 µM B) 0.1 µM C) 1 µM tipifarnib. Images were taken as described in Figure 15.

Positive Markers of Senescence

Senescence often involves p53 and p21 activation for cell cycle arrest. These checkpoint regulators are involved in regulating cellular response to DNA damage. OS187 cells were treated with 0.1µM tipifarnib for 12, 14, 48 or 72 hours. Lysates were collected at these times, run on immunoblots, and probed for regulators of cell stress/damage and cell cycle. With tipifarnib treatment total and phosphorylated p53 are both increased (A III 6). p21 levels are also dramatically increased in response to tipifarnib treatment over time. The cyclins are proteins which are involved in different phases of the cell cycle. Cyclins interact with Cyclin Dependent Kinases (CDKs) to promote transitions into the next phase of the cell cycle, from G1 thru S and G2/M. 72 hours of tipifarnib treatment results in decreased expression of Cyclin A, B, and E. Cyclin D has increased expression over time.

A III 6

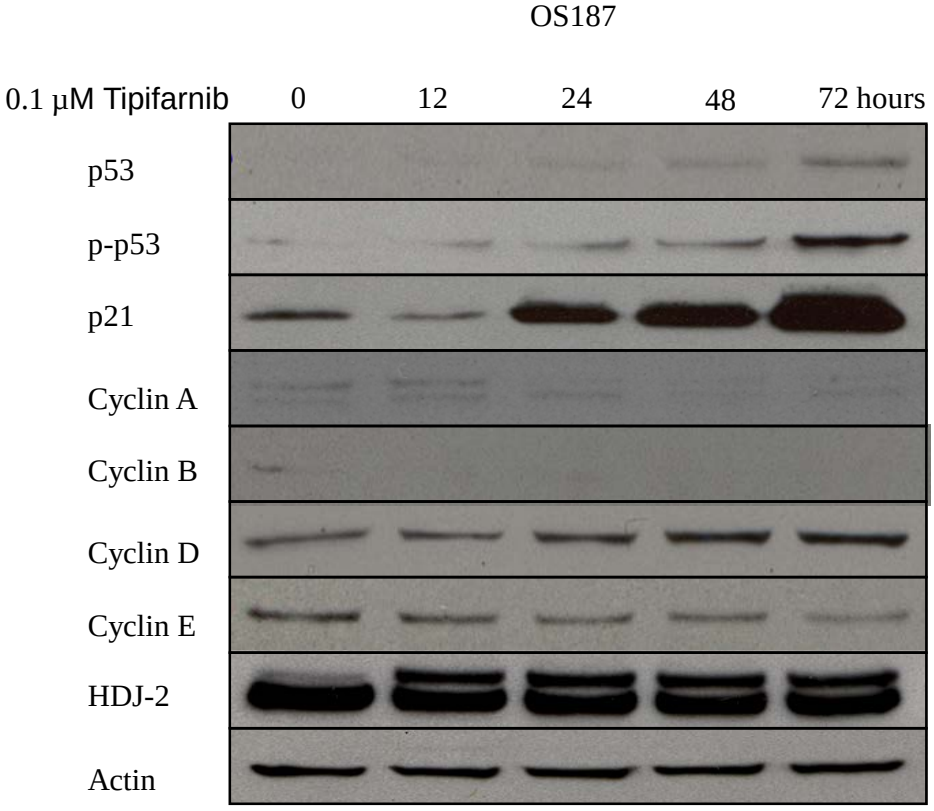

A III 6. Active p53, p21, and Cyclin D all increase over time in response to FTI. OS187 cells were treated with 0.1 µM tipifarnib for 12, 24, 48, or 72 hours, lysates were collected and run on immunoblots and probed for the indicated protein. HDJ-2 demonstrates that farnesylation is inhibited at the time points collected.

A common marker of senescence is increased β-galactosidase activity at pH 6. To determine if low concentrations of tipifarnib treatment were resulting in OS187 cells transitioning to senescence, cells were plated and treated with 0.001, 0.01, or 0.1μM tipifarnib for one week and then allowed to continue growing for an additional week. After treatment, cells were fixed and stained with β-galactosidase. Cells were then imaged as described in Figure 12. After two weeks tipifarnib treatment all treated groups had increased β-galactosidase activity as indicated by a blue color which is produced in senescent cells (A III 7)

A III 7

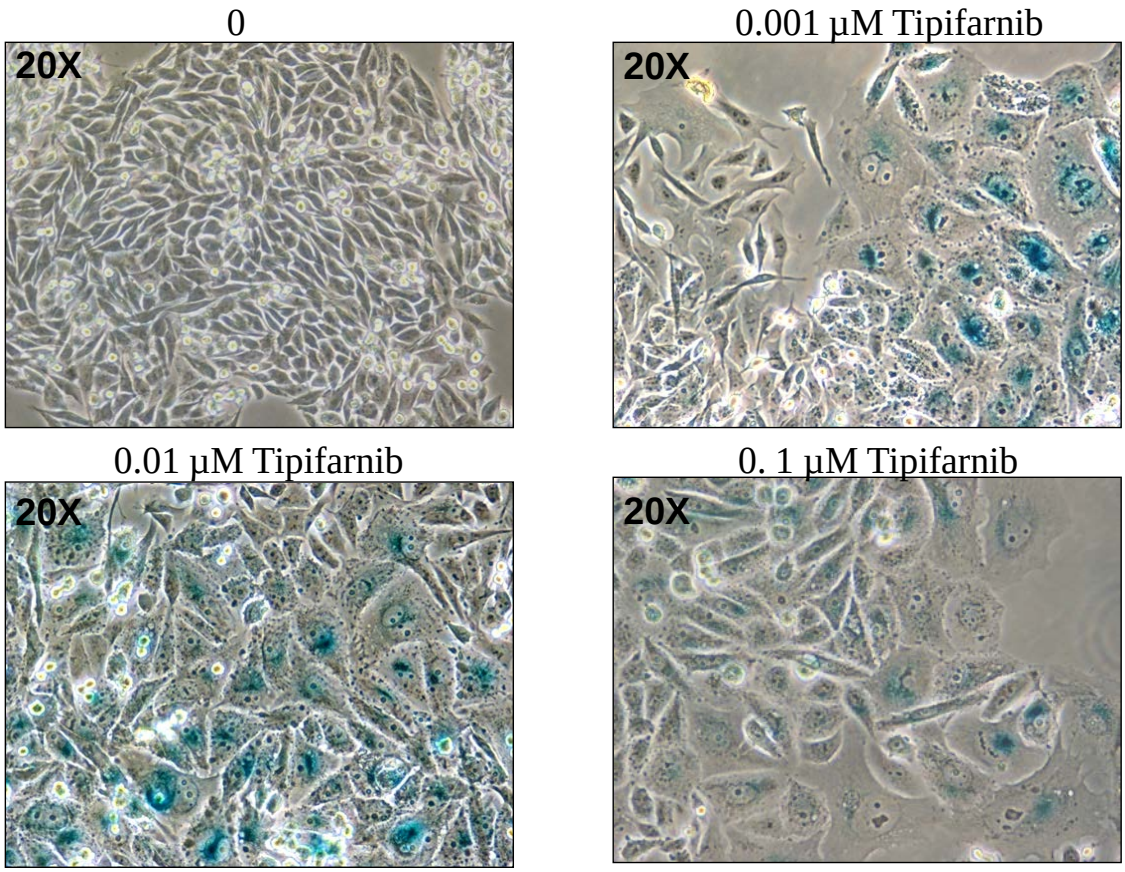

A III 7. OS187 cells treated with tipifarnib for 2 weeks stain positive for β-galactosidase. Cells were plated and treated with 0.001, 0.01, 0.1 μM tipifarnib for 2 weeks and then stained as directed in the Cell Signaling manual. Images were taken as described in Figure 15.

Senescent cells often are described as arresting in the G1 phase of the cell cycle. To determine if this occurs at low doses of tipifarnib treatment, OS187 cells were incubated with

0.001 or 0.1 µM tipifarnib for various exposure times. OS187 cells were exposed for 24 hours, 24 hours with different recovery times, or continuously for 96 hours. After 24 hours the drug and media were removed and cells were maintained with fresh media for 24, 48, or 72 hours. After 96 hours cells were collected and stained with BrdU, a marker that stains actively proliferating cells. Only cells treated with 0.001 µM tipifarnib show an increase of cells in the G1 phase of the cell cycle (A III 8). Both 0.001 and 0.1 µM treatments have an increased percentage of cells in sub G1 and G2/M, although with 0.001 µM treatment takes 96 hours after initial tipifarnib treatment to have increases in these phases of the cell cycle.

A III 8

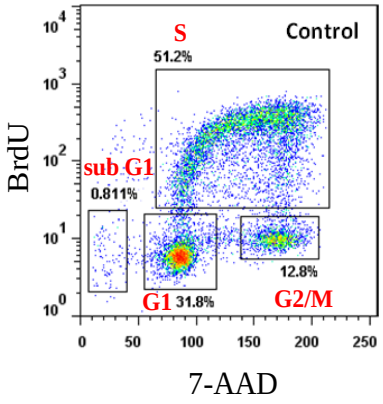

Tipifarnib **0.001 µM**	sub G1	G1	S	G2 / M
OS187	0.8	31.8	51.2	12.8
24	0.7	35.1	42.4	16.4
24 / 24	1	39	37.1	17.4
24 / 48	3	43.7	31.3	16.4
24 / 72	8	41.1	10.3	30.1
96	7.5	39.6	8.2	35.6
0.1 µM				
OS187	0.9	37.8	45	12
24	1.9	32	36.7	24.2
24 / 24	8.6	24.2	6.9	54
24 / 48	8.4	26	7.9	54
24 / 72	8.4	33	7.8	46.6
96	11	26.5	5	46.2

A III 8. OS187 cells treated with 0.001 µM tipifarnib have an increased percentage of cells in G1. OS187 cells were treated with 0.001 or 0.1 µM tipifarnib for 24 or 96 hours. Cells treated for 24 hours were assayed immediately or after 24, 48, or 72 hours with refreshed media without tipifarnib. BrdU staining was conducted as described in materials and methods.

p53 induced senescence

SaOS2 is a p53-null cell line which also demonstrates cytotoxity to FTI. However, this only occurs with longer duration of tipifarnib treatment. The increase of phosphorylated and

total p53 in OS187 in response to tipifarnib treatment at low concentrations indicated p53 may be an important requirement for a drastic growth inhibitory response to FTI treatment. To determine if p53 is important for response to FTI we used shRNA to knockdown p53 (shTP53) expression. OS187 cells were transduced with scrambled or shTP53 shRNA. Positively transduced cells were selected by cell sorting using a GFP tag that was incorporated into the pGFP-V-RS retroviral plasmid with scrambled or shTP53. Single clones of shTP53 were isolated and grown to select a clone which had nearly complete knockdown of TP53. Scrambled and shTP53 cells were treated with 0.1 μM of tipifarnib for 72 hours. Lysates were collected and immunoblots were performed. After treatment with tipifarnib phosphorylated p53 and p21 expression levels were both increased in scrambled shRNA-control cells. Phosphorylated p53 and total p21 were increased in response to tipifarnib treatment, but expression of both proteins was markedly reduced in tipifarnib treated shTP53 cells when compared to scrambled shRNA transduced cells (A III 9).

A III 9

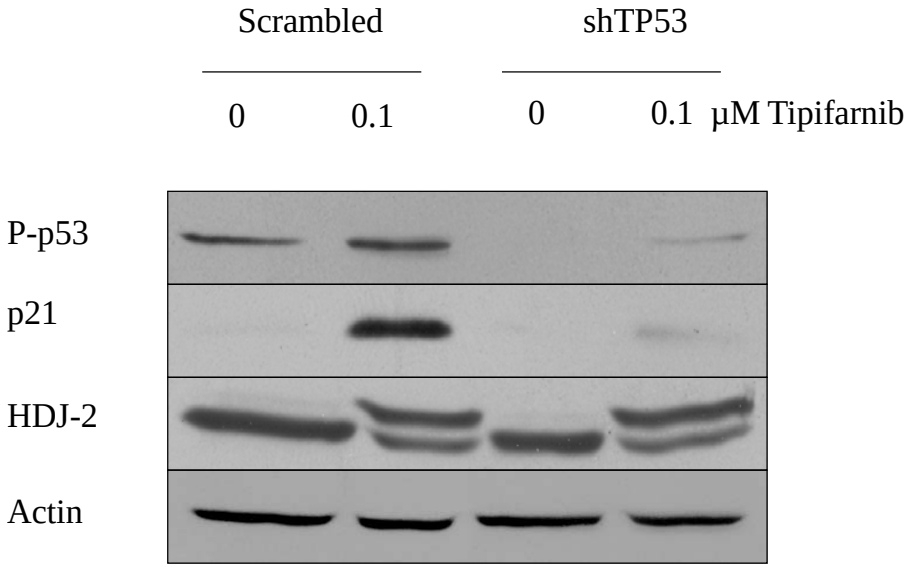

A III 9. Loss of phosphorylated p53 expression reduces activation of cell cycle inhibitor p21 with tipifarnib treatment in OS187 cells. Stably transduced shTPp53 and scrambled control cells were treated with 0.1 μM tipifarnib for 72 hours, lysates were collected, run on immunoblots, and probed with the indicated antibodies.

shTP53 and scrambled control transduced cells were treated with 0.1 μM tipifarnib for 72 hours and photographed under 20X magnification. shTP53 cells treated with tipifarnib do not have a morphology change when compared to untreated shTP53 cells (A III 10). Knocking down p53 expression reversed the swollen senescent morphology with tipifarnib treatment, suggesting that p53 is an important mediator of senescence.

A III 10

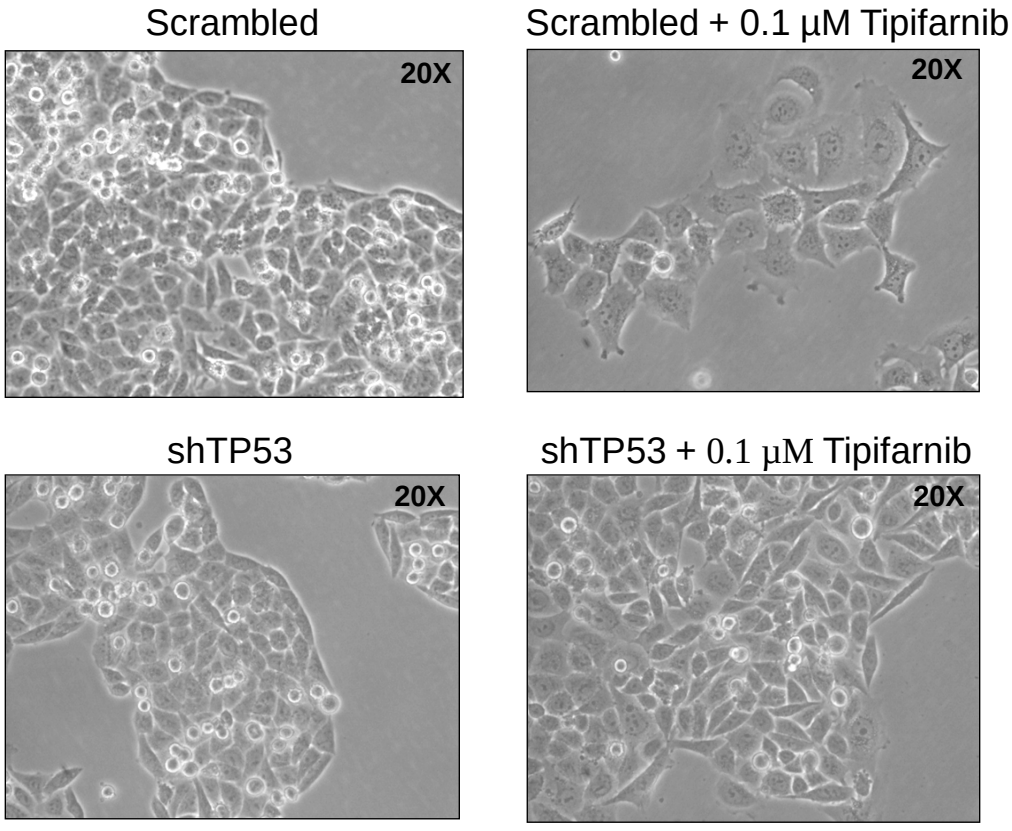

A III 10. Loss of p53 reverses the swollen senescent-like morphology that tipifarnib treatment induces on p53 WT OS187 cells. OS187 cells transduced with scrambled or shRNA to p53 were plated in a 6-well dish and left untreated or treated with 0.1 μM tipifarnib for 72 hours. Images were taken as described in Figure 15.

Summary

Cells respond to stress by adapting, repair and recovery, permanent cell cycle arrest (senescence), or cell death (apoptosis or necrosis) (152). Our initial observation of treatment with tipifarnib resulting in swollen OS187 cells raised the question of senescence occurring in response to FTI. The size of OS187 cells is visually and quantitatively increased with tipifarnib treatment. This cell line has functioning p53 and presumably Rb. With these indications we assessed the possibility of senescence occurring in response to FTI.

Duration of 1 μM tipifarnib treatment did not influence the ability of OS187 to proliferate when cell yield was assayed over one week. Tipifarnib exposure at lower concentrations does influence what proportion of cells respond to short exposures. Cells which do not respond at lower concentrations with short durations of treatment out-compete non-responding cells faster than at high concentrations. Even with continuous treatment some cells are unaffected morphologically by 0.01 or 0.1 μM tipifarnib treatments. However with continuous treatment of 1 μM tipifarnib nearly all cells are dead and the remaining cells are swollen. When cells which did not initially undergo morphological changes in response to tipifarnib treatment are allowed to grow and then undergo a second round of treatment, some cells which did not originally respond are still sensitive to tipifarnib treatment. This implies duration is important in order to keep cells sensitized to tipifarnib treatment regardless of the concentration used.

Over a 72 hour treatment, expression of phosphorylated and total p53, p21 and Cyclin D were increased. This indicates OS187 cells are attempting to respond to the stress of FTI. Cyclin A, B, and C all decreased. Cyclin D did not decrease but slightly increased at 12 and 24 hours and then remained constant. This is not surprising as Cyclin D is involved in the growth phases (G1 and G2) of the cell cycle (153), and when treated with 0.1μM tipifarnib OS187 cells undergo a cell cycle arrest in the G2/M phases of the cell cycle. Cyclin B1 is associated in the G2/M transition and its expression decreases as cells transition into anaphase of mitosis (154). This implies the cells are arresting during anaphase or telophase as cyclin B1 expression is increased in growth phase II and in prophase and metaphase portions of mitosis.

An indicator of senescence is an increase of β-galactosidase activity at pH6. Cells treated with low dose tipifarnib for two weeks had a marked increase of β-galactosidase activity. This indicates tipifarnib treatment does result in senescence with all concentrations tested. Cells at lower dose tipifarnib treatment show increased β-galactosidase staining. This suggests higher concentration tipifarnib treatment results in less senescence but perhaps more

cell death, which also is confirmed by continuous treatment resulting in much fewer cells for analysis. This finding is consistent with the model of higher stress on the cell reduces senescence and increases cell death, because cells are unable to adapt under more stringent treatments.

Low dose tipifarnib treatment did result in an increase of cells in the G1 phase of the cell cycle. However, at higher concentrations of tipifarnib treatment OS187 cells accumulated in sub G1 and G2/M. Cells treated with higher concentrations of tipifarnib may need to be assayed after 2 weeks to determine if there is a permanent increase and accumulation in the G1 phase of the cell cycle. Although some senescent cells may be arrested in the G1 phase, a larger portion at shorter time points are arrested in sub G1 and G2/M, allowing senescent cells to be overlooked. After longer treatment, the cells which are arrested in sub G1 or G2/M are likely to undergo cell death or adapt, allowing for cells which are arrested in G1 to be assessed. It is also possible that cells treated with higher concentrations of tipifarnib are too stressed to undergo senescence and turn to apoptosis or G2/M arrest instead. As we did not see a G1 arrest but a G2/M arrest, it is possible that some cells are senescent and others are only cell cycle arrested.

To assess if the activation and function of p53 were involved in activating a senescent response to FTI, shTP53 was utilized. As p53 and p21 are important regulators of the cell cycle, we wanted to assess the effects of reduced p53 expression in FTI-treated cells. OS187 cells with shTP53 had decreased activation of p53 and p21 as compared to scrambled control cells after FTI. This suggests p53 is an important regulator of the stress response induced by tipifarnib in OS187 cells. Cells with shTP53 also retained the parental morphology when treated with tipifarnib. This confirms that p53 is important for inducing a senescent or a senescent-like phenotype when farnesylation is inhibited. Increasing tipifarnib results in increased cleaved PARP indicating apoptosis also occurs in some cells as a result of FTI (data not shown).

It is likely there are a variety of cytotoxic and cytostatic effects resulting from tipifarnib treatment, and that senescence is just one. We investigated this affect because of preliminary data in OS187 treated with tipifarnib which showed no change in proliferation rate with different durations of treatment and a swollen morphology. Knocking down p53 showed that this protein is important in reversing the morphological changes tipifarnib induces in OS187. This p53 pathway seems to be acting through p21 as its expression is correlated with p53

activation and expression. **Our results demonstrate senescence or a senescent-like phenotype that occurs in response to tipifarnib treatment in OS187 cells is p53 dependent.** This may be dependent or independent of increased Ras activity from FTI (A III 11).

A III 11

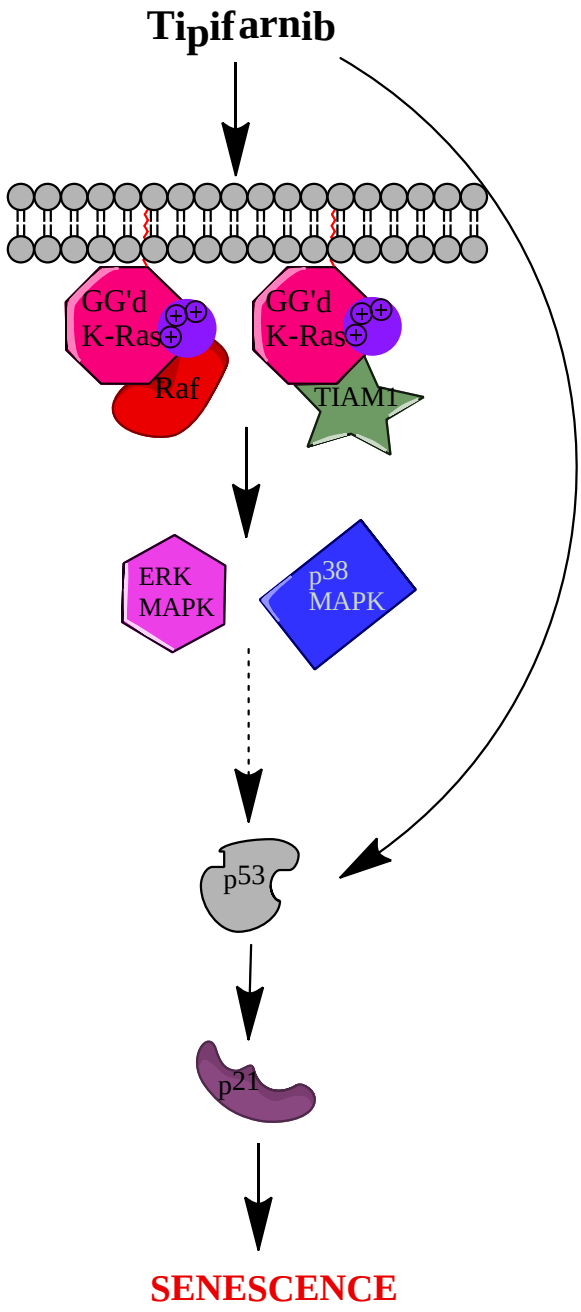

A III 11. Tipifarnib induced senescence pathway in OS187 tumor cell line. Tipifarnib increases p53 activity to activate p21 and result in senescence. This pathway may be mediated through increased ERK and p38 MAPKs from the increased active GG'd K-Ras after tipifarnib treatment.

Works Cited

1. Khwaja A, Dockrell ME, Hendry BM, Sharpe CC. Prenylation is not necessary for endogenous Ras activation in non-malignant cells. J Cell Biochem 2006;97:412-22.
2. Ashery U, Yizhar O, Rotblat B, Kloog Y. Nonconventional trafficking of Ras associated with Ras signal organization. Traffic 2006;7:119-26.
3. Sherman LS, Ratner N. Immunocytochemical Assay for Ras Activity. In: Press A, editor. Methods in Enzymology: Academic Press; 2001. p. 348-55.
4. Hingorani SR, Tuveson DA. Ras redux: rethinking how and where Ras acts. Curr Opin Genet Dev 2003;13:6-13.
5. Sprang SR. G proteins, effectors and GAPs: structure and mechanism. Curr Opin Struct Biol 1997;7:849-56.
6. Hall BE, Yang SS, Boriack-Sjodin PA, Kuriyan J, Bar-Sagi D. Structure-based Mutagenesis Reveals Distinct Functions for Ras Switch 1 and Switch 2 in Sos-catalyzed Guanine Nucleotide Exchange. J Biol Chem 2001;276:27629-37.
7. Yan J, Roy S, Apolloni A, Lane A, Hancock JF. Ras Isoforms Vary in Their Ability to Activate Raf-1 and Phosphoinositide 3-Kinase. J Biol Chem 1998;273:24052-6.
8. Prior IA, Hancock JF. Compartmentalization of Ras proteins. J Cell Sci 2001;114:1603-8.
9. Prior IA, Muncke C, Parton RG, Hancock JF. Direct visualization of Ras proteins in spatially distinct cell surface microdomains. J Cell Biol 2003;160:165-70.
10. Hancock JF, Prior IA. Electron microscopic imaging of Ras signaling domains. Methods 2005;37:165-72.
11. Laude AJ, Prior IA. Palmitoylation and localisation of RAS isoforms are modulated by the hypervariable linker domain. J Cell Sci 2008;121:421-7.
12. Henis YI, Hancock JF, Prior IA. Ras acylation, compartmentalization and signaling nanoclusters (Review). Mol Membr Biol 2009;26:80-92.
13. Hancock JF, Magee AI, Childs JE, Marshall CJ. All ras proteins are polyisoprenylated but only some are palmitoylated. Cell 1989;57:1167-77.
14. Hancock JF, Cadwallader K, Marshall CJ. Methylation and proteolysis are essential for efficient membrane binding of prenylated p21K-ras(B). EMBO J 1991;10:641-6.

15. Hancock JF, Cadwallader K, Paterson H, Marshall CJ. A CAAX or a CAAL motif and a second signal are sufficient for plasma membrane targeting of ras proteins. EMBO J 1991;10:4033-9.

16. Magee AI, Newman CM, Giannakouros T, Hancock JF, Fawell E, Armstrong J. Lipid modifications and function of the ras superfamily of proteins. Biochem Soc Trans 1992;20:497-9.

17. Hancock JF. Ras proteins: different signals from different locations. Nat Rev Mol Cell Biol 2003;4:373-84.

18. Plowman SJ, Muncke C, Parton RG, Hancock JF. H-ras, K-ras, and inner plasma membrane raft proteins operate in nanoclusters with differential dependence on the actin cytoskeleton. PNAS 2005;102:15500-5.

19. Brunner TB, Hahn SM, Gupta AK, Muschel RJ, McKenna WG, Bernhard EJ. Farnesyltransferase Inhibitors: An Overview of the Results of Preclinical and Clinical Investigations. Cancer Res 2003;63:5656-68.

20. Casey PJ. Biochemistry of protein prenylation. J Lipid Res 1992;33:1731-40.

21. Winter-Vann AM, Casey PJ. Post-prenylation-processing enzymes as new targets in oncogenesis. Nat Rev Cancer 2005;5:405-12.

22. Adjei AA. Blocking Oncogenic Ras Signaling for Cancer Therapy. J Natl Cancer Inst 2001;93:1062-74.

23. Zujewski J, Horak ID, Bol CJ, et al. Phase I and Pharmacokinetic Study of Farnesyl Protein Transferase Inhibitor R115777 in Advanced Cancer. J Clin Oncol 2000;18:927-.

24. Maurer-Stroh S, Eisenhaber F. Refinement and prediction of protein prenylation motifs. Genome Biol 2005;6:R55.

25. Whyte DB, Kirschmeier P, Hockenberry TN, et al. K- and N-Ras Are Geranylgeranylated in Cells Treated with Farnesyl Protein Transferase Inhibitors. J Biol Chem 1997;272:14459-64.

26. Michaelson D, Ali W, Chiu VK, et al. Postprenylation CAAX Processing Is Required for Proper Localization of Ras but Not Rho GTPases. Mol Biol Cell 2005;16:1606-16.

27. Chen Z, Otto JC, Bergo MO, Young SG, Casey PJ. The C-terminal Polylysine Region and Methylation of K-Ras Are Critical for the Interaction between K-Ras and Microtubules. J Biol Chem 2000;275:41251-7.

28. Berthiaume LG. Insider Information: How Palmitoylation of Ras Makes It a Signaling Double Agent. Sci STKE 2002;2002:pe41-.

29. Rocks O, Peyker A, Bastiaens PI. Spatio-temporal segregation of Ras signals: one ship, three anchors, many harbors. Curr Opin Cell Biol 2006;18:351-7.

30. Sasaki AT, Carracedo A, Locasale JW, et al. Ubiquitination of K-Ras Enhances Activation and Facilitates Binding to Select Downstream Effectors. Sci Signal;4:ra13-.

31. Jura N, Bar-Sagi D. Mapping cellular routes of Ras: a ubiquitin trail. Cell Cycle 2006;5:2744-7.

32. de la Vega M, Burrows JF, McFarlane C, Govender U, Scott CJ, Johnston JA. The Deubiquitinating Enzyme USP17 Blocks N-Ras Membrane Trafficking and Activation but Leaves K-Ras Unaffected. J Biol Chem;285:12028-36.

33. Yoo Y, Watts S, Rechsteiner M. Ubiquitin-RAS peptide extensions as substrates for farnesyl-protein transferase and carboxymethyltransferase. Biochem J 1992;285 (Pt 1):55-60.

34. Miyake M, Mizutani S, Koide H, Kaziro Y. Unfarnesylated transforming Ras mutant inhibits the Ras-signaling pathway by forming a stable Ras.Raf complex in the cytosol. FEBS Lett 1996;378:15-8.

35. Thissen JA, Gross JM, Subramanian K, Meyer T, Casey PJ. Prenylation-dependent Association of Ki-Ras with Microtubules. EVIDENCE FOR A ROLE IN SUBCELLULAR TRAFFICKING. J Biol Chem 1997;272:30362-70.

36. Eisenberg S, Beckett AJ, Prior IA, et al. Raft Protein Clustering Alters N-Ras Membrane Interactions and Activation Pattern. Mol Cell Biol;31:3938-52.

37. Chiu VK, Bivona T, Hach A, et al. Ras signalling on the endoplasmic reticulum and the Golgi. Nat Cell Biol 2002;4:343-50.

38. Matallanas D, Sanz-Moreno V, Arozarena I, et al. Distinct Utilization of Effectors and Biological Outcomes Resulting from Site-Specific Ras Activation: Ras Functions in Lipid Rafts and Golgi Complex Are Dispensable for Proliferation and Transformation. Mol Cell Biol 2006;26:100-16.

39. Barbacid M. ras genes. Annu Rev Biochem 1987;56:779-827.

40. Lemmon MA, Schlessinger J. Cell signaling by receptor tyrosine kinases. Cell;141:1117-34.

41. Caloca MJ, Zugaza JL, Bustelo XR. Exchange Factors of the RasGRP Family Mediate Ras Activation in the Golgi. J Biol Chem 2003;278:33465-73.

42. Clyde-Smith J, Silins G, Gartside M, et al. Characterization of RasGRP2, a Plasma Membrane-targeted, Dual Specificity Ras/Rap Exchange Factor. J Biol Chem 2000;275:32260-7.

43. Adari H, Lowy DR, Willumsen BM, Der CJ, McCormick F. Guanosine triphosphatase activating protein (GAP) interacts with the p21 ras effector binding domain. Science 1988;240:518-21.

44. Lockyer PJ, Kupzig S, Cullen PJ. CAPRI regulates Ca(2+)-dependent inactivation of the Ras-MAPK pathway. Curr Biol 2001;11:981-6.

45. Walker SA, Lockyer PJ, Cullen PJ. The Ras binary switch: an ideal processor for decoding complex Ca2+ signals? Biochem Soc Trans 2003;31:966-9.

46. Rajalingam K, Schreck R, Rapp UR, Albert S. Ras oncogenes and their downstream targets. Biochim Biophys Acta 2007;1773:1177-95.

47. Cichowski K, Santiago S, Jardim M, Johnson BW, Jacks T. Dynamic regulation of the Ras pathway via proteolysis of the NF1 tumor suppressor. Genes & Dev 2003;17:449-54.

48. Serrano M, Lin AW, McCurrach ME, Beach D, Lowe SW. Oncogenic ras provokes premature cell senescence associated with accumulation of p53 and p16INK4a. Cell 1997;88:593-602.

49. Wang Z, Li Y, Liu ET, Yu Q. Susceptibility to cell death induced by blockade of MAPK pathway in human colorectal cancer cells carrying Ras mutations is dependent on p53 status. Biochem Biophys Res Commun 2004;322:609-13.

50. Woessmann W, Chen X, Borkhardt A. Ras-mediated activation of ERK by cisplatin induces cell death independently of p53 in osteosarcoma and neuroblastoma cell lines. Cancer Chemother Pharmacol 2002;50:397-404.

51. Roux PP, Blenis J. ERK and p38 MAPK-Activated Protein Kinases: a Family of Protein Kinases with Diverse Biological Functions. Microbiol Mol Biol Rev 2004;68:320-44.

52. Yang R, Piperdi S, Gorlick R. Activation of the RAF/Mitogen-Activated Protein/Extracellular Signal-Regulated Kinase Kinase/Extracellular Signal-Regulated Kinase Pathway Mediates Apoptosis Induced by Chelerythrine in Osteosarcoma. Clin Cancer Res 2008;14:6396-404.

53. Casar B, Arozarena I, Sanz-Moreno V, et al. Ras Subcellular Localization Defines Extracellular Signal-Regulated Kinase 1 and 2 Substrate Specificity through Distinct Utilization of Scaffold Proteins. Mol Cell Biol 2009;29:1338-53.

54. Voice JK, Klemke RL, Le A, Jackson JH. Four Human Ras Homologs Differ in Their Abilities to Activate Raf-1, Induce Transformation, and Stimulate Cell Motility. J Biol Chem 1999;274:17164-70.

55. Junttila MR, Li S-P, Westermarck J. Phosphatase-mediated crosstalk between MAPK signaling pathways in the regulation of cell survival. FASEB J 2008;22:954-65.

56. Colicelli J. Human RAS Superfamily Proteins and Related GTPases. Sci STKE 2004;2004:re13-.

57. Jin K, Park S, Ewton DZ, Friedman E. The Survival Kinase Mirk/Dyrk1B Is a Downstream Effector of Oncogenic K-ras in Pancreatic Cancer. Cancer Res 2007;67:7247-55.

58. Chen G, Hitomi M, Han J, Stacey DW. The p38 Pathway Provides Negative Feedback for Ras Proliferative Signaling. J Biol Chem 2000;275:38973-80.

59. Cozzi S-J, Parsons PG, Ogbourne SM, Pedley J, Boyle GM. Induction of Senescence in Diterpene Ester-Treated Melanoma Cells via Protein Kinase C-Dependent Hyperactivation of the Mitogen-Activated Protein Kinase Pathway. Cancer Res 2006;66:10083-91.

60. Sanz-Moreno V, Casar B, Crespo P. p38{alpha} Isoform Mxi2 Binds to Extracellular Signal-Regulated Kinase 1 and 2 Mitogen-Activated Protein Kinase and Regulates Its Nuclear Activity by Sustaining Its Phosphorylation Levels. Mol Cell Biol 2003;23:3079-90.

61. Deora AA, Win T, Vanhaesebroeck B, Lander HM. A Redox-triggered Ras-Effector Interaction. RECRUITMENT OF PHOSPHATIDYLINOSITOL 3'-KINASE TO Ras BY REDOX STRESS. J Biol Chem 1998;273:29923-8.

62. Wolfman JC, Wolfman A. Endogenous c-N-Ras Provides a Steady-state Anti-apoptotic Signal. J Biol Chem 2000;275:19315-23.

63. Wolfman JC, Palmby T, Der CJ, Wolfman A. Cellular N-Ras Promotes Cell Survival by Downregulation of Jun N-Terminal Protein Kinase and p38. Mol Cell Biol 2002;22:1589-606.

64. Zha J, Harada H, Yang E, Jockel J, Korsmeyer SJ. Serine phosphorylation of death agonist BAD in response to survival factor results in binding to 14-3-3 not BCL-X(L). Cell 1996;87:619-28.

65. Ninomiya Y, Kato K, Takahashi A, et al. K-Ras and H-Ras Activation Promote Distinct Consequences on Endometrial Cell Survival. Cancer Res 2004;64:2759-65.

66. Bivona TG, Quatela SE, Bodemann BO, et al. PKC regulates a farnesyl-electrostatic switch on K-Ras that promotes its association with Bcl-XL on mitochondria and induces apoptosis. Mol Cell 2006;21:481-93.

67. Dumic J, Dabelic S, Flogel M. Galectin-3: an open-ended story. Biochim Biophys Acta 2006;1760:616-35.

68. Elad-Sfadia G, Haklai R, Balan E, Kloog Y. Galectin-3 Augments K-Ras Activation and Triggers a Ras Signal That Attenuates ERK but Not Phosphoinositide 3-Kinase Activity. J Biol Chem 2004;279:34922-30.

69. Shalom-Feuerstein R, Cooks T, Raz A, Kloog Y. Galectin-3 Regulates a Molecular Switch from N-Ras to K-Ras Usage in Human Breast Carcinoma Cells. Cancer Res 2005;65:7292-300.

70. Torii S, Kusakabe M, Yamamoto T, Maekawa M, Nishida E. Sef is a spatial regulator for Ras/MAP kinase signaling. Dev Cell 2004;7:33-44.

71. Krengel U, Schlichting I, Scherer A, et al. Three-dimensional structures of H-ras p21 mutants: molecular basis for their inability to function as signal switch molecules. Cell 1990;62:539-48.

72. Kiaris H, Spandidos D. Mutations of ras genes in human tumors (review). Int J Oncol 1995;7:413-21.

73. Illmer T, Thiede C, Fredersdorf A, et al. Activation of the RAS Pathway Is Predictive for a Chemosensitive Phenotype of Acute Myelogenous Leukemia Blasts. Clin Cancer Res 2005;11:3217-24.

74. Plowman SJ, Hancock JF. Ras signaling from plasma membrane and endomembrane microdomains. Biochim Biophys Acta 2005;1746:274-83.

75. Lobell RB, Omer CA, Abrams MT, et al. Evaluation of Farnesyl:Protein Transferase and Geranylgeranyl:Protein Transferase Inhibitor Combinations in Preclinical Models. Cancer Res 2001;61:8758-68.

76. Lancet JE, Karp JE. Farnesyltransferase inhibitors in hematologic malignancies: new horizons in therapy. Blood 2003;102:3880-9.

77. Pan J, Yeung S-CJ. Recent Advances in Understanding the Antineoplastic Mechanisms of Farnesyltransferase Inhibitors. Cancer Res 2005;65:9109-12.

78. Caraglia M, Marra M, Leonetti C, et al. R115777 (Zarnestra)/Zoledronic acid (Zometa) cooperation on inhibition of prostate cancer proliferation is paralleled by Erk/Akt inactivation and reduced Bcl-2 and bad phosphorylation. J Cell Physiol 2007;211:533-43.

79. Feldkamp MM, Lau N, Roncari L, Guha A. Isotype-specific Ras{middle dot}GTP-Levels Predict the Efficacy of Farnesyl Transferase Inhibitors against Human Astrocytomas Regardless of Ras Mutational Status. Cancer Res 2001;61:4425-31.

80. Moasser MM, Rosen N. The use of molecular markers in farnesyltransferase inhibitor (FTI) therapy of breast cancer. Breast Cancer Res Treat 2002;73:135-44.

81. Schafer-Hales K, Iaconelli J, Snyder JP, et al. Farnesyl transferase inhibitors impair chromosomal maintenance in cell lines and human tumors by compromising CENP-E and CENP-F function. Mol Cancer Ther 2007;6:1317-28.

82. End DW, Smets G, Todd AV, et al. Characterization of the Antitumor Effects of the Selective Farnesyl Protein Transferase Inhibitor R115777 in Vivo and in Vitro. Cancer Res 2001;61:131-7.

83. Ma P, Magut M, Chen X, Chen C-Y. p53 Is Necessary for the Apoptotic Response Mediated by a Transient Increase of Ras Activity. Mol Cell Biol 2002;22:2928-38.

84. Shao J, Sheng H, DuBois RN, Beauchamp RD. Oncogenic Ras-mediated Cell Growth Arrest and Apoptosis are Associated with Increased Ubiquitin-dependent Cyclin D1 Degradation. J Biol Chem 2000;275:22916-24.

85. Cox AD, Garcia AM, Westwick JK, et al. The CAAX peptidomimetic compound B581 specifically blocks farnesylated, but not geranylgeranylated or myristylated, oncogenic ras signaling and transformation. J Biol Chem 1994;269:19203-6.

86. Sun J, Qian Y, Hamilton AD, Sebti SM. Both farnesyltransferase and geranylgeranyltransferase I inhibitors are required for inhibition of oncogenic K-Ras prenylation but each alone is sufficient to suppress human tumor growth in nude mouse xenografts. Oncogene 1998;16:1467-73.

87. Du W, Prendergast GC. Geranylgeranylated RhoB Mediates Suppression of Human Tumor Cell Growth by Farnesyltransferase Inhibitors. Cancer Res 1999;59:5492-6.

88. Jiang K, Coppola D, Crespo NC, et al. The Phosphoinositide 3-OH Kinase/AKT2 Pathway as a Critical Target for Farnesyltransferase Inhibitor-Induced Apoptosis. Mol Cell Biol 2000;20:139-48.

89. Liu A-x, Du W, Liu J-P, Jessell TM, Prendergast GC. RhoB Alteration Is Necessary for Apoptotic and Antineoplastic Responses to Farnesyltransferase Inhibitors. Mol Cell Biol 2000;20:6105-13.

90. Fiordalisi JJ, Johnson RL, II, Weinbaum CA, et al. High Affinity for Farnesyltransferase and Alternative Prenylation Contribute Individually to K-Ras4B Resistance to Farnesyltransferase Inhibitors. J Biol Chem 2003;278:41718-27.

91. Efuet ET, Keyomarsi K. Farnesyl and Geranylgeranyl Transferase Inhibitors Induce G1 Arrest by Targeting the Proteasome. Cancer Res 2006;66:1040-51.

92. Wang C-C, Liao Y-P, Mischel PS, Iwamoto KS, Cacalano NA, McBride WH. HDJ-2 as a Target for Radiosensitization of Glioblastoma Multiforme Cells by the Farnesyltransferase Inhibitor R115777 and the Role of the p53/p21 Pathway. Cancer Res 2006;66:6756-62.

93. Qiu Y, Liu X, Zou W, et al. The Farnesyltransferase Inhibitor R115777 Up-regulates the Expression of Death Receptor 5 and Enhances TRAIL-Induced Apoptosis in Human Lung Cancer Cells. Cancer Res 2007;67:4973-80.

94. Mavrakis KJ, Zhu H, Silva RLA, et al. Tumorigenic activity and therapeutic inhibition of Rheb GTPase. Genes & Dev 2008;22:2178-88.

95. Venkatasubbarao K, Choudary A, Freeman JW. Farnesyl Transferase Inhibitor (R115777)-Induced Inhibition of STAT3(Tyr705) Phosphorylation in Human Pancreatic Cancer Cell Lines Require Extracellular Signal-Regulated Kinases. Cancer Res 2005;65:2861-71.

96. Ashar HR, James L, Gray K, et al. Farnesyl Transferase Inhibitors Block the Farnesylation of CENP-E and CENP-F and Alter the Association of CENP-E with the Microtubules. J Biol Chem 2000;275:30451-7.

97. Adnane J, Muro-Cacho C, Mathews L, Sebti SM, Munoz-Antonia T. Suppression of Rho B Expression in Invasive Carcinoma from Head and Neck Cancer Patients. Clin Cancer Res 2002;8:2225-32.

98. Alsina M, Fonseca R, Wilson EF, et al. Farnesyltransferase inhibitor tipifarnib is well tolerated, induces stabilization of disease, and inhibits farnesylation and oncogenic/tumor survival pathways in patients with advanced multiple myeloma. Blood 2004;103:3271-7.

99. Biagi C, Astolfi A, Masetti R, et al. Pediatric early T-cell precursor leukemia with NF1 deletion and high-sensitivity in vitro to tipifarnib. Leukemia;24:1230-3.

100. Fouladi M, Nicholson HS, Zhou T, et al. A phase II study of the farnesyl transferase inhibitor, tipifarnib, in children with recurrent or progressive high-grade glioma, medulloblastoma/primitive neuroectodermal tumor, or brainstem glioma: a Children's Oncology Group study. Cancer 2007;110:2535-41.

101. Haas-Kogan DA, Banerjee A, Kocak M, et al. Phase I trial of tipifarnib in children with newly diagnosed intrinsic diffuse brainstem glioma. Neuro Oncology 2008;10:341-7.

102. Widemann BC, Arceci RJ, Jayaprakash N, et al. Phase 1 trial and pharmacokinetic study of the farnesyl transferase inhibitor tipifarnib in children and adolescents with refractory leukemias: a report from the Children's Oncology Group. Pediatr Blood Cancer;56:226-33.

103. Widemann BC, Salzer WL, Arceci RJ, et al. Phase I Trial and Pharmacokinetic Study of the Farnesyltransferase Inhibitor Tipifarnib in Children With Refractory Solid Tumors or Neurofibromatosis Type I and Plexiform Neurofibromas. J Clin Oncol 2006;24:507-16.

104. Johnston SR, Kelland LR. Farnesyl transferase inhibitors--a novel therapy for breast cancer. Endocr Relat Cancer 2001;8:227-35.

105. Kurzrock R, Kantarjian HM, Cortes JE, et al. Farnesyltransferase inhibitor R115777 in myelodysplastic syndrome: clinical and biologic activities in the phase 1 setting. Blood 2003;102:4527-34.

106. Clark GJ, Der CJ. Aberrant function of the Ras signal transduction pathway in human breast cancer. Breast Cancer Res Treat 1995;35:133-44.

107. Clark JW, Santos-Moore A, Stevenson LE, Frackelton AR. Effects of tyrosine kinase inhibitors on the proliferation of human breast cancer cell lines and proteins important in the ras signaling pathway. Int J Cancer 1996;65:186-91.

108. Martin L-A, Head JE, Pancholi S, et al. The farnesyltransferase inhibitor R115777 (tipifarnib) in combination with tamoxifen acts synergistically to inhibit MCF-7 breast cancer cell proliferation and cell cycle progression in vitro and in vivo. Mol Cancer Ther 2007;6:2458-67.

109. Haas-Kogan DA, Banerjee A, Poussaint TY, et al. Phase II trial of tipifarnib and radiation in children with newly diagnosed diffuse intrinsic pontine gliomas. Neuro Oncology;13:298-306.

110. Raponi M, Belly RT, Karp JE, Lancet JE, Atkins D, Wang Y. Microarray analysis reveals genetic pathways modulated by tipifarnib in acute myeloid leukemia. BMC Cancer 2004;4:56.

111. Raponi M, Harousseau J-L, Lancet JE, et al. Identification of Molecular Predictors of Response in a Study of Tipifarnib Treatment in Relapsed and Refractory Acute Myelogenous Leukemia. Clin Cancer Res 2007;13:2254-60.

112. Kancha RK, von Bubnoff N, Miething C, Peschel C, Gotze KS, Duyster J. Imatinib and leptomycin B are effective in overcoming imatinib-resistance due to Bcr-Abl amplification and clonal evolution but not due to Bcr-Abl kinase domain mutation. Haematologica 2008;93:1718-22.

113. Shah NP, Lee FY, Luo R, Jiang Y, Donker M, Akin C. Dasatinib (BMS-354825) inhibits KITD816V, an imatinib-resistant activating mutation that triggers neoplastic growth in most patients with systemic mastocytosis. Blood 2006;108:286-91.

114. Raz T, Nardi V, Azam M, Cortes J, Daley GQ. Farnesyl transferase inhibitor resistance probed by target mutagenesis. Blood 2007;110:2102-9.

115. Pear WS, Miller JP, Xu L, et al. Efficient and Rapid Induction of a Chronic Myelogenous Leukemia-Like Myeloproliferative Disease in Mice Receiving P210 bcr/abl-Transduced Bone Marrow. Blood 1998;92:3780-92.

116. Hussein D, Taylor SS. Farnesylation of Cenp-F is required for G2/M progression and degradation after mitosis. J Cell Sci 2002;115:3403-14.

117. Hall-Geryk M YY, Hughes DPM. Inhibiting Farnesylation Increases Ras Activity. Cancer Res Submitted.

118. Abankwa D, Gorfe AA, Inder K, Hancock JF. Ras membrane orientation and nanodomain localization generate isoform diversity. PNAS;107:1130-5.

119. Yanamandra N, Colaco NM, Parquet NA, et al. Tipifarnib and Bortezomib Are Synergistic and Overcome Cell Adhesion-Mediated Drug Resistance in Multiple Myeloma and Acute Myeloid Leukemia. Clin Cancer Res 2006;12:591-9.

120. Deng Q, Liao R, Wu B-L, Sun P. High Intensity ras Signaling Induces Premature Senescence by Activating p38 Pathway in Primary Human Fibroblasts. J Biol Chem 2004;279:1050-9.

121. Wang W, Chen JX, Liao R, et al. Sequential Activation of the MEK-Extracellular Signal-Regulated Kinase and MKK3/6-p38 Mitogen-Activated Protein Kinase Pathways Mediates Oncogenic ras-Induced Premature Senescence. Mol Cell Biol 2002;22:3389-403.

122. Sato T, Koseki T, Yamato K, et al. p53-Independent Expression of p21CIP1/WAF1 in Plasmacytic Cells during G2 Cell Cycle Arrest Induced by Actinobacillus actinomycetemcomitans Cytolethal Distending Toxin. Infect Immun 2002;70:528-34.
123. Cox AD, Hisaka MM, Buss JE, Der CJ. Specific isoprenoid modification is required for function of normal, but not oncogenic, Ras protein. Mol Cell Biol 1992;12:2606-15.
124. Kaddoum L, Magdeleine E, Waldo GS, Joly E, Cabantous S. One-step split GFP staining for sensitive protein detection and localization in mammalian cells. Biotechniques;49:727-8, 30, 32 passim.
125. Benanti JA, Galloway DA. Normal Human Fibroblasts Are Resistant to RAS-Induced Senescence. Mol Cell Biol 2004;24:2842-52.
126. Bihani T, Chicas A, Lo CP-K, Lin AW. Dissecting the Senescence-like Program in Tumor Cells Activated by Ras Signaling. J Biol Chem 2007;282:2666-75.
127. Bihani T, Mason DX, Jackson TJ, Chen SC, Boettner B, Lin AW. Differential oncogenic Ras signaling and senescence in tumor cells. Cell Cycle 2004;3:1201-7.
128. Ferbeyre G, de Stanchina E, Lin AW, et al. Oncogenic ras and p53 Cooperate To Induce Cellular Senescence. Mol Cell Biol 2002;22:3497-508.
129. Lin AW, Barradas M, Stone JC, van Aelst L, Serrano M, Lowe SW. Premature senescence involving p53 and p16 is activated in response to constitutive MEK/MAPK mitogenic signaling. Genes & Dev 1998;12:3008-19.
130. Roninson IB. Tumor Cell Senescence in Cancer Treatment. Cancer Res 2003;63:2705-15.
131. Mathon NF, Lloyd AC. Cell senescence and cancer. Nat Rev Cancer 2001;1:203-13.
132. Harley CB, Futcher AB, Greider CW. Telomeres shorten during ageing of human fibroblasts. Nature 1990;345:458-60.
133. Shay JW, Wright WE. Senescence and immortalization: role of telomeres and telomerase. Carcinogenesis 2005;26:867-74.
134. Elmore LW, Rehder CW, Di X, et al. Adriamycin-induced Senescence in Breast Tumor Cells Involves Functional p53 and Telomere Dysfunction. J Biol Chem 2002;277:35509-15.
135. Shay JW, Roninson IB. Hallmarks of senescence in carcinogenesis and cancer therapy. Oncogene 2004;23:2919-33.
136. Lee AC, Fenster BE, Ito H, et al. Ras Proteins Induce Senescence by Altering the Intracellular Levels of Reactive Oxygen Species. J Biol Chem 1999;274:7936-40.

137. van Doorn WG, Woltering EJ. Senescence and programmed cell death: substance or semantics? J Exp Bot 2004;55:2147-53.

138. Campisi J. Cellular senescence: putting the paradoxes in perspective. Curr Opin Genet Dev;21:107-12.

139. Itahana K, Dimri G, Campisi J. Regulation of cellular senescence by p53. Eur J Biochem 2001;268:2784-91.

140. Alcorta DA, Xiong Y, Phelps D, Hannon G, Beach D, Barrett JC. Involvement of the cyclin-dependent kinase inhibitor p16 (INK4a) in replicative senescence of normal human fibroblasts. PNAS 1996;93:13742-7.

141. Castro ME, del Valle Guijarr M, Moneo V, Carnero A. Cellular senescence induced by p53-ras cooperation is independent of p21waf1 in murine embryo fibroblasts. J Cell Biochem 2004;92:514-24.

142. Chang B-D, Swift ME, Shen M, Fang J, Broude EV, Roninson IB. Molecular determinants of terminal growth arrest induced in tumor cells by a chemotherapeutic agent. PNAS 2002;99:389-94.

143. Dimri GP, Lee X, Basile G, et al. A biomarker that identifies senescent human cells in culture and in aging skin in vivo. PNAS 1995;92:9363-7.

144. Kurz DJ, Decary S, Hong Y, Erusalimsky JD. Senescence-associated (beta)-galactosidase reflects an increase in lysosomal mass during replicative ageing of human endothelial cells. J Cell Sci 2000;113:3613-22.

145. Sherr CJ, DePinho RA. Cellular senescence: mitotic clock or culture shock? Cell 2000;102:407-10.

146. Hemann MT, Narita M. Oncogenes and senescence: breaking down in the fast lane. Genes & Dev 2007;21:1-5.

147. Hydbring P, Larsson L-G. Tipping the Balance: Cdk2 Enables Myc to Suppress Senescence. Cancer Res;70:6687-91.

148. Shay JW, Pereira-Smith OM, Wright WE. A role for both RB and p53 in the regulation of human cellular senescence. Exp Cell Res 1991;196:33-9.

149. Thaler S, Hahnel PS, Schad A, Dammann R, Schuler M. RASSF1A Mediates p21Cip1/Waf1-Dependent Cell Cycle Arrest and Senescence through Modulation of the Raf-MEK-ERK Pathway and Inhibition of Akt. Cancer Res 2009;69:1748-57.

150. Haferkamp S, Tran SL, Becker TM, Scurr LL, Kefford RF, Rizos H. The relative contributions of the p53 and pRb pathways in oncogene-induced melanocyte senescence. Aging (Albany NY) 2009;1:542-56.

151. Nevins JR. The Rb/E2F pathway and cancer. Hum Mol Genet 2001;10:699-703.

152. White E, Lowe SW. Eating to exit: autophagy-enabled senescence revealed. Genes & Dev 2009;23:784-7.

153. Yang K, Hitomi M, Stacey DW. Variations in cyclin D1 levels through the cell cycle determine the proliferative fate of a cell. Cell Div 2006;1:32.

154. Morgan DO. SnapShot: cell-cycle regulators I. Cell 2008;135:764-.e1.

Vita

Mandy Ann Geryk Hall was born in Houston, Texas on March 16, 1983. She is the daughter of Rocky Joe Geryk and Patti Clair Geryk. After completing her work at Cypress Falls High School , Houston, Texas in 2001, she entered Texas Tech University in Lubbock, Texas. She was a Howard Hughes Research Fellow Summer 2004 through Summer 2005. She received the degree of Bachelor of Science with a major in Biochemistry and minor in Biology from Texas Tech University in May, 2005. In August of 2005 she entered The University of Texas Health Science Center at Houston Graduate School of Biomedical Sciences and MD Anderson Cancer Center. Spring 2012 she received the degree of Doctorate of Philosophy with the majors of Cancer Biology and Biochemistry.

This dissertation was typed by Mandy Geryk Hall.